PART I. RATES OF PARAMAGNETIC PULSE REACTIONS BY NUCLEAR MAGNETIC RESONANCE

PART II. THE ELECTRON PARAMAGNETIC RESONANCE SPECTRUM OF GAS PHASE $^{14}N^{16}O_2$ AND ITS PRESSURE DEPENDENCE

Thesis by

Stuart Brooke Berger

In Partial Fulfillment of the Requirements

For the Degree of

Doctor of Philosophy

California Institute of Technology

Pasadena, California

1961

ACKNOWLEDGEMENT

It is a pleasurable and yet difficult task to fairly assay and proportionately attribute the benefits derived from my association with the professors and staff of the Institute. I have been indeed fortunate to have been affiliated with a most gracious, helpful and, in general, wonderful group of people during these very beneficial years of graduate study.

I am deeply grateful to have had the opportunity to study under the very able supervision of Professor Harden M. McConnell. I am certain that the inspiration gained from these years spent in his resourceful hands will serve as a guiding light in my future endeavor. His patience and direction are sincerely appreciated.

I would like to express my gratitude to Professors Richard M. Badger, Norman R. Davidson, G. Wilse Robinson and Ernest H. Swift for the many pleasant and informative discussions that I had with them.

The years spent in association with the students of the Molecular Spectra and Structure groups have been made especially pleasant by them. I hope to be as fortunate in my associations in the future.

Thanks go to Mrs. Lucille Lozoya who patiently and judiciously typed this thesis and to Dr. Robert Poynter who proof read this thesis and discussed many of the points contained herein.

I am indebted to the Sloan Foundation for the three Summer Fellowships which were awarded to me.

Finally and to me certainly very important, I wish to dedicate this thesis to my mother and father, Madeline and Morris Berger. Their faith, encouragement, support and devotion is a personal treasure and cannot be assayed.

Abstract

Part I of this thesis concerns the classically derived theory of the effect on the nuclear magnetic resonance line width and shape of a species which has a nucleus under investigation and is involved in an electron exchange reaction. The result is that the pseudo-first order reaction rate constant is added, under certain conditions, directly onto the no electron exchange line width of the species investigated, thereby increasing that line width. A reprint of a published article is included.

Part II of this thesis concerns the investigation of the gas phase E.P.R. spectrum of $^{14}N^{16}O_2$ at a total pressure of 0.65 millimeters of mercury to 1.3 atmospheres. A many lined spectrum is recorded at low pressures which upon increase of pressure loses intensity in the portion away from the center of the spectrum and gains intensity in the central region, especially in three positions. Upon further increase in pressure the many lines broaden into a triplet at the three positions cited which continues to broaden with increase of pressure, eventually forming a singlet. This singlet continues to broaden with increase in pressure. A linear relation between line width and pressure is approached at the intermediate to high end of the pressure range investigated. The data is consistent with the assignment of a Fermi contact interaction equal to 131 Mcps and a spin-rotation interaction equal to 73 Mcps. The

comparison to the theory of the electronic distribution of NO_2 and to the work done on the NO_2 E.P.R. spectrum in liquid CS_2 and CCl_4 and in the argon matrix is discussed. The broadening is interpreted in terms of the spin-rotation and spin-spin coupling (spin-lattice interaction) and collision theory. A treatment of the overlapping of three spectral lines at ν_o and $\nu_o \pm A$ is given.

TABLE OF CONTENTS

PART I

RATES OF PARAMAGNETIC PULSE REACTIONS BY NUCLEAR MAGNETIC RESONANCE

A. INTRODUCTION

In 1946, Bloch, Hansen and Packard (1) and Purcell, Torrey and Pound (2) performed the pioneer experiments in nuclear induction and nuclear magnetic resonance absorption, respectively. Their work triggered a vast research effort which has afforded a deeper insight into intra- and intermolecular interactions. The field of nuclear magnetic resonance (hereon referred to as N.M.R.) is well documented by review articles (for example: 3, 4, 5, 6) and by books (for example: 7, 8).

A classical description of the phenomenon involved has been presented by Bloch (9). The torque resulting from the coupling of an applied magnetic field to the macroscopic magnetization of a nuclear spin system is expressed mathematically as the vector product of the magnetization (M) and the magnetic field (H) vectors and is equal to the time rate of change of angular momentum. The angular momentum is related to the magnetization by the gyromagnetic ratio, γ (the ratio of the magnetization to the angular momentum in the electromagnetic cgs units of gauss-radian per second).

$$\frac{d\vec{M}}{dt} = \gamma \vec{M} \times \vec{H} .$$

The magnetic field vector is composed of a static component, H_o, taken to be in the z direction of the laboratory and a circularly polarized

component in the xy plane of the laboratory which oscillates with frequency ω and has an amplitude H_1. Then,

$$\frac{dM_x}{dt} + i \frac{dM_y}{dt} = \gamma (M_y - i M_x) H_o$$

$$\frac{dM_z}{dt} = - \gamma (M_x \sin \omega t + M_y \cos \omega t) H_1 .$$

These equations may be expressed in terms of u and v, defined by (7):

$$u = M_x \cos \omega t - M_y \sin \omega t$$

$$v = - (M_x \sin \omega t + M_y \cos \omega t) ;$$

thus:

$$\frac{du}{dt} + (\gamma H_o - \omega) v = 0$$

$$\frac{dv}{dt} - (\gamma H_o - \omega) u = - \gamma H_1 M_z$$

$$\frac{dM_z}{dt} - \gamma H_1 v = 0 .$$

Bloch realized that the motion must satisfy both the classical and the quantum mechanical equations in the limit of large action. In this limit, the quantum mechanical expectation value of any quantity exhibits the same time dependence as its classical mechanical analogue, which means that the above equation expressing the classical time dependence of the z magnetization component also expresses the time dependence

of the expectation value of I_z, the projection of the nuclear spin angular momentum, I, in the z direction.

For simplicity, consider $I = 1/2$; therefore, $I_z = \pm \frac{1}{2}$. The energy difference between the two nuclear spin states, equal to $2\mu H_o$, where μ is the nuclear magnetic moment, determines the population ratio of the nuclear spin states at thermal equilibrium. Using Maxwell-Boltzmann statistics:

$$\frac{N(+\frac{1}{2})}{N(-\frac{1}{2})} = \exp\left(\frac{2\mu H_o}{kT}\right),$$

where $N(m)$ is the population of the $I_z = m$ level, k is the Boltzmann constant and T is the absolute temperature. The population difference leads to a corresponding difference between the probabilities of absorption (W_+) and stimulated emission (W_-):

$$\frac{W_+}{W_-} = \exp\left(\frac{2\mu H_o}{kT}\right).$$

The net preponderance of the absorptive process, at resonance $(\gamma H_o = \omega)$, is observed experimentally as a power loss in the H_1 circuitry as the longitudinal magnetic field is slowly varied at constant $\omega = \omega_o$ and leads to a heating up of the spin system relative to the surroundings. The spin system tends toward thermal equilibrium with its surroundings (lattice) because of various interactions which exist

between the spin system and the lattice and which result in a net transfer of energy from the spin system to the lattice. One such interaction results from the thermal motion of the molecules, which produces a fluctuating local field and which, then, adds vectorally to the H_o field; the resultant fluctuating magnetic field contains, in general, Fourier components of sufficient magnitude and necessary frequency to induce significant numbers of transitions. Bloch postulated an exponential return to equilibrium in characteristic time T_1, called variously the "longitudinal," "spin-lattice," or "thermal" relaxation time, and is expressed mathematically as:

$$\frac{dM_z}{dt} = \frac{M_o - M_z}{T_1} ;$$

where $M_o = \chi_o H_o$ and χ_o is the magnetic susceptibility. The T_1 type relaxation interactions are said to be "lifetime limiting" and have an effect on the line width and line shape of the N.M.R. spectral lines. If $T_1^{-1} >> \omega_o$ (where $\omega_o = \gamma H_o$ and $2\pi/\omega_o$ is a precessional period), line narrowing is observed; if $T_1^{-1} << \omega_o$, line broadening results with an attendant Lorentzian line shape characteristic of damping a harmonic oscillator. Bloembergen, Purcell and Pound developed the theory concerning T_1 type interactions and should be consulted for further details (10).

Distinct from the T_1 mechanism for line broadening are those interactions which involve no exchange of energy with the lattice, and which merely involve a loss in phase coherence of the macroscopic magnetization component in the xy or "transverse" plane. Local field perturbations, resulting in no net energy transfer, such as those arising from nearby magnetic moments, produce an effect analogous to inhomogeneity in the logitudinal magnetic field and which lead to a distribution of magnetic field values. Experimentally, the absorption spectrum shows the distribution of magnetic fields when the longitudinal magnetic field is varied adiabatically (slowly) at constant $\omega = \omega_o$. The transverse magnetization component is decreased to e^{-1} of its coherent value in characteristic time T_2, called variously the "spin-spin" and "transverse" relaxation time. The appropriate classical equations of motion with both types of relaxation effects included are (7):

$$\frac{du}{dt} + \frac{u}{T_2} + (\gamma H_o - \omega) v = 0$$

$$\frac{dv}{dt} + \frac{v}{T_2} - (\gamma H_o - \omega) u = - \gamma H_1 M_z$$

$$\frac{dM_z}{dt} + \frac{M_z}{T_2} - \gamma H_1 v = \frac{M_o}{T_2} \quad .$$

If T_1 is much shorter than T_2, the relaxation process will be dominated by the spin-lattice mechanism. The half height-half line width is equal to $(4\pi T_1)^{-1}$. On the other hand, if T_2 is the shorter

time, one would expect an approximately Gaussian line shape which reflects the normal distribution (to a first approximation) of the magnetic fields "seen" by the nuclear magnetic moment arising from the inhomogeneity of the external magnetic field or the local magnetic field.

In this research, the effect of an electron exchange reaction on the line width and frequency is investigated. A description of an electron exchange is:

$$Y_1 + (Y_2 + \bar{e}) \rightleftharpoons (Y_1 + \bar{e}) + Y_2$$

where Y_n is species n and $\bar{e}$ is the electron. The problem is approached through consideration of the magnetization of nucleus X in a given molecule in its various "environments." The term "environment" describes local magnetic fields that the nucleus "sees." The environments under consideration for electron exchange involve the presence or absence of an unpaired electron in an orbital about nucleus X. The present work deals only with $S = 1/2$; the cases for which $S > 1/2$ may be treated in an analogous manner. The lifetimes of the various environments are correlated with the kinetic reaction rate constant and the environmental concentrations. Finally, the conditions suitable to a particular solution are imposed to obtain the equation describing the magnetization including the effects of the electron exchange.

B. DISCUSSION

One chooses as the starting point the set of Bloch equations (7) describing the behavior of the classical magnetization of nucleus X in each of its magnetic environments. These environments are, specifically, the diamagnetic denoted D and the paramagnetic denoted (P + (P-); the +(-) signifying that the electron is parallel (antiparallel) to the magnetic field direction. As does Andrew (7), one transforms the dynamic magnetization equations from laboratory cartesian coordinates into a primed system of cartesian coordinates rotating with H_1 along x' about the z = z' axis with frequency ω_o. One then defines the total transverse magnetization, G = u + iv ; where u is the in-phase magnetization and v is the out-of-phase magnetization (with respect to H_1). One chooses H_1 small enough such that no saturation results. One may then require $M_z \approx M_o$, a static value. The equation describing the time dependence of the M_z component is then of no further interest and is excluded from further discussion.

As shown mathematically in M.B.*, one integrates the transverse magnetization in the various magnetic environments over all time

---

*M.B. will be used as shorthand for reference (11) which is also to be found on pages 16 through 21 of this thesis.

up to time t. The resultant expression is given in equation 24 of M.B. One now requires an average value for the magnetization over all time, since it is the average value that one observes experimentally. In constructing this time average, one must account for the mean lifetime of nucleus X in its various environments. One accomplishes this by using a normalized correlation function, namely $T^{-1}\exp(-t\,T^{-1})$; where T represents the mean lifetime of nucleus X with respect to its existing in a specific environment. For the present case, τ_D represents the mean lifetime of X in environment D with respect to a jump(jump used to denote a quantized transition) to P+ or P-. The probability that the electron spin be up is very nearly the same as it is to be down. The mean lifetime of D with respect to the jump to environment P+(P-) is $(2\tau_D)^{-1}$. The difference in population of the two electron spin states is very nearly equal to $g|\beta|H/kT$; where g is the spectroscopic splitting factor for the electron in question, $|\beta|$ is the Bohr magneton, H the z-external field, k the Boltzmann constant and T the absolute temperature. Similarly, τ denotes the mean lifetime of X in environment P+(P-) with respect to any transition. τ is comprised of, for the case under investigation, τ_P and τ_p:

$$(1) \qquad \frac{1}{\tau} = \frac{1}{\tau_P} + \frac{1}{\tau_p} \,.$$

τ_P is the mean lifetime of nucleus X in environment P+(P-) with respect to the jump to D. τ_p is the mean lifetime of nucleus X in environment P+(P-) with respect to a jump to P-(P+). Actually, the probability of transition from environment P+ is not the same as that for P-. The probabilities differ by the amount $g|\beta|H/kT$, which is being neglected.

The time average obtained by integration over all time, of the transverse magnetization, results in equations 26-28 of M.B. It is seen that these equations involve initial values for the magnetization upon the entering by nucleus X into the various environments. Since there are definite transitions from one environment to another, a restriction is imposed as to what these initial values may be. One must perform an ensemble average to incorporate the fact that the initial value of the magnetization may be of many different values depending on the molecule of the system being considered. For example, nucleus X in environment P+ may have originated from a transition either from D or from P-. The former transition has relative probability $(2\tau_D)^{-1} F_D$ and the latter transition has relative probability $(\tau_p)^{-1} F_{P-} = \frac{1}{2}(\tau_p)^{-1} F_P$ (F_j is the fraction of nuclei X in environment j). The average initial value of the magnetization of nucleus X in environment P+ is then equal to the fraction of magnetization of nuclei X in environment D plus the fraction of magnetization of

nuclei X in environment P- entering the P+ environment. The fraction of nuclei undergoing a specific environmental transition is equal to the number of nuclei X in a given environment undergoing a transition to another specific environment per unit time divided by the total number of nuclei X undergoing an environmental jump per unit time. The explicit form of these fractions is found in equations 15-17 of M.B.

One also requires an expression for the fraction of molecules in each environment. The fractions may be simply deduced from the rate equation:

$$\frac{dN_D}{dt} = \frac{1}{\tau_P} N_{P+} + \frac{1}{\tau_P} N_{P-} - \frac{1}{\tau_D} N_D$$

(2)

$$= \frac{1}{\tau_P} N_P - \frac{1}{\tau_D} N_D \ .$$

Since the present interest lies in the steady state (where the time rate of transition into a given environment is equal to that out), $\frac{dN_D}{dt} = 0$ and

$$N_D = \frac{\tau_D}{\tau_P} N_P \ . \qquad (3)$$

The fraction of nuclei X in a given environment j is simply:

$$F_j = \frac{N_j}{\Sigma_j N_j} \ . \qquad (4)$$

The various F_j's are given in equations 13 and 14 of M.B.

One now evaluates the initial values of the magnetization of nuclei X in their various environments. This is done in equations 30-32 of M.B. The time and ensemble averaged values of the magnetization of the nuclei X in their respective environments can now be expressed in terms of τ, τ_p and τ_D. See equations 33 and 34 of M.B. The total magnetization of nuclei X is obtained by use of these equations in conjunction with the proper weighting fractions. The weighting fractions are, obviously, just the fraction of nuclei in each environment and have been discussed above. The result is given in equation 37 of M.B. and is seen to contain, aside from the usual terms obtained from the slow passage, no saturation solution, a dependency on τ, τ_p, τ_D and $\delta\omega$.

This equation may be simplified to pertain to specific cases if certain restrictions are imposed. In other words, one examines the limiting cases. In order to observe the N.M.R. signal of nucleus X in environment D it is necessary that nucleus X spend only a small fraction of time in environment P in comparison to the length of time spent in environment D. This is tantamount to the statement that a large majority of nuclei X are in environment D. Therefore, one requires:

(5) $$\tau_D \gg \tau_P ,$$

which is the same as equation 6 of M.B. Furthermore, it is necessary that the electron exchange occur at a comparable frequency with or more often than the mean time of occurrence of the other relaxation processes. This is the requirement that an effect be observable. If this were not the case then the line width would be dominated by the other relaxation processes and the present solution would prove superfluous. Mathematically:

$$(T_2)_D \geq T_D \,. \tag{6}$$

A final condition requires the nucleus X to be in a specific P environment for a long enough time to lose its phase memory with respect to the rotating magnetization vector. This condition is also the condition that the multiplets be separated. That is, one should be able to resolve the hyperfine structure of the electron paramagnetic resonance spectrum due to the interaction of the electron spin and the nuclear spin of nucleus X. The energy separation of the hyperfine structure is just $\delta\omega$. Mathematically this condition is:

$$\left(\frac{\delta\omega}{2}\,\tau\right)^2 \gg 1 \,. \tag{7}$$

The result of the imposition of the conditions expressed by equations 5, 6 and 7 results in equation 38 of M.B. for the total transverse magnetization:

$$(8) \qquad \left\langle \bar{G} \right\rangle = \frac{-i\omega_1 M_o}{\frac{1}{\tau_D} + \left(\frac{1}{T_2}\right)_D - i\Delta\omega} \quad .$$

This equation directly implicates the correlation time or mean lifetime, τ_D, in a way obviously analogous to the other relaxation times. One may then write:

$$(9) \qquad \left(\frac{1}{T_2}\right)_{DP} = \frac{1}{\tau_D} + \left(\frac{1}{T_2}\right)_D ;$$

where $\left(\frac{1}{T_2}\right)_{DP}$ is the measured line width for the D plus P environmental mixture when the equations 5-7 are satisfied. This equation 9 was used by McConnell and Weaver (12) in their work on the electron exchange between cuprous and cupric chloride complexes in hydrochloric acid solution. In this case,the cuprous state is the diamagnetic whereas the cupric state is the paramagnetic with S = 1/2. Similarly, Bruce, Norberg and Weissman (13) obtained a rate constant for the electron exchange between N,N' tetramethylparaphenylene diamine and its positive ion. In this case the former is the diamagnetic and the latter is the paramagnetic species.

In order to correlate the second order rate constant, k, of the electron exchange reaction:

$$(10) \qquad D + P \rightleftharpoons P + D$$

to τ_D, one writes the rate equation:

$$\frac{dN_e}{dt} = k N_D N_P \quad ; \tag{11}$$

where N_e is the number of electrons being transferred. The pseudo-first order rate constants $\frac{1}{\tau_D}$ and $\frac{1}{\tau_P}$ are then seen to be:

$$\frac{1}{N_D} \frac{dN_e}{dt} = \frac{1}{\tau_D} = k N_P \quad , \tag{12}$$

$$\frac{1}{N_P} \frac{dN_e}{dt} = \frac{1}{\tau_P} = k N_D \quad . \tag{13}$$

Since the concentration, N_P, is known or measurable and τ_D is experimentally derivable with the use of equation 9, k is obtainable.

It is to be noted that the lack of inclusion of the difference in probability between transitions involving P+ and P- is expected to have excluded the effect of a line shift. In addition, because of this probability difference one would expect a skewness (slight though it may be) to occur. Since the other cases, which may be described as limiting, are expected to involve a line shift, it will not prove satisfactory to discuss them in light of the approximation concerning the probability made.

Reprinted from THE JOURNAL OF CHEMICAL PHYSICS, Vol. 27, No. 1, 230–234, July, 1957
Printed in U. S. A.

Rates of Paramagnetic Pulse Reactions by Nuclear Magnetic Resonance*

HARDEN M. MCCONNELL AND STUART B. BERGER
Gates and Crellin Laboratories of Chemistry, California Institute of Technology, Pasadena 4, California
(Received December 12, 1956)

Certain fast chemical reactions involving both paramagnetic and diamagnetic molecular species are termed "paramagnetic pulse" reactions when each reaction event results in a change in a large hyperfine magnetic field acting at one or more of the molecular nuclei. The frequency distribution of the magnetic pulses is directly related to the reaction rate. The hyperfine intensity and frequency distribution of the paramagnetic pulses affects the nuclear magnetic resonance (NMR) line shapes. The Bloch equations are used to establish a quantitative relation between nuclear resonance line shape, nuclear, and electron relaxation times, and the reaction rate. The theory is discussed in terms of the Cu^{63} NMR work of McConnell and Weaver on electron exchange between Cu^{++} and Cu^{+} ions in hydrochloric acid solutions, and the H^1 NMR work of Bruce, Norberg, and Weissman on the electron exchange between neutral and positive ion molecules of *N,N'*-tetramethyl-*p*-phenylenediamine.

I. INTRODUCTION

TWO recent publications have illustrated the possibility of using NMR spectroscopy to measure the rates of very fast electron transfer reactions. McConnell and Weaver[1] have used the Cu^{63} NMR line widths in hydrochloric acid solutions of cuprous and cupric ions to estimate the bimolecular rate constant k for the electron transfer reaction:

$$Cu^{++}+Cu^{+}\rightleftharpoons Cu^{+}+Cu^{++}, \tag{1}$$

$k\sim 0.5\times 10^8$ liter/mole-second. Similarly, Bruce, Norberg, and Weissman[2] have studied aromatic proton line widths in mixtures of *N,N'*-tetramethylparaphenylenediamine and *N,N'*-tetramethylparaphenylenediamine positive ion to estimate the bimolecular rate constant for the electron transfer reaction:

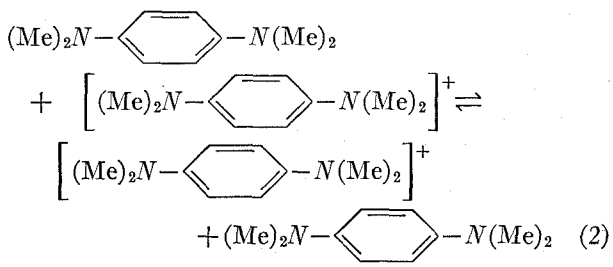

$$+(\mathrm{Me})_2N-\langle\rangle-N(\mathrm{Me})_2 \tag{2}$$

$k=2.5\times 10^4$ liter/mole-sec.

Both of the above electron transfer reactions involve one diamagnetic species D and one paramagnetic species P, and the electron transfer reaction can be written:

$$D+P\rightleftharpoons P+D. \tag{3}$$

If it is assumed that the electron transfer process in (3) is bimolecular in the species D and P, then the bimolecular rate constant k is defined by the equation:

$$N=k(D)(P), \tag{4}$$

where N is the number of moles of electrons transferred between species D and P per liter per second, and (D) and (P) are the molar concentrations of the diamagnetic and paramagnetic species, respectively. Let X be some magnetic nuclear species contained in both P and D. *Under certain conditions* the nuclear resonance line widths of species X, as measured in solutions containing both P and D, can lead to a direct determination of the bimolecular rate constant k. That is, under these conditions:

$$k=\frac{1}{(P)}\left[\left(\frac{1}{T_2}\right)_{DP}-\left(\frac{1}{T_2}\right)_{D}\right]. \tag{5}$$

In (5) $(T_2)_{DP}$ is the transverse nuclear relaxation time in a DP mixture containing (P) moles per liter of P; $(T_2)_D$ is the transverse nuclear relaxation time of X when $(P)=0$. The present work requires that the resonance line shapes be Lorentzian.

The physical arguments which lead to Eq. (5), and which also suggest important limitations on the validity of this equation, have been discussed previously by McConnell and Weaver,[1] and will not be repeated here. A set of *sufficient* conditions for the validity of (5) are summarized below.

$$\tau_D\gg\tau_P, \tag{6}$$

$$\left(\frac{\delta\omega\tau_P}{2}\right)^2\gg 1, \tag{7}$$

$$\tau_p\gg\tau_P, \tag{8}$$

$$(T_2)_D\gtrsim\tau_D. \tag{9}$$

In (6), τ_D is the average lifetime of the diamagnetic species D, with respect to the electron transfer process, τ_P is the average lifetime of the species P, τ_p is the paramagnetic spin lattice relaxation time for species P. $\hbar\delta\omega$ is the energy of the magnetic hyperfine interaction between the unpaired electron spin in P and nucleus X. By simple chemical kinetics the lifetimes τ_D and τ_P are related to the rate constant, k, and the concentra-

* Contribution No. 2153.
[1] H. M. McConnell and H. E. Weaver, Jr., J. Chem. Phys. **25**, 307 (1956).
[2] Bruce, Norberg, and Weissman, J. Chem. Phys. **24**, 473 (1956).

tions (P) and (D) by the equations,

$$\tau_D=\frac{1}{(P)k}, \tag{10}$$

$$\tau_P=\frac{1}{(D)k}. \tag{11}$$

Some of the conditions (6)–(9) have also been mentioned by Bruce, Norberg, and Weissman.

The purpose of the present paper is to use the Bloch equations to give a theoretical treatment of nuclear resonance line widths in systems containing species P and D which undergo rapid electron exchange. The solution of the Bloch equations[3] for this problem automatically shows Eqs. (6)–(9) to be necessary conditions for the validity of (5). That is, under these conditions the line width is a direct measure of τ_D and hence, from (10), of k. In addition, these solutions of the Bloch equations give general formulas for line shapes in intermediate cases as well. The final quantitative results are, of course, entirely dependent on the validity and applicability of the Bloch equations. In future work we hope to give a more general treatment of the effects of electron transfer on nuclear resonance line shapes.

II. KINETIC CONSIDERATIONS

We focus our attention on some particular nucleus, say nucleus X, which exists part of the time in molecule P and part of the time in molecule D. Actually, nucleus X can be considered to be in three distinct magnetic environments, symbolized by the three circles in Fig. 1. Circle "D" represents the magnetic environment of nucleus X when X is contained in molecule D. In this case the magnetic field acting at X is essentially equal to the intensity of the externally applied magnetic field. We neglect the effects of long range dipolar fields at X arising from unpaired electrons in other molecules. In the experimental work on exchange reactions mentioned above, this approximation has been justified.

For simplicity we assume the electronic state of P to be a doublet, $S_z=\pm 1/2\hbar$. Thus, when X is contained in P the electron spin may be up or down, and these two possible magnetic environments of X are indicated by the two circles with $P+$ and $P-$ in Fig. 1. When nucleus X is in the $P+$ "state" (environment) it is acted on by a magnetic field $\delta\omega/2\gamma_X$ in addition to the externally applied field. Here $\delta\omega$ (radians/sec) is the hyperfine splitting of the electron resonance of P due to nucleus X, and γ_X is the magnetogyric ratio of nucleus X. Similarly, in state $P-$ nucleus X sees a field of $-\delta\omega/2\gamma_X$ in addition to the applied magnetic field.

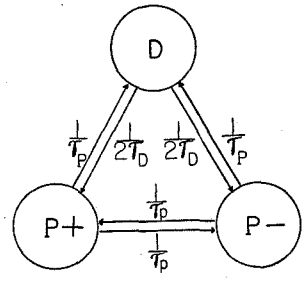

FIG. 1. The three possible magnetic environments of a nucleus X. In D nucleus X is in a diamagnetic molecule; in $P+$ nucleus X is in a paramagnetic molecule (doublet state) with electron spin "up"; in P nucleus X is in a paramagnetic molecule with electron spin "down."

The arrows in Fig. 1 indicate the six possible "transitions" whereby the magnetic environment of X can change. The specific probability (sec^{-1}) that X jumps out of D is τ_D^{-1}; the specific probability that X jumps from D to $P+$ is $(2\tau_D)^{-1}$. The jump from the $P+$ state to the $P-$ state corresponds to paramagnetic relaxation, with specific probability τ_p^{-1}. The specific probability that X jumps from the $P+$ state to the D state is the specific probability of electron transfer, τ_P^{-1}. In the subsequent discussion of the Bloch equations it is convenient to introduce a time τ such that τ^{-1} is the specific probability that X leave the $P+$ state, going either to the D state or to the $P-$ state.

$$\frac{1}{\tau}=\frac{1}{\tau_P}+\frac{1}{\tau_p}. \tag{12}$$

Also in our subsequent discussion we shall wish to have expressions for F_D, F_+, F_- where these quantities represent the fractions of an ensemble of X nuclei which are in the states D, $P+$, and $P-$. These F's may be related to the τ's by considerations of chemical kinetics:

$$F_D=(\tau_P)^{-1}/((\tau_P)^{-1}+(\tau_D)^{-1}), \tag{13}$$

$$F_+=F_-=(2\tau_D)^{-1}/((\tau_P)^{-1}+(\tau_D)^{-1}). \tag{14}$$

Finally, we shall wish to know the fraction of systems entering one state which come from some other specific state. For example, we shall wish to know f_{+D}, the fraction of the X nuclei which enter the $P+$ state from D. Once we have f_{+D} we also have f_{+-}, since $f_{+D}+f_{+-}=1$. For example, f_{+D} must be proportional to the rate at which one system in D moves to $P+$, and also proportional to the fraction of all X nuclei which are in the D state, F_D. This consideration thus leads to the following equations for the f's:

$$f_{+D}=\frac{(2\tau_D)^{-1}F_D}{(2\tau_D)^{-1}F_D+(\tau_p)^{-1}F_-}, \tag{15}$$

$$f_{+-}=\frac{(\tau_p)^{-1}F_-}{(2\tau_D)^{-1}F_D+(\tau_p)^{-1}F_-}, \tag{16}$$

$$f_{D+}=\tfrac{1}{2}. \tag{17}$$

The other f's are obtained from (15)–(17) by everywhere replacing $+$ with $-$ and vice versa.

III. SOLUTION OF THE BLOCH EQUATIONS

The method used here for the solution of the Bloch equations is a relatively straightforward extension of the

[3] F. Bloch, Phys. Rev. **70**, 460 (1946).

procedure used by Gutowsky, McCall, and Slichter[4] in their treatment of the effects of spin-lattice relaxation and chemical exchange on spin-spin multiplets in nuclear magnetic resonance. For the present problem the Bloch equations have the form:

$$\dot{G}_D+\alpha_D G_D=-i\omega_1 M_0, \tag{18}$$

$$\dot{G}_+ +\alpha_+ G_+ =-i\omega_1 M_0, \tag{19}$$

$$\dot{G}_- +\alpha_- G_- =-i\omega_1 M_0, \tag{20}$$

$$\alpha_D=\left(\frac{1}{T_2}\right)_D-i\Delta\omega, \tag{21}$$

$$\alpha_+=\left(\frac{1}{T_2}\right)_D-i\left(\Delta\omega+\frac{\delta\omega}{2}\right), \tag{22}$$

$$\alpha_-=\left(\frac{1}{T_2}\right)_D-i\left(\Delta\omega-\frac{\delta\omega}{2}\right). \tag{23}$$

In (18)–(20) $G=u+iv$ where u and v are the in-phase and out-of-phase nuclear magnetizations. Equation (18) applies when nucleus X is in the diamagnetic molecule, D; Eqs. (19) and (20) apply when X is in the $P+$ and $P-$ states, respectively. When X is in D, the nuclear resonance is centered at ω_0, and $\Delta\omega$ in (21)–(23) is $\omega_0-\omega$, where ω is the rf angular frequency. In writing (18)–(20), it is assumed that the rf amplitude, $H_1=\omega_1/\gamma_X$, is so small that there is no saturation, and $M_z\approx M_0$. The subscript D on $1/T_2$ in Eqs. (21)–(23) indicate that this T_2 is the line width relaxation time appropriate to nucleus X contained in molecule D, in the absence of molecules P.

Following the work of Gutowsky, McCall, and Slichter, solutions of (18)–(20) are, e.g.:

$$G_D=\frac{-i\omega_1 M_0}{D}(1-e^{-\alpha_D t})+G_D{}^0 e^{-\alpha_D t}, \tag{24}$$

where $G_D{}^0$ is the value of G at time $t=0$, i.e., when nucleus X first enters state D. The average value of G_D before nucleus X jumps to some other environment, $\bar{G}_D$, is

$$\bar{G}_D=\int_0^\infty \tau_D{}^{-1}e^{-t/\tau_D}G_D(t)dt, \tag{25}$$

$$\bar{G}_D=\frac{-i\omega_1 M_0\tau_D}{1+\alpha_D\tau_D}+\frac{G_D{}^0}{1+\alpha_D\tau_D}. \tag{26}$$

Similarly,

$$\bar{G}_+=\frac{-i\omega_1 M_0\tau}{1+\alpha_+\tau}+\frac{G_+{}^0}{1+\alpha_+\tau}, \tag{27}$$

$$\bar{G}_-=\frac{-i\omega_1 M_0\tau}{1+\alpha_-\tau}+\frac{G_-{}^0}{1+\alpha_-\tau}. \tag{28}$$

To obtain a true average value of G_D, $\langle\bar{G}_D\rangle$, we must also average over various possible starting values of $G_D{}^0$, $\langle G_D{}^0\rangle$. For example,

$$\langle\bar{G}_D\rangle=\frac{-i\omega_1 M_0\tau_D}{1+\alpha_D\tau_D}+\frac{\langle G_D{}^0\rangle}{1+\alpha_D\tau_D}. \tag{29}$$

By a straightforward extension of the discussion given by Gutowsky, McCall, and Slichter,[4] we have for the present case:

$$\langle G_D{}^0\rangle=f_{D+}\langle\bar{G}_+\rangle+f_{D-}\langle\bar{G}_-\rangle, \tag{30}$$

$$\langle G_+{}^0\rangle=f_{+D}\langle\bar{G}_D\rangle+f_{+-}\langle\bar{G}_-\rangle, \tag{31}$$

$$\langle G_-{}^0\rangle=f_{-D}\langle\bar{G}_D\rangle+f_{-+}\langle\bar{G}_+\rangle. \tag{32}$$

Equations (30)–(32), and Eq. (29), and two equations similar to (29) (obtained by replacing τ_D with τ, and otherwise replacing D's by $+$ or $-$, respectively) can then be combined to give $\langle\bar{G}_D\rangle$, $\langle\bar{G}_+\rangle$ and $\langle\bar{G}_-\rangle$:

$$\langle\bar{G}_D\rangle=\frac{-i\omega_1 M_0}{R}\left\{\tau_D\left[\left(\frac{\tau}{\tau_p}\right)^2-(1+\alpha_+\tau)(1+\alpha_-\tau)\right]-\tau\left[\frac{\tau}{\tau_p}+1+\alpha_D\tau\right]\right\}, \tag{33}$$

$$\langle\bar{G}_+\rangle=\frac{-i\omega_1 M_0}{R}\left\{-\tau(1+\alpha_D\tau_D)\left[\frac{\tau}{\tau_p}+1+\alpha_-\tau\right]-\tau_D\left[1-\frac{\tau}{\tau_p}\right]\left[\frac{\tau}{\tau_p}+1+\alpha_-\tau\right]\right\}, \tag{34}$$

$$R=(1+\alpha_D\tau_D)\left\{\left(\frac{\tau}{\tau_p}\right)^2-(1+\alpha_+\tau)(1+\alpha_-\tau)\right\}+\left(1-\frac{\tau}{\tau_p}\right)\left(\frac{\tau}{\tau_p}+1+\alpha_D\tau\right). \tag{35}$$

The equation for $\langle\bar{G}_-\rangle$ is obtained from (34) by symmetry. The net average nuclear magnetization of species X, $\langle\bar{G}\rangle$, is then

$$\langle\bar{G}\rangle=F_D\langle\bar{G}_D\rangle+F_+\langle\bar{G}_+\rangle+F_-\langle\bar{G}_-\rangle. \tag{36}$$

From (33)–(35), and from (13) and (14) we obtain finally for $\langle\bar{G}\rangle$:

$$\langle\bar{G}\rangle=-i\omega_1 M_0\frac{\tau_D{}^2\left(1-\frac{\tau}{\tau_p}\right)\left[\left(\frac{\tau}{\tau_p}\right)^2-(1+\alpha_+\tau)(1+\alpha_-\tau)\right]-2\left(1-\frac{\tau}{\tau_p}\right)\left[\frac{\tau}{\tau_p}+1+\alpha_D\tau\right]\tau\tau_D-\tau^2(1+\alpha_D\tau_D)\left[\frac{\tau}{\tau_p}+1+\alpha_D\tau\right]}{\left[\tau+\tau_D-\frac{\tau\tau_D}{\tau_p}\right]\left[(1+\alpha_D\tau_D)\left\{\left(\frac{\tau}{\tau_p}\right)^2-(1+\alpha_+\tau)(1+\alpha_-\tau)\right\}+\left(1-\frac{\tau}{\tau_p}\right)\left\{\frac{\tau}{\tau_p}+1+\alpha_D\tau\right\}\right]}. \tag{37}$$

[4] Gutowsky, McCall, and Slichter, J. Chem. Phys. 21, 279 (1953).

IV. DISCUSSION AND APPLICATIONS

Equation (37) represents the general solution of the problem. When inequalities (6)–(8) are applied to (37), we obtain the simple Lorentzian line-shape formula:

$$\langle \bar{G} \rangle = \frac{-i\omega_1 M_0}{\frac{1}{\tau_D} + \left(\frac{1}{T_2}\right)_D - i\Delta\omega}. \tag{38}$$

Equation (38) for the complex magnetization of nucleus X in a DP mixture leads to a transverse relaxation time $(T_2)_{DP}$ given by the equation,

$$\left(\frac{1}{T_2}\right)_{DP} = \frac{1}{\tau_D} + \left(\frac{1}{T_2}\right)_D. \tag{39}$$

Equations (39) and (10) thus yield (5). Note that condition (9) is not essential to the simplification of (37) to give (38) but is merely a statement of a condition that there be an observable broadening in the nuclear resonance of X.

Conditions (6)–(9), which are those proposed previously,[1] are somewhat more restrictive than necessary. In particular, one can obtain (38), and hence (5), from (37) by replacing conditions (7) and (8) by the more general sufficient condition,

$$\left(\frac{\delta\omega\tau}{2}\right)^2 \gg 1. \tag{40}$$

In obtaining (38) from (37) using (40) instead of (7) and (8) it is important to note that τ must be smaller than τ_p by a finite amount since otherwise condition (6) could not be satisfied.

One can easily generalize the present development to include the effects of electron exchange between paramagnetic species:

$$\frac{1}{\tau} = \frac{1}{\tau_P} + \frac{1}{\tau_p} + \frac{1}{\tau_e}, \tag{41}$$

where τ_e is the effective time for electron exchange between paramagnetic species.

It will now be seen that Eq. (40) has an extremely important practical implication. Equation (40) is a necessary condition that X-nuclear hyperfine splittings be resolved in the paramagnetic resonance spectrum of the DP mixture. One has, therefore, a direct experimental method for testing the validity of (40) for any DP mixture. Likewise, condition (9) is easily tested from the experimental results. Condition (6) is readily established by using appropriate relative concentrations of the species D and P.

The development given in the present paper appears to be particularly well suited to studies of electron transfer rates between aromatic ions and neutral molecules, such as the electron transfer reaction in (2). This is because in dilute solutions of these paramagnetic ion radicals, the paramagnetic relaxation times are quite long and rather well resolved proton hyperfine splittings can be observed. In the work of Bruce, Norberg, and Weissman on reaction (2), condition (40) was satisfied with respect to the contribution of τ_p to τ, and was also satisfied with respect to the τ_P contribution since τ_P was $\sim 2\times 10^{-5}$ sec and $\delta\omega/2\pi$ was greater than 1 Mc.

It is actually possible for condition (40) to be satisfied even though hyperfine splittings are not resolved. This situation can occur when the paramagnetic $t_1(\tau_p)$ is related to t_2 by the inequality, $t_1 \gg t_2$. Let us consider the work of McConnell and Weaver[1] on $Cu^{++}-Cu^{+}$ electron transfer in connection with this situation. In this work all of the above mentioned sufficient conditions for the validity of (38) are met except possibly condition (40). Condition (40) could only be satisfied with $\tau_p \geq 3\times 10^{-9}$ sec since $\delta\omega \sim 6\times 10^{9}$ radian/sec and the derived value of $\tau_{Cu^{++}}$ was 2×10^{-8} sec. The actual value of τ_p in the $Cu^{++}-Cu^{+}-HCl$ system[1] is not known. However the hyperfine splittings in aqueous solutions of Cu^{++} are poorly resolved, at best, and a similar situation probably prevails in HCl solutions. Theoretical estimates[5] indicate quite strongly, however, that (at least for hydrated Cu^{++} in aqueous solution) the paramagnetic line broadening is exclusively a t_2 effect, and that condition (40) actually does hold, even though the hyperfine splitting is not resolved.

It may be mentioned further that (40) is only a sufficient condition for the validity of (38). The X resonance broadening which leads to (38) is essentially a T_2' effect, and strong T_1 relaxation of nucleus X in the paramagnetic species should also lead to (38). If we denote by $(T_1)_P$ the nuclear relaxation time of X in the paramagnetic species P, then it is qualitatively plausible that conditions (6) and (9) and

$$(T_1)_P \ll \tau_P \tag{42}$$

are also a set of sufficient conditions for the validity of (38). Since we are considering rather short paramagnetic species lifetimes in the present work $\tau_P \sim 10^{-6}-10^{-8}$ sec, condition (42) is quite severe and requires a nuclear T_1 relaxation time of the same order as typical paramagnetic relaxation times. A possible example of condition (42) would be just the Cu^{++} ion, where there is a strong *anisotropic* hyperfine interaction which brings about interdependent nuclear and electron T_1 relaxation.[5]

In conclusion it should be noted that in all the experimental work to date in which (38) has been used to infer a rate constant, paramagnetic dipolar broadening of the X nuclear resonance was shown to be negligible. If this were not the case it might be necessary to correct $(T_2)_D$ from independent experimental dipolar broadening data *if* the corrected $(T_2)_D$ was of the order of magnitude of τ_D. The problem of electron-nucleus dipolar broadening is only one reason that we have not at-

[5] H. M. McConnell, J. Chem. Phys. **25**, 709 (1956).

tempted to treat the (line-shape)-(reaction-rate) problem for the case $\tau_D \leq \tau_P$. Under certain conditions (which tend to be rather involved) one can formally obtain from (37) a line shape formula in which τ_D^{-1} dominates the width. We believe, however, that to treat properly the case for $\tau_D \leq \tau_P$ one must allow for the Boltzmann distribution in population between the $P+$ and $P-$ states so that the calculated line shape formula will give both the broadening effect and also the "paramagnetic shift" of the nuclear resonance.

ACKNOWLEDGMENTS

We are indebted to Professor Norman Davidson, Professor S. I. Weissman, and Dr. R. G. Shulman for helpful discussions and correspondence concerning this work.

Bibliography

1. F. Bloch, W. W. Hansen and M. E. Packard, Phys. Rev., 69, 127 (1946); 70, 474-485 (1946).

2. E. M. Purcell, H. C. Torrey and R. V. Pound, Phys. Rev., 69, 37-38 (1946).

3. G. E. Pake, Am. J. Phys., 18, 438-452 (1950).

4. G. E. Pake, Am. J. Phys., 18, 473-486 (1950).

5. G. E. Pake, Solid State Physics (edited by F. Seitz and D. Turnbull), 2, 1-91, Academic Press, New York (1956).

6. J. E. Wertz, Chem. Rev., 55, 829-955 (1955).

7. E. R. Andrew, Nuclear Magnetic Resonance, Cambridge Monographs on Physics, Cambridge University Press, Cambridge (1955).

8. A. K. Saha and T. P. Das, Theory and Applications of Nuclear Induction, Saha Institute of Nuclear Physics, Calcutta, India (1957), esp. Chapters 1, 2 and 4, pages 1-73, 113-282.

9. F. Bloch, Phys. Rev., 70, 460-474 (1946).

10. N. Bloembergen, E. M. Purcell and R. V. Pound, Phys. Rev., 73, 679-712 (1948).

11. H. M. McConnell and S. B. Berger, J. Chem. Phys., 27, 230-234 (1957).

12. H. M. McConnell and H. E. Weaver, Jr., J. Chem. Phys., 25, 307-311 (1956).

13. C. R. Bruce, R. E. Norberg and S. I. Weissman, J. Chem. Phys., 24, 473-475 (1956).

PART II

THE ELECTRON PARAMAGNETIC RESONANCE SPECTRUM OF GAS PHASE $^{14}N^{16}O_2$ AND ITS PRESSURE DEPENDENCE

A. INTRODUCTION

This research was initiated to investigate a possible correlation between the observed broadening of the gas phase E.P.R. (Electron Paramagnetic Resonance) spectrum of NO_2 and the second order rate constant, k_1, of the Lindemann process (1), described by:

$$\text{(1)} \qquad \begin{aligned} NO_2 + NO_2 &\underset{k_1'}{\overset{k_1}{\rightleftharpoons}} N_2O_4^* \\ N_2O_4^* + M &\underset{k_2'}{\overset{k_2}{\rightleftharpoons}} N_2O_4 + M \,. \end{aligned}$$

The star (*) on the N_2O_4 indicates an energized state (in contradistinction to an activated state) and M represents a "deenergizer." The latter may be a container wall, an NO_2 or an N_2O_4 molecule or some other gaseous constituent that is present. Carrington and Davidson (2) have measured the low pressure rate constant, k_2', by shock tube methods. k_1 was estimated as 5.2×10^8 liters/mole/second from the rate of formation of NO_2, $k = \dfrac{k_1' k_2'}{k_2}$, and the equilibrium constant (gas phase). The expectation of obtaining a rate constant from spectral broadening due to the dimerization is a natural consequence of extension of the theory presented in Part I of this thesis. Unfortunately, this result is not obtained because the broadening produced by this lifetime limiting interaction is small compared to other mechanisms, especially

collision broadening. The work is by no means fruitless, since the investigation of the gas phase spectral broadening proves convenient for investigation of pertinent interactions. Likewise from a study of the magnetic interactions resulting from the coupling of the electron magnetic moment with a nuclear magnetic moment one can draw conclusions concerning the odd-electron's distribution. In so doing one tries to corroborate existent theories concerning the electronic distribution in NO_2 and the magnetic interactions involved.

With the advent of E.P.R., the study of the well-known, stable free-radical, paramagnetic gases (nitric oxide, nitrogen dioxide, chlorine dioxide and the singular even-electron molecule, oxygen) was given a new direction. It is true that information concerning the various magnetic perturbations could be discerned by other available techniques; specifically, magnetic susceptibility and microwave, infrared and optical spectroscopic measurements. Magnetic susceptibility measurements distinguish between diamagnetism and paramagnetism. In other words, this method proves NO_2 to contain one unpaired electron. The various spectroscopic methods afford information concerning the spectroscopic state, the contribution of spin-orbit coupling, the interaction between the electron magnetic moment and the molecular rotation and the coupling of the nuclear magnetic moment of nitrogen (in the case of N^{14}, $I = 1$, and for N^{15}, $I = 1/2$) to the electron moment. Microwave spectroscopy, in view of the magnitude of the energy involved, turns out to be particularly well suited to the investigation of the perturbations due to magnetic

interactions. These perturbations manifest themselves as transition fine structure in the absorption spectrum of the molecule of interest. The energy absorptions other than those due to E.P.R. which occur in the microwave range are either a result of a rotational state change or arise from an inversion level transition (the case of the ammonia levels is well known). One can also use a small magnetic field in the study of the rotational absorption spectrum (Zeeman effect). The charge produced in the spectrum due to the Zeeman effect may be correlated with theoretical prediction based upon a model of interest to the investigator. One, therefore, is afforded another method with which the molecule can be further studied. The reader interested in pursuing this topic further may consult a standard reference such as the book by Townes and Schawlow (3) which includes a complete reference list with subjects noted through 1954.

In a task as complicated as the assignment of spectral lines, it is advantageous to be able to cross-reference the information available both from the standpoint of simplification and additional substantiation. This is where E.P.R. comes into play. That is, E.P.R. is a tool which allows one to directly observe the magnetic interactions. For example, one can obtain from the E.P.R. spectrum information concerning the importance of the spin-orbit interaction (the g-value is a measure of this coupling), the magnitude of a nuclear magnetic moment and the nature of the orbitals that the electron occupies through the

nuclear spin-electron spin coupling, the effect of the rotational states on the internal magnetic field (that field produced by the molecule in question), the effect of motion and exchange of energy from line shape and width, etc. The list is indeed impressive.

For the case at hand, Castle and Beringer (4) observed the E.P.R. spectrum in the gas phase over a small variation of pressure in the millimeter mercury range. Between 5 and 15 millimeters of mercury pressure, their spectrum consisted of a triplet which they attributed to the magnetic interaction between the nuclear magnetic moment of nitrogen (N^{14}) ($I = 1$, therefore, since the multiplicity is $2I + 1$ and $\Delta I_z = 0$, one expects a triplet) and the electron magnetic moment of the unpaired spin. At the value of the magnetic field strength which they used, namely, 3300 oersteds, one would expect virtually complete coupling of the electron magnetic moment to the external field since the energy of this interaction is large in comparison to the other interaction energies (spin-spin and spin-rotation coupling). At a pressure of 1.3 millimeters mercury, these investigators noted several lines. They interpreted these lines to be those arising from the interaction of the electron magnetic moment with the rotation of the molecule in addition to the nuclear spin-electron spin interaction. Beringer (5) noted that one should expect the nuclear magnetic dipole-electron magnetic dipole coupling to be dependent on the rotational level. Lin,

in his thesis (6) and later in an article (7), described an elegant theory which bore out this rotational energy state dependence. The energy Hamiltonian, $\mathcal{H}$, given by Lin (6, 7) is:

$$(2) \qquad \mathcal{H} = -g|\beta| HS_z + AS_z I_z + BS_z M_N$$

where g is the spectroscopic splitting factor; $|\beta|$ is the absolute value of the Bohr magneton; H is the magnitude of the external magnetic field; S_z and I_z are, respectively, the electron and nuclear spin quantum number projection upon the external magnetic field direction; and M_N is the projection upon the external magnetic field direction of the molecular angular momentum quantum number, N. The constant A, which is electron configuration dependent, will be shown later to contain an isotropic part and an anisotropic part. The anisotropic part will also be shown to be rotation level dependent. The constant B is dependent upon the rotation. Therefore, A and B do behave as Castle and Beringer (4) and Beringer (5) have asserted.

The information gleaned from the microwave work allows a very precise structural determination. The N--O bond length is 1.197 Å and the O-N-O angle is 134° 15' as reported by Bird (8). There are not enough rotational transitions investigated at the present time due to the limitations imposed by the lack of electronic technique in the very short microwave range for one to obtain the harmonic force constants, the moments of inertia of the undistorted molecule and the

effect of centrifugal distortion from the pure rotational spectra (see, for example, Bird (8)). By the combination of the infrared data that they obtained and the existent microwave data, Arakawa and Nielsen (9) have been able to get all the above except the effect of centrifugal distortion.

The quest for fuller understanding of this molecule has spurred Bird and Baird (10, 11) to an interpretation of the magnetic effects. With simplification in mind, Bird, Baird, and Williams (12) studied the triplet that they observed in the E.P.R. spectrum of NO_2 in dilute solution in CCl_4 and CS_2. The outer lines are symmetrically displaced from the central absorption peak by an amount F. The splitting is attributed to an isotropic hyperfine interaction since the time average over a precessional period of the orientation of the NO_2 molecule is expected to be spherically symmetric. This spherically symmetric positioning is the result of the large number of collisions which the molecule undergoes during a precessional period. The isotropic coupling is the Fermi contact interaction (13). This interaction is the result of the breakdown of the dipole-dipole approximation near the nucleus. In the region close to the nucleus a magnetostatic calculation may be made assuming that the distribution of spin is constant and the region under consideration is large compared to the size of the electron and the nucleus (14). It can be shown that, in terms of atomic orbitals, the contribution of p-orbitals to this coupling is very much smaller

than that for the s-orbital of the same principal quantum number. In other words, this interaction affords a measure of the amount of s-character that the unpaired electron has at that nucleus about which the orbit is centered. Since this term depends on the probability of finding the electron at the nucleus, one should have a fair idea of the wave functions involved before making an ironclad estimate. F for NO_2 is 300 Mcps (megacycles per second), which corresponds to about 18% s-character on the nitrogen atom on the assumption that the nature of the 2s-orbital is the same as that for a nitrogen atom (12). A recent theoretical work (15) accounts for about one-half of the contribution, which, owing to the necessarily crude approximations made, may be considered to be in fair agreement. Bird et al. expected this term, F, to be a part of the spin-spin term, A, of equation 2. One additional point may be made in the nature of information. Namely, the term F used is the average of the values obtained from the data of the splitting in CCl_4 and CS_2; the two values differ by what may be expected to be negligible, specifically, 4.2 Mcps. No more will be said of this term now, since it is the subject of later discussion. As far as the other terms are concerned, Bird (10) has indicated that he has obtained the other constants that occur in equation 2 as given by Lin (6,7).

The present research will be presented in the following manner. A discussion of the Hamiltonian will be undertaken and, where feasible, the magnitudes of the interaction parameters will be estimated from

theoretical calculations. The theoretical aspects of the factors governing line shapes and widths will be considered. The effects of collisions will be treated therein. The experimental procedure will next be explained including the purification and preparation of samples of NO_2, the instruments and the various apparatus described, and the spectral calibration discussed. The data will be presented including the method used to prepare its presentation in terms of theoretically interesting quantities. The final consideration will be the correlation between theory and experiment.

B. THEORY

1.. Hamiltonian

It will prove advantageous to understand the theoretical considerations before passing on to the results of the experiments. The general high field spin Hamiltonian is:

$$(3) \qquad \mathcal{H} = \mathcal{H}_o + \mathcal{H}_{SI} + \mathcal{H}_F + \mathcal{H}_{SR} + \mathcal{H}_Q \,.$$

The terms will be treated in their order of appearance in equation 3.

$\mathcal{H}_o$ is the unperturbed spin Hamiltonian for the strong magnetic field case. The restriction to strong fields means that the various other interactions are small in energy as compared to the energy of interaction of the electron spin with the external magnetic field. If the situation were not this, one would have to diagonalize the electron spin matrix along a resultant magnetic field vector produced by adding vectorially the external magnetic field and the local magnetic fields produced by the effects of nuclear magnetic moments, rotational magnetic moments on the electron magnetic moment, etc.

$$(4) \qquad \mathcal{H}_o = -g\,|\beta|\,\vec{S}\cdot\vec{H} + g_N\,\beta_N\,\vec{I}\cdot\vec{H}\,;$$

where the arrows denote vectors; g and g_N are the electron and ^{14}N

nuclear splitting factors; β and β_N are the Bohr and nuclear magnetons; S and I are the electron and nuclear spin quantum numbers, and H is the magnetic field strength. For H taken in the z laboratory cartesian coordinate direction:

$$(5) \qquad \mathcal{H}_o = g|\beta| HS_z + g_N \beta_N HI_z \ .$$

It can be shown that I_z is almost a good quantum number (14). For the present case, it will be shown that $\mathcal{H}_o >> \mathcal{H}_F, \mathcal{H}_{SI}$ and that $\mathcal{H}_F >> \mathcal{H}_{SI}$ which are approximate requirements for I_z to be good. The selection rules for the strong field case are $\Delta S_z = \pm 1$ and $\Delta I_z = 0$. The second term in equation 5 is then seen to be superfluous and hence is dropped.

$\mathcal{H}_{SI}$ arises from the coupling of the electron spin to the nuclear spin:

$$(6) \qquad \mathcal{H}_{SI} = g|\beta| g_N \beta_N \left(\vec{S}\cdot\vec{I} - 3 \frac{(\vec{S}\cdot\vec{r})(\vec{r}\cdot\vec{I})}{r^2} \right) \frac{1}{r^3} \ ,$$

everywhere except where the dipole-dipole approximation fails. This latter situation occurs at a distance from the nucleus (considered as a point) which is comparable to the "length" of the electron dipole. For this condition one must include another term to account for the probability of finding the electron spin very close to the nucleus. This term, as noted earlier, is the Fermi contact term $\mathcal{H}_F$(13), which is

considered below. $\vec{r}$ is the vector connecting the two point dipoles. The expression in the brackets may be expanded:

$$
\begin{aligned}
(7)\quad \left(\vec{S}\cdot\vec{I} - 3\,\frac{(\vec{S}\cdot\vec{r})(\vec{r}\cdot\vec{I})}{r^2} \right) &= (3\underline{\beta}^2 - 1)(\vec{I}\cdot\vec{S} - 3\, I_B S_B) \\
&- \frac{3}{4}(\alpha - i\gamma)^2 (I_A + iI_C)(S_A + iS_C) - \frac{3}{4}(\alpha - i\gamma)^2 (I_A - iI_C)(S_A - iS_C) \\
&- \frac{3}{2}\underline{\beta}(\alpha - i\gamma) I_B (S_A + iS_C) - \frac{3}{2}\underline{\beta}(\alpha + i\gamma) I_B (S_A - iS_C) \\
&- \frac{3}{2}\underline{\beta}(\alpha - i\gamma) S_B (I_A + iI_C) - \frac{3}{2}\underline{\beta}(\alpha + i\gamma) S_B (I_A - iI_C) \ ;
\end{aligned}
$$

where:

$$
\begin{aligned}
&(a)\quad \alpha = \sin\theta'\cos\phi' \\
(8)\qquad &(b)\quad \underline{\beta} = \cos\theta' \\
&(c)\quad \gamma = \sin\theta'\sin\phi'
\end{aligned}
$$

θ' and ϕ' are the spherical polar coordinates referred to the axes A, B and C centered at the nitrogen nucleus. B is the symmetry axis; A is perpendicular to B and in the molecular plane; C is orthogonal to A and B and satisfies the vector product of unit vectors (denoted by $\hat{g}_i$):

$$
(9)\qquad \hat{g}_C = \hat{g}_B \times \hat{g}_A \ .
$$

This choice of the coordinates is prompted by their relation to the Euler angles. The Euler angles are defined for a right hand coordinate

system in the following way. One chooses a set of axes in the rigid body of concern about the center of mass (in NO_2 the center of mass lies on the symmetry axis B, and is $\frac{16}{23}$ the distance from the nitrogen atom to the line intersecting both oxygen atoms). For convenience, the symmetry axis is chosen as the z' axis, the x' axis is chosen parallel to and displaced an amount, a (described above as the displacement of the center of mass from the nitrogen atom), from the C axis, and the y' axis is chosen parallel to and displaced by a from the A axis. Likewise, one selects a set of laboratory coordinates whose origin is at the molecular center of mass and initially coincident with the molecular coordinates: $z' = z$; $y' = y$, $x' = x$. A rotation of the molecule about the z axis will describe the Euler angle ϕ. Next a molecular rotation about the x' axis will describe the second Euler angle, θ. Finally, a rotation of the molecule about the z' axis will describe the Euler angle, χ. See Figure 1 for a pictorial description.

The wave function describing the molecular rotation is written in terms of the Euler angles (3a):

$$\Psi_R = \Theta(\theta)\, e^{iM_N\phi}\, e^{iK\chi} \quad ; \tag{10}$$

where $\Theta(\theta)$ is a complicated hypergeometric function. $\Theta(\theta)$ is a function of θ, K and M_N. Through the solution of $\Theta(\theta)$, N, the total rotational angular quantum number is defined. The solution of $\Theta(\theta)$ is not of interest here and will not be presented (see

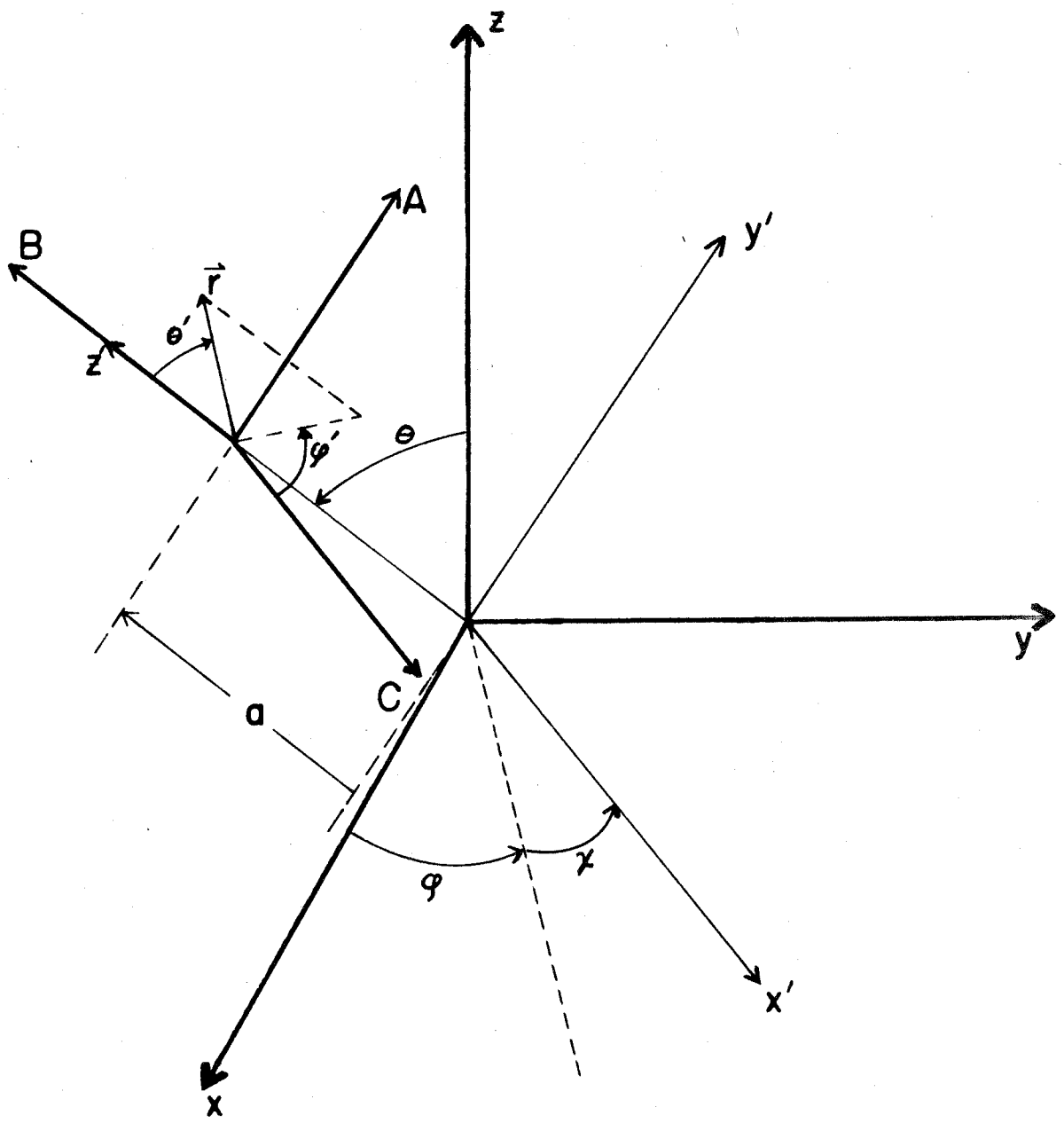

Fig. 1. - The space-fixed and molecular coordinate systems as described in the text.

ref. 3a). K is the projection of N on the symmetry axis, z' = B (though there are alternate means of presentation, this is the one herein used), and M_N is the projection of N on z. The energy expression for the rotation is approximately:

$$E = \frac{B+C}{2} N(N+1) + (A - \frac{B+C}{2}) K^2 ;$$

where for example: $B = \frac{h}{8\pi^2 I_B}$; I_B is the principal moment of inertia about the B axis. $(A - \frac{B+C}{2}) = 227,020$ Mcps and $\frac{B+C}{2} = 12648.6$ Mcps (8). The NO_2 molecule is very nearly a prolate symmetric top with $B \approx C$. A, B and C are reciprocal moments of inertia in the order of decreasing magnitude. The energy equation is independent of M_N in the absence of an externally applied field.

In order to transform the terms of equation 7 into laboratory coordinates, it is necessary to define a set of direction cosines, λ_{Fg}, where F refers to the laboratory coordinates (x, y, z) and g refers to the center of mass molecular coordinates (x', y', z'). Because the molecular coordinates relative to the nitrogen atom position may be transformed into the center of mass molecular coordinate system by a simple translation along the axis z' by an amount a, the direction cosines with respect to the space-fixed coordinates remain unchanged. The elements of the direction cosine matrix with respect to the Euler angles are well known and may be found in a standard treatise on the

mechanics of rigid bodies, e.g., see reference 16 . The transformation into laboratory coordinates now requires the z direction to be parallel to the static external magnetic field and gives as a result:

$$S_B = S_z\lambda_{zB} + S_y\lambda_{yB} + S_x\lambda_{xB} \tag{11a}$$

$$I_B = I_z\lambda_{zB} + I_y\lambda_{yB} + I_x\lambda_{xB} \tag{11b}$$

$$(S_A \pm iS_C) = S_z(\lambda_{zA} \pm i\lambda_{zC}) + S_y(\lambda_{yA} \pm i\lambda_{yC}) + S_x(\lambda_{xA} \pm i\lambda_{xC}) \tag{11c}$$

$$(I_A \pm iI_C) = I_z(\lambda_{zA} \pm i\lambda_{zC}) + I_y(\lambda_{yA} \pm \lambda_{yC}) + I_x(\lambda_{xA} \pm \lambda_{xC}) \tag{11d}$$

$$\vec{I}\cdot\vec{S} = I_zS_z + I_yS_y + I_xS_x \ . \tag{11e}$$

The various direction cosines involved either do or do not commute with the rotational Hamiltonian. For a symmetric rotor, N and K are good quantum numbers. For a very near symmetric top such as NO_2, this is approximately true. The only states for which $\Delta K = \pm 2$ will not be neglected are those with $|K| = 1$. In other words, the diagonal terms of the four energy submatrices resulting from the Wang transformation (19) of the energy matrix for given N are retained (see King, Hainer and Cross (20) or Strandberg (18a)). For J even and $|K| = 1$, Ψ^- is symmetric with respect to C_{2v} (symmetry axis) and for J odd and $|K| = 1$, Ψ^+ is symmetric with respect to C_{2v}:

$$(12a)\qquad \Psi^{+} = \frac{1}{2}\left(\Psi\,(N, K = +1) + \Psi\,(N, K = -1) \right)$$

$$(12b)\qquad \Psi^{-} = \frac{1}{2}\left(\Psi\,(N, K = +1) - \Psi\,(N, K = -1) \right).$$

Thus, direction cosine matrix elements connect states with $\Delta K = \pm 2$. The direction cosine matrix elements were derived by Cross et al. (17) and are tabulated in reference 3b or reference 18b.

Inspection of equation 7 shows that the last four terms on the right hand side contain direction cosines of the form: $\lambda_{FB}(\lambda_{FA} \pm i\,\lambda_{FC})$. Examination of the table of direction cosine matrix elements shows that terms of this type mix K and $K \pm 1$ states and are therefore not diagonal with respect to K. These terms are dropped.

Next, the first term on the right hand side of equation 7 may be transformed and written in the form:

$$(3\beta^2 - 1)(\vec{I}\cdot\vec{S} - 3I_B S_B) = (3\beta^2 - 1)\,[I_x S_x + I_y S_y + I_z S_z - 3(I_x\lambda_{xB} + I_y\lambda_{yB} + I_z\lambda_{zB}) *$$

$$(S_x\lambda_{xB} + S_y\lambda_{yB} + S_z\lambda_{zB})\,].$$

Since $\Delta I_z = 0$ for the strong magnetic field case, terms in I_x and I_y are zero:

$$(3\beta^2 - 1)(\vec{I}\cdot\vec{S} - 3I_B S_B) = (3\beta^2 - 1)\,[S_z - 3\lambda_{zB}(S_x\lambda_{xB} + S_y\lambda_{yB} + S_z\lambda_{zB})\,]\,I_z.$$

Terms in λ_{xB} and λ_{yB} mix states of $\Delta M_N = \pm 1$, where for low pressures

M_N is considered to be a good quantum number:

(13a) $(3\underline{\beta}^2-1)(\vec{I}\cdot\vec{S} - 3I_B S_B) = (3\underline{\beta}^2-1)(1 - 3\lambda_{zB}^2)S_z I_z$.

Lin (6, 7) has shown the matrix elements:

(13b) $(N, K, M_N | 1-3\lambda_{zB}^2 | N, K, M_N) = -2[N(N+1)(2N-1)(2N+3)]^{-1}$

$$[N(N+1)-3M_N^2][N(N+1)-3K^2] .$$

The two remaining terms on the right side of equation 7 contain a direction cosine dependence of the form $(\lambda_{FA} \pm i\lambda_{FC})(\lambda_{F'A} \pm i\lambda_{F'C})$. Again, terms containing I_x and I_y are dropped, leaving only those terms in $(\lambda_{FA} \pm i\lambda_{FC})(\lambda_{zA} \pm i\lambda_{zC})$. Terms in $(\lambda_{zA} \pm i\lambda_{zC})$ are diagonal with respect to M_N whereas those in $(\lambda_{F'A} \pm i\lambda_{F'C})$ where $F' \neq z$ are not. The latter terms are dropped. The remaining terms contain $(\lambda_{zA} \pm i\lambda_{zC})^2 S_z I_z$. They, through the direction cosine matrix, mix states of $\Delta K = \pm 2$ which, as stated before, are important for certain K values, specifically for $K = \pm 1$. For NO_2, Lin (6, 7) has shown:

(14) $(N, K=1, M_N | (\lambda_{zA} + i\lambda_{zC})^2 | N, K=1, M_N) = 2[(2N-1)(2N+3)]^{-1}[N(N+1)-3M_N^2]$.

Combining the results of equations 13b and 14 with the average over the electron distribution:

$$(15)\quad \mathcal{H}_{SI} = 2g|\beta|\, g_N\beta_N\left(\left\langle\frac{3\beta^2-1}{r^3}\right\rangle_{ave}[N(N+1)-3K^2] \pm \delta^1_{|K|}\,\frac{3}{4}\left\langle\frac{a^2+\gamma^2}{r^3}\right\rangle_{ave} N(N+1)\right)$$

$$\times\,[N(N+1)(2N-1)(2N-3)]^{-1}\,[N(N+1)-3M_N^2]\quad ;$$

where $\delta^1_{|K|}$ is zero for $|K| \neq 1$ or one if $|K| = 1$, and the $\pm$ modifying $\delta^1_{|K|}$ refers to the symmetric and antisymmetric Wang (18) functions described above.

$\mathcal{H}_F$ as stated above is the Fermi contact interaction Hamiltonian. Fermi (13) was the first to treat the problem of an electron in an s-orbital magnetically interacting with the nuclear magnetic moment. As previously noted, the dipole approximation is not useful when the distance between the magnetic dipoles is comparable to the effective lengths of the dipoles. One must treat this problem in an alternate way. As described by Ramsey (21,14), a semiclassical treatment may be utilized. One considers a distance large with respect to the size of the nucleus and of the electron, but small enough such that the electron density is essentially constant over that distance. The problem is then treated as one in classical magnetostatics. The energy of interaction is:

$$(16a)\qquad -\vec{u}_N\cdot\vec{B} = -g_N\beta_N\vec{I}\cdot\vec{B}\ ;$$

where:

$$(16b)\qquad \vec{B} = \frac{8\pi}{3}\,\vec{m}(o)\ .$$

The electron distribution is considered constant for the distance involved and must therefore be equal to the probability of finding the unpaired electron at the nucleus. $\vec{m}(o)$ is the magnetization at the nucleus:

$$\vec{m}(o) = -g|\beta||\psi(o)|^2\vec{S}. \tag{17}$$

Therefore:

$$\mathcal{H}_F = \frac{8\pi}{3} g|\beta| g_N\beta_N |\psi(o)|^2 \vec{I}\cdot\vec{S}. \tag{18}$$

For the strong field case:

$$\mathcal{H}_F = \frac{8\pi}{3} g|\beta| g_N\beta_N |\psi(o)|^2 I_z S_z = \sigma I_z S_z. \tag{19}$$

It has been shown that by substituting the justifiable value of 10^{-2} Å as the distance from the nucleus into the hydrogen-like wave functions for an s and p orbital of identical principal quantum number, the contribution to $\mathcal{H}_F$ from the s-orbital is very many times larger than that from the p-orbital (14). One may say, therefore, that the contact interaction is a virtual measure of the s-character about a given atom of the electron in question.

$\mathcal{H}_{SR}$ is that part of the Hamiltonian which describes the interaction of the electron magnetic moment with the rotation induced magnetic moment. Qualitatively, the rotational magnetic moment results

from the rotationally induced orbital angular momentum of the electrons and the magnetic fields produced by the rotating charges of the nucleus and other electrons. As shown by Lin (6,7), the two types of interaction are of the same consequence and their contributions to the energy are therefore inseparable. The latter interaction is dependent on the isotope used since it depends on the moments of inertia. In addition, it is a function of the internuclear distances, the average distance of the odd electron to the various nuclei of the molecule and the centrifugal distortion. Lin expects:

$$(20) \quad \mathcal{H}_{SR} = [N(N+1)]^{-1} (\vec{N}\cdot\vec{S}) \sum_{ij} \epsilon_{ij} N_i N_j \quad ;$$

where $\epsilon_{ij} = \epsilon_{ji}$ are the coefficients which represent the sum of the two interactions described above. Again, the selection rules are imposed (with the proper treatment of the $|K| = 1$ state as mentioned earlier). The result is:

$$(21) \quad \mathcal{H}_{SR} = \kappa (\vec{N}\cdot\vec{S}) \quad ;$$

where:

$$(22) \quad \kappa = \frac{1}{2}(\epsilon_{CC} + \epsilon_{BB}) + [N(N+1)]^{-1}[\epsilon_{AA} - \frac{1}{2}(\epsilon_{BB} + \epsilon_{CC})] K^2 \pm \frac{1}{4} \delta_{|K|,1} (\epsilon_{BB} - \epsilon_{CC})$$

Since:

$$(23) \quad \vec{N}\cdot\vec{S} = N_x S_x + N_y S_y + M_N S_z$$

for the strong field case:

$$(24) \qquad \mathcal{H}_{SR} = \kappa M_N S_z .$$

$\mathcal{H}_Q$, the final term of the total Hamiltonian of equation 3, represents the electric quadrupole interaction which is expected to be of small consequence in view of the small nitrogen quadrupole moment. It shall be neglected.

The Hamiltonian is then:

$$(25) \quad \mathcal{H} = -\left(g|\beta| H_o + 2g|\beta| g_N\beta_N \left[f_\lambda \left\langle \frac{3\beta^2 - 1}{2r^3} \right\rangle_{ave} \pm \delta'_{|K|} \frac{3}{4} f_\tau \left\langle \frac{a^2 + \gamma^2}{r^2} \right\rangle_{ave} \right] I_z \right.$$

$$\left. - \frac{8\pi}{3} |\psi(o)|^2 g|\beta| g_N\beta_N I_z - \kappa M_N \right) S_z ;$$

where:

$$(26) \quad (a) \qquad f_\lambda = [N(N+1)(2N-1)(2N+3)]^{-1} [N(N+1) - 3M_N^2] [N(N+1) - 3K^2]$$

$$(b) \qquad f_\tau = [(2N-1)(2N+3)]^{-1} [N(N+1) - 3M_N^2] .$$

One would like to know what magnitude to expect for the various coupling parameters. This problem is, for the anisotropic spin spin coupling, solvable from theoretical considerations. First, $g|\beta| g_N\beta_N$ is equal to 5.71×10^2 Mcps - $Å^{-3}$ for ^{14}N interaction with the unpaired electron of nitrogen dioxide. By using the ground state wave

function, if it is known or, if not, by making a suitable approximation, $\left\langle \frac{3\beta^2-1}{2r^3} \right\rangle_{ave}$ may be calculated. A computation of this quantity has been carried out by Dousmanis (22), who obtained a value of 22.5×10^{24} cm^{-3} for $\left\langle \frac{1}{r^3} \right\rangle_{ave}$. This calculation was based on the Hartree orbitals (23) and was "corrected" in an artificial manner. The "correction" was obtained from the experimentally well-known oxygen case which for a similar computation exhibited an 8% discrepancy. For a wave function which has the same angular dependence as a $2p_z$ hydrogen-like wave function:

$$(27) \quad \left\langle \frac{3\beta^2-1}{2r^3} \right\rangle_{ave} = \frac{2}{5} \left\langle \frac{1}{r^3} \right\rangle_{ave} ;$$

$$(28) \quad \left\langle \frac{\alpha^2+\gamma^2}{r^3} \right\rangle_{ave} = -\frac{2}{5} \left\langle \frac{1}{r^3} \right\rangle_{ave} .$$

Using equations 31 and 32 and the above values of $g|\beta|g_N\beta_N$ and $\left\langle \frac{1}{r^3} \right\rangle_{ave}$, one expects:

$$(29) \quad g|\beta|g_N\beta_N \left\langle \frac{3\beta^2-1}{2r^3} \right\rangle_{ave} = 51.4 \text{ Mcps};$$

$$(30) \quad g|\beta|g_N\beta_N \left\langle \frac{\alpha^2+\gamma^2}{r^3} \right\rangle_{ave} = -38.5 \text{ Mcps}.$$

However, these values are not directly applicable to NO_2, since these quantities refer to 100% $2p_B$ character.

Recently, McEwen (15) carried through a calculation which resulted in the wave functions for NO_2 in its various electronic states. The present interest lies in the ground state configuration. The method employed was that of the self-consistent field theory molecular orbitals expressed in terms of atomic orbitals. Hückel-type molecular orbitals were used for the non-bonding σ-electron system. The approach was semi-empirical. For details, the paper should be consulted (15). Considering only the orbital configuration of the unpaired electron of the ground state, one obtains:

$$(31) \qquad \psi_e = 0.985\, a_1^* + 0.18\, b_2 ;$$

where ψ_e is the part of the spatial wave function describing the motion of the unpaired electron and:

$$(32) \qquad a_1^* = 0.68\, O_t^+ - 0.41\, O_r^+ + 0.01\, O_s^+ + \left(\frac{0.60}{\sqrt{3}}\right)(N_s - \sqrt{2}\, N_B) - \left(\frac{0.04}{\sqrt{3}}\right)(\sqrt{2}\, N_s + N_B),$$

$$(33) \qquad b_2 = 0.99\, O_t^- - 0.14\, O_r^- \pm 0.01\, O_s^- \pm 0.02\, N_A .$$

The asterisk (*) indicates antibonding character. The O_t^+, O_r^+ and O_s^+ are linear combinations of the oxygen orbitals:

$$(34) \quad (a) \qquad O_r^+ = \frac{1}{\sqrt{2}}\,(O_r \pm O_r')$$

$$(b) \qquad O_t^+ = \frac{1}{\sqrt{2}}\,(O_t \pm O_t')$$

$$(c) \qquad O_s^+ = \frac{1}{\sqrt{2}}\,(O_s \pm O_s') ;$$

where the primes distinguish the two oxygen atoms of NO_2. O_r is the 2p orbital along the N-O bond; O_t is orthogonal to O_r and in the molecular plane; O_s is the 2s orbital of oxygen. Due to their small size, the last two terms of equation 37 may be neglected for the purposes of this thesis. The letters a and b and the subscripts 1 and 2 of equations 36 and 37 concern the behavior of the wave function with respect to certain symmetry conditions (24). Namely, the letters a and b refer to symmetric and antisymmetric functions with respect to a rotation of 180° about the symmetry axis. The subscripts 1 and 2 refer, respectively to the symmetric and antisymmetric behavior of the functions with respect to a reflection through the BC plane. Since the distance from the oxygen nuclei to the nitrogen nucleus is large, one expects little contribution to the dipole-dipole interaction energy when the electron is near the oxygen nuclei. Therefore, the part of the wave function concerning the oxygen orbitals is neglected. From the wave function one deduces approximately 21.2% N_B character (the $2p_B$ orbital discussed above) and about 10.6% N_s character (the 2s orbital of nitrogen). Modifying the coupling constant discussed above by the probability of finding the unpaired electron in the $2p_B$ orbital gives:

$$(35) \qquad g\,|\beta|\,g_N\beta_N\left(\left\langle \frac{3\beta^2-1}{2r^3}\right\rangle_{\text{ave } 2p_B}\right) = \lambda = 10.9 \text{ Mcps}$$

$$(36) \qquad \frac{3}{4}\,g\,|\beta|\,g_N\beta_N\left(\left\langle \frac{\alpha^2+\gamma^2}{r^3}\right\rangle_{\text{ave } 2p_B}\right) = \tau = -8.7 \text{ Mcps}\,.$$

The next topic of discussion is the factors f_λ and f_τ defined in equation 26a and 26b respectively. These factors are obviously rotation energy state dependent. f_τ will not be treated directly, since any remarks concerning f_λ with $K = 0$ also apply to f_τ. By inspection of the total Hamiltonian of equation 25, it is evident that the most sensible treatment of f_λ involves the discussion in terms of M_N sublevels. Figure 2 shows the distribution of f_λ values weighted by the relative population of the energy levels for several values of N. In order to obtain the relative rotational energy level populations, it is necessary to consider the symmetry restrictions. A good discussion of symmetry, if one is careful with the notation, is found in Herzberg (25). For an asymmetric top, with the symmetry axis as the principal axis of the intermediate moment of inertia, the wave functions of the components of the principal rotational angular momentum quantum number (N), designated $\tau = K_{-1} - K_{+1}$ (where K_{-1} is the limiting value of K for a prolate symmetric top and K_{+1} is the limiting value of for an oblate symmetric top; τ then takes on values:

-N, -N+1, ... , N-1, N), are symmetric for τ even and antisymmetric for τ odd with respect to an 180° rotation about the symmetry axis. Since, for the present interest, NO_2 (1). is in its lowest vibrational energy state, which is totally symmetric, (2). is in its ground electronic energy state, which is designated $^2A_1$ (15) and is totally symmetric, and (3). has two identical nuclei with zero nuclear spin symmetrically

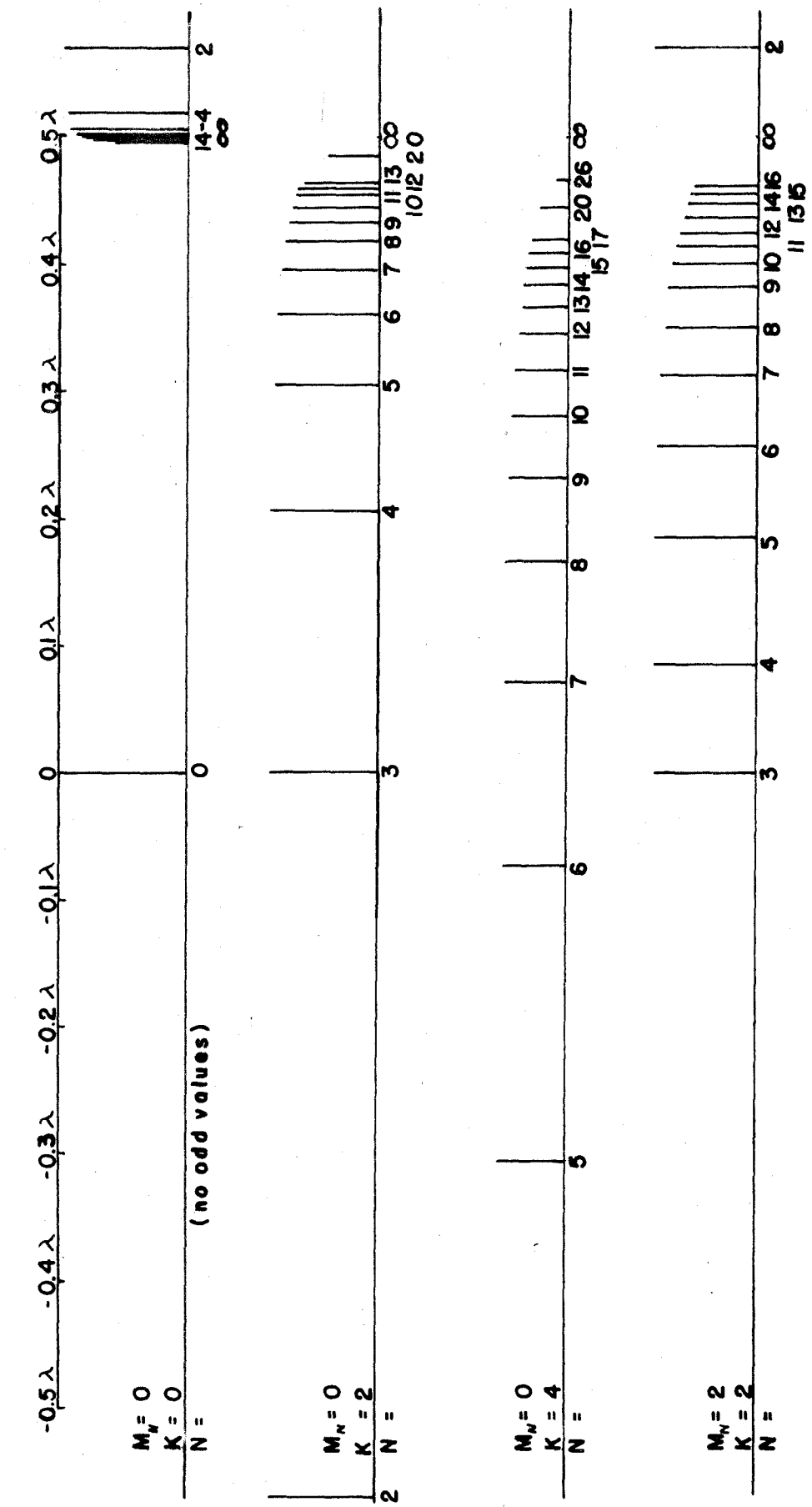

Fig. 2a.- Behavior of f_λ with respect to N, K and M_n. The height of the lines is a measure of the relative population of the various rotation levels.

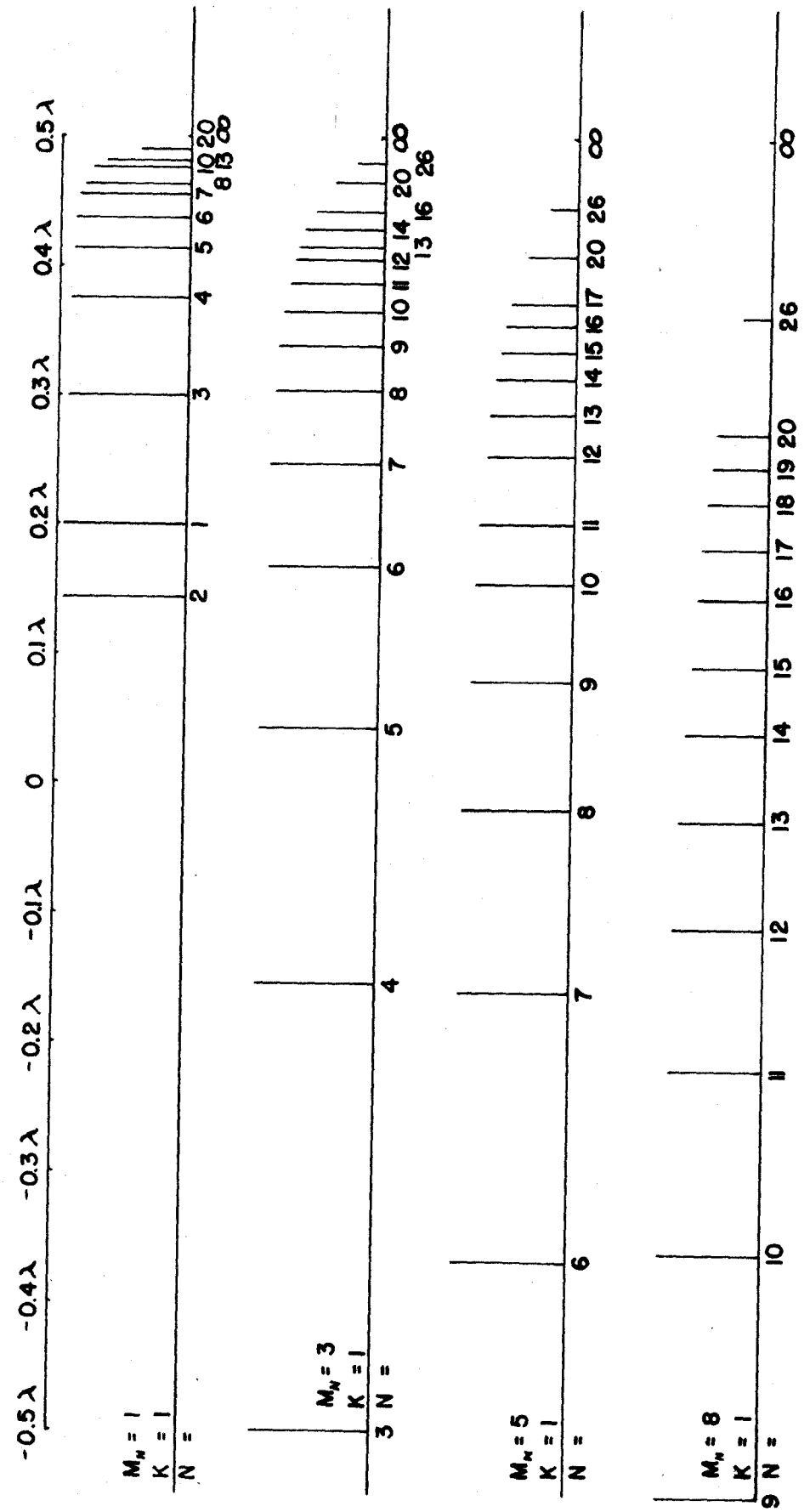

Fig. 2.- Behavior of f_λ with respect to N, K and M_N. The height of the lines is a measure of the relative population of the various rotation levels.

disposed about the symmetry axis, then all of the rotational energy levels which are antisymmetric with respect to C_{2v} are disallowed. Since NO_2 is a very near prolate symmetric top, the K = 0 levels will be missing for N odd. In terms of a symmetric top, the K levels, when they are allowed, are non-degenerate.

The values of f_λ have been sorted according to their M_N value. One notes that the main body of lines on the graph lie very close. This situation leads to the conclusion that a great number of energy levels will be nearly degenerate producing an overlap of spectral lines. This is to say that the individual transitions will not be observed, but, rather, groups of transitions appearing to have the same energy will produce single absorption lines. For example, consider the ability to resolve a line of 2 Mcps. half line width. This value of the half line width is approximately $0.2\,\lambda$. Referring to Figure II, one can see that the spectrum observed experimentally will consist of a superposition of many lines into "packets." One may also conclude from Figure II that for $M_N > 8$ (approximately) the intensity of any line (for $I_z = \pm 1$) will be very weak. As far as the $K = \pm 1$ states are concerned, an analysis of f_τ will reveal that it fast approaches a value of 0.25 for $M_N = 0$ with variations of N and decreasing ever increasingly (square law dependence) with increasing M_N. One would expect a spectral triplet about the energy $\bar{f}_\lambda \lambda$; where $\bar{f}_\lambda$ is an average f_λ for a given M_N value. The satellite lines will be of low intensity relative to the

central $|K| \neq 1$ state line. The separation between lines will be $\bar{f}_\tau \tau$; where $\bar{f}_\tau$ is the average f_τ for a given M_N value. It is not possible to estimate for what value these satellite lines will no longer be discernible. This is so since $\bar{f}_\tau$ decreases with increasing M_N resulting in the coalescing of the triplet and its subsequent resplitting. Also the intensity of the satellite lines decreases with increasing M_N.

One can estimate the isotropic coupling constant (the Fermi interaction) from theory using the calculated 2s character of the unpaired electron discussed earlier and the value of $|\psi(o)|^2$. Dousmanis (22) has given $|\psi(o)|^2$ for a 2s electron on nitrogen as 34×10^{24} cm^{-3}. $|\psi(o)|^2$ could have been calculated by setting the magnitude of the radius vector in a suitable wave function equal to about 0.01 Å (as noted earlier). Such a calculation has been made using a simple Slater function (26). The effective nuclear charge, Z^*, has been obtained by neglecting the 2p electrons. Using Slater's rules, one obtains $Z^* = 4.95$. After manipulating the wave function:

$$(37) \qquad |\psi(o)|^2 = \frac{1}{8\pi}\left(\frac{Z^*}{a_o}\right)^3 \quad ;$$

where a_o is the Bohr radius. Substituting the values for the symbols, one obtains $|\psi(o)|^2 = 32.8 \times 10^{24}$ cm^{-3} which bears a close resemblance to Dousmanis' value. Using Dousmanis' value one obtains a Fermi contact constant of 1620 Mcps for a 2s electron of nitrogen. With this value and the expected probability of finding the unpaired electron of

NO_2 in a 2s nitrogen orbit one expects $\sigma = 1620 \times 0.109 = 177$ Mcps.

It is felt that the spin-rotational coupling is too complex to estimate theoretically at this time. One requires more definite information concerning the molecule to carry through a computation. The various spin-rotation coupling constants will be left for experimental fit, if it is possible.

2. Line Shape and Width

The several factors governing the gas phase E.P.R. spectral line shape and width are of interest. Namely, in order of treatment, these factors are (3, 27):

1. Natural line width
2. Doppler effect
3. Spin-Lattice relaxation
4. Spin-Spin relaxation
5. Saturation.

1. Natural line width. The natural line width may be considered to arise from the Heisenberg uncertainty principle. In other words, since a molecule spends a finite length of time, Δt, in a given energy state, there results an uncertainty in the energy according to:

$$\Delta E \, \Delta t = h \, \Delta \nu \, \Delta t \approx h . \tag{38}$$

It has been shown that (3c, 27a):

$$(39) \qquad \Delta\nu = \frac{32\pi^3 \nu_o^3 |\mu_{mn}|^2}{3h} \quad \text{cps}$$

where $|\mu_{mn}|^2$ is the magnetic dipole matrix element. For the microwave range, the magnitude of the half line width due to the phenomenon is roughly 10^{-4} cps and is therefore of totally negligible consequence.

2. The Doppler Effect. The Doppler effect is the name given to the change in frequency that results when a molecule has a component of velocity in the direction of the propagation of the radiation (3d). The shift in resonant frequency is proportional to the zero molecular velocity resonant frequency multiplied by the rate of the molecular velocity component in the direction of the radiation propagation to the propagation velocity. The propagation velocity is approximately the velocity of light. The velocity distribution may be expressed as a Gaussian distribution. The intensity function, $I(\nu)$, is given by (27b):

$$(40) \qquad I(\nu) = I(\nu_o) \exp\left(- \frac{mc^2}{2kT} \frac{(\nu - \nu_o)^2}{\nu_o^2} \right) .$$

The Doppler effect line width for NO_2 at room temperature and for ν_o = 10 K Mcps (the K abbreviates kilo) is about 17 Kcps. The line width is defined as twice the half intensity half line width, $\Delta\nu$.

3. Spin-Lattice relaxation. Spin-Lattice relaxation is that process which produces an exchange of energy between the spin system and the surroundings (lattice). The terminology is that usually applied to N.M.R. and E.P.R. The relaxation proceeds with a characteristic time, T_1. There is no specific theoretical treatment available for gas phase E.P.R., but the problem of spin-lattice relaxation is well documented for the nuclear magnetic resonance counterpart. An excellent treatment is that of Saha and Das (28). No attempt at a rigorous treatment shall be attempted here, but, rather, a comparison will be made to the nuclear case.

The only mechanisms which are available for the exchange of energy from the spin system to the lattice in a gas are those involving the fluctuating magnetic fields produced by molecular motion and those involving changes in the rotational energy state. The latter is incorporated into the Hamiltonian as described above. It is apparent from the Hamiltonian that both mechanisms involve molecular motion. The expected line shape for this case is that of a damped harmonic oscillator or Lorentzian distribution:

$$(41) \qquad a = a_\nu{}^2 \left[\frac{\Delta\nu}{(\nu - \nu_o)^2 + \Delta\nu^2} + \frac{\Delta\nu}{(\nu + \nu_o)^2 + \Delta\nu^2} \right] \quad ;$$

where $\Delta\nu = (4\pi T_1)^{-1}$ and is the half intensity half line width (not the line width = $2\Delta\nu$). Equation 41 is due to Van Vleck and

Weisskopf (29). They have expressed the absorption, α, for a damped harmonic oscillator (actually treated for spectral pressure broadening in general) such that it obeys the limiting Debye case ($\nu_o = 0$). The second term in the bracket of equation 41 will not be of interest (see Appendix A). The differences between equation 41 and the original Lorentz line shape are (1) the sign modifying the second term in the bracket of equation 41, and (2) the factor of ν_o/ν missing in front of the bracket of equation 41. The differences arise from the assumptions made in the two treatments. Both were classical mechanical treatments requiring "strong" collisions (a collision which allows no retention of memory of the previous state or, alternately, a collision such that the duration of the collision is short compared to a precessional period). Lorentz assumed that the distribution after collision was random, whereas Van Vleck and Weisskopf required adiabaticity. Anderson (30) obtains an equation similar to that of the latter authors. Anderson's treatment, which is specifically derived for the effect of collisions on rotational energy states, is of interest here in order to predict the cross-sectional diameters for collision, b, and hence the mean times between collisions, τ, for the various rotational energy states. Anderson's theory considers not only the effect of adiabatic collisions which result in a change of phase, but also diabatic collisions, which account for collision induced transitions (energy exchanged between rotation and translational degrees of freedom). The theory is based on the usual

assumptions of a classical path and a short duration of collision with respect to τ defined above. The resultant equation (30):

$$(42)\quad \alpha = \alpha_o \nu^2 \left[\frac{\Delta\nu}{(\nu-\nu_o-a\Delta\nu)^2+\Delta\nu^2} + \frac{\Delta\nu}{(\nu+\nu_o+a\Delta\nu)^2+\Delta\nu^2} \right] ;$$

where a is a constant. This theory predicts a line shift which for the microwave region is usually negligible and is therefore dropped. The result is equation 41; however, in this case $\Delta\nu$ is $(2\pi\tau)^{-1}$ (the present interest is with respect to the rotational state perturbation due to collision). The beauty of Anderson's treatment manifests itself in the possibility of the theoretical calculation of τ and the effective cross-sectional diameter, b. The computation is, unfortunately, very difficult for a large number of situations encountered. For a dipolar interaction of the type:

$$(43)\quad \mathcal{H} = \left[\vec{\mu}_1 \cdot \vec{\mu}_2 - 3 \frac{(\vec{\mu}_1 \cdot \vec{r})(\vec{\mu}_2 \cdot \vec{r})}{r^2} \right] r^{-3} ;$$

one calculates (3e):

$$(44)\quad \Delta\nu = N v b^2 = \frac{4\pi\sqrt{2}\ N\ |\mu_1 K_1|}{3h\sqrt{N_1(N_1+1)}} \sum_{\mu_2 K_2 N_2} \frac{|\mu_2 K_2|}{\sqrt{N_2(N_2+1)}}\ f_{N_2 K_2 \mu_2} ;$$

where N is the number of molecules per cubic centimeter; μ_i is the dipole moment for molecule i; $f_{N_2 K_2 \mu_2}$ is the fraction of molecules having dipole moment μ_2 and quantum numbers N_2 and K_2; v is the

mean molecular velocity. For collisions between NO_2 molecules, $\mu_1 = \mu_2 = 0.3$ debye (31a):

$$(45) \quad \Delta\nu = \frac{4\pi\sqrt{2}\, N \mu^2}{3h} \frac{|K_1|}{\sqrt{N_1(N_1+1)}} \sum_{N_2 K_2} \frac{|K_2|}{\sqrt{N_2(N_2+1)}} \; f_{N_2 K_2} \; .$$

For NO_2, $v = [\, 3RT/M_{NO_2} \,]^{1/2}_{T=300°K} = 4.0 \times 10^4$ cm/sec:

$$(46) \quad b = 6.35 \times 10^{-8} \text{cm} \left[\frac{|K_1|}{\sqrt{N_1(N_1+1)}} \sum_{N_2 K_2} \frac{|K_2|}{\sqrt{N_2(N_2+1)}} \; f_{N_2 K_2} \right]^{1/2} .$$

One readily surmises that 6.35×10^{-8} cm is the maximum b predicted on the basis of this interaction. There is another effect which could increase b. This involves what is termed a "rotational resonance collision." However, since for NO_2 the dipole moment is small and the partition function large (the probability that a molecule with N differing by ± 1, the necessary condition for collisional rotation resonance, colliding with a given molecule being small), this effect is expected to be of little consequence (3e). There is a factor, however, which tends to offset this argument, namely, that when the duration of collision is small compared to the reciprocal of the rotational frequency, the molecule does not have time to find out what state the colliding molecule is in and can therefore undergo a pseudo-resonant collision. For molecules other than NO_2 colliding with NO_2, this effect is not operative

(except for an accidental degeneracy of rotational energy states such that the molecule colliding with NO_2 apparently fulfills the necessary requirement (mentioned above). Most molecules which one would mix physically with NO_2 (those which do not react) have dipole moments which in general are smaller than that of NO_2 and would therefore exhibit a smaller collision diameter than NO_2 as the colliding molecule. For a non-polar molecule, the interaction may involve an electric quadrupole, an induced dipole, etc.

The other type of interaction involved in a collision, that is of interest, is that of a magnetic dipole interaction. This interaction may be shown to require very small collision diameters. In fact, the collision diameter required would be much smaller than the effective size of the molecule concerned. If one considers the electron to be distributed over the molecule, the magnetic interaction would be effective at a distance of the order of the "hard sphere" collision diameter. This is only true where the colliding molecule has a resultant electron magnetic moment. This interaction would just make the close collisions "stronger."

From the previous discussion, one may recall that there were terms which were dropped because the selection rules $\Delta N = \Delta K = \Delta M_N = 0$ were imposed. In a collision, these restrictions are lifted. Since the interaction Hamiltonian during a collision may involve terms which

mix the spin states, a mechanism is provided by which energy may be exchanged between the spin system and the lattice. The result is:

$$(47) \qquad \left(\frac{1}{2T_1}\right) = \left(g|\beta|H_{SR}\right)^2 \frac{N(N+1)}{3} \frac{\tau}{1+(2\pi\nu_o\tau)^2}$$

for the spin-rotation energy, where H_{SR} is the magnetic field associated with the interaction. The field, H_{SR}, is the magnetic field at the electron produced by the rotation and is approximately $\frac{\kappa M_N}{2g|\beta|}$ from equation 24. The spin-spin interaction is the only other interaction which is present to produce mixing. The Fermi interaction requires very strong collisions since it is rotational energy state independent. At high pressures, this interaction can add a possibly discernible contribution. As for the magnetic dipole-dipole type of $\mathcal{H}_{SI}$, one expects only a small contribution due to its small value. Since it is much more difficult to treat, it shall be neglected.

Therefore, on the basis of the spin-lattice interaction, one would expect a Lorentz line shape and a collision diameter of about 6 Å. Since $2\pi\nu_o$ is about 6×10^{10} radians/second, one may show that the one in the denominator of equation 47 may be neglected for all τ greater than approximately $10 \times \frac{1}{2\pi\nu_o}$ or 1.7×10^{-10} sec. Finally, one can see that the relaxation will be rotation state dependent, the greater relaxation occurring for the higher N states.

4. Spin-Spin relaxation. For electron magnetic resonance there is virtually no relaxation due to this mechanism, except in certain cases not of interest here. The reason for this is that the electron is smeared out over the total molecule or can be considered to assume all positions within the molecule in a time very short compared to the precessional frequency. The effect observed experimentally is an average over the molecule and an average over orientation; the result is zero contribution to the line width.

5. Saturation. Saturation occurs when a non-equilibrium condition is produced by excessive radiation. More specifically, it is a term used to describe the situation which occurs when the rate of transition exceeds the rate of relaxation. This process disturbs the equilibrium population of the energy levels with the result that the population difference between the upper and lower energy state equalizes so that there is a zero net absorption of energy. The spectral intensity with the saturation term included is (3f):

$$(48)\quad I(\nu) = I(\nu_o)\,\frac{1/2\pi\tau}{(\nu-\nu_o)^2+(1/2\pi\tau)^2+[8\pi^2 T_1|\mu_{mn}|^2 \nu I_o 2\pi\tau/3ch](1/2\pi\tau)^2}$$

where I_o is the microwave radiation intensity (in units of quanta per unit cross-sectional area); T_1 is the lifetime with respect to electron spin transition by collision; τ the mean time between collisions. I_o

is related to the incident power per unit cross-sectional area, P; $\hbar \nu I_o = P$. T_1 is related to τ, ν_o and an interaction constant as shown above.

C. EXPERIMENTAL

The NO_2 that was used in this research was supplied by Olin Matheson Co. (cylinder #AP4167). To assure purity, the NO_2 was processed in the following manner. See figure A. NO_2 from the cylinder was condensed into the initial tube. This tube was transferred to a vacuum system. Oxygen was passed over the liquid, which was kept at about 0°C, to oxidize the lower valence state nitrogen oxides to NO_2. The resultant gas mixture flowed through a drying tube which contained P_2O_5 which was deposited on 4 millimeter glass beads in order to permit a free flow of the gas mixture. The NO_2 was frozen out from the oxygen in a carbon dioxide cold trap of commercial design. A trap that consists of a u-tube section is felt to be a better design for this operation since it allows better thermal contact. The system was then evacuated. The NO_2 was allowed to warm up in an isolated section and was then refrozen. The system was again pumped out and the procedure was repeated. A vacuum distillation was next performed. The NO_2 was frozen in the tube it originated from (on the other side of the drying tube) and a second vacuum distillation was performed through the drying tube. The first and last 10% of the NO_2 was discarded and the distillate was collected in a reservoir tube. The reservoir tube was removed under reduced pressure from this apparatus and placed on the manifold of a high vacuum line. See figure B.

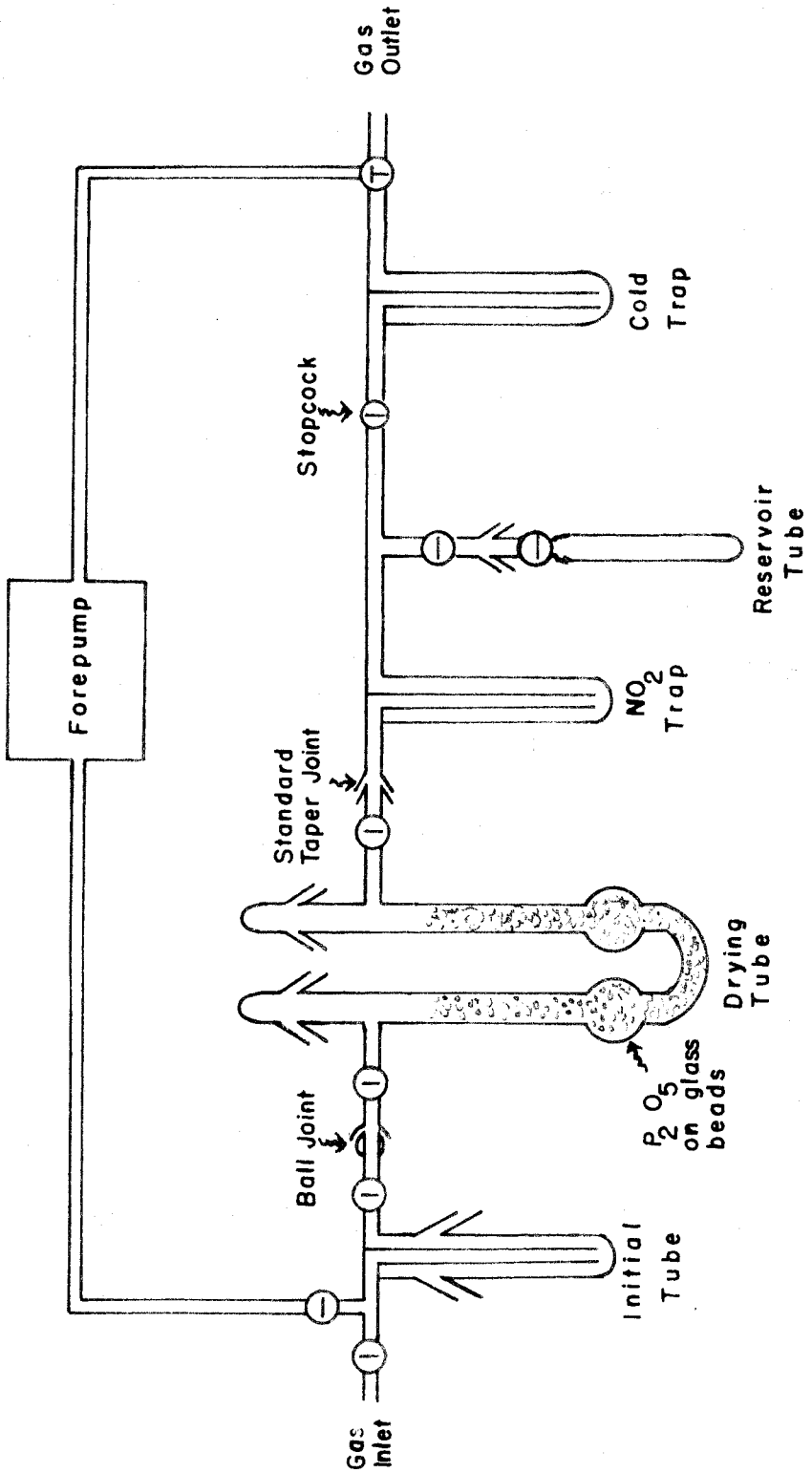

Figure A. Diagram of purification apparatus.

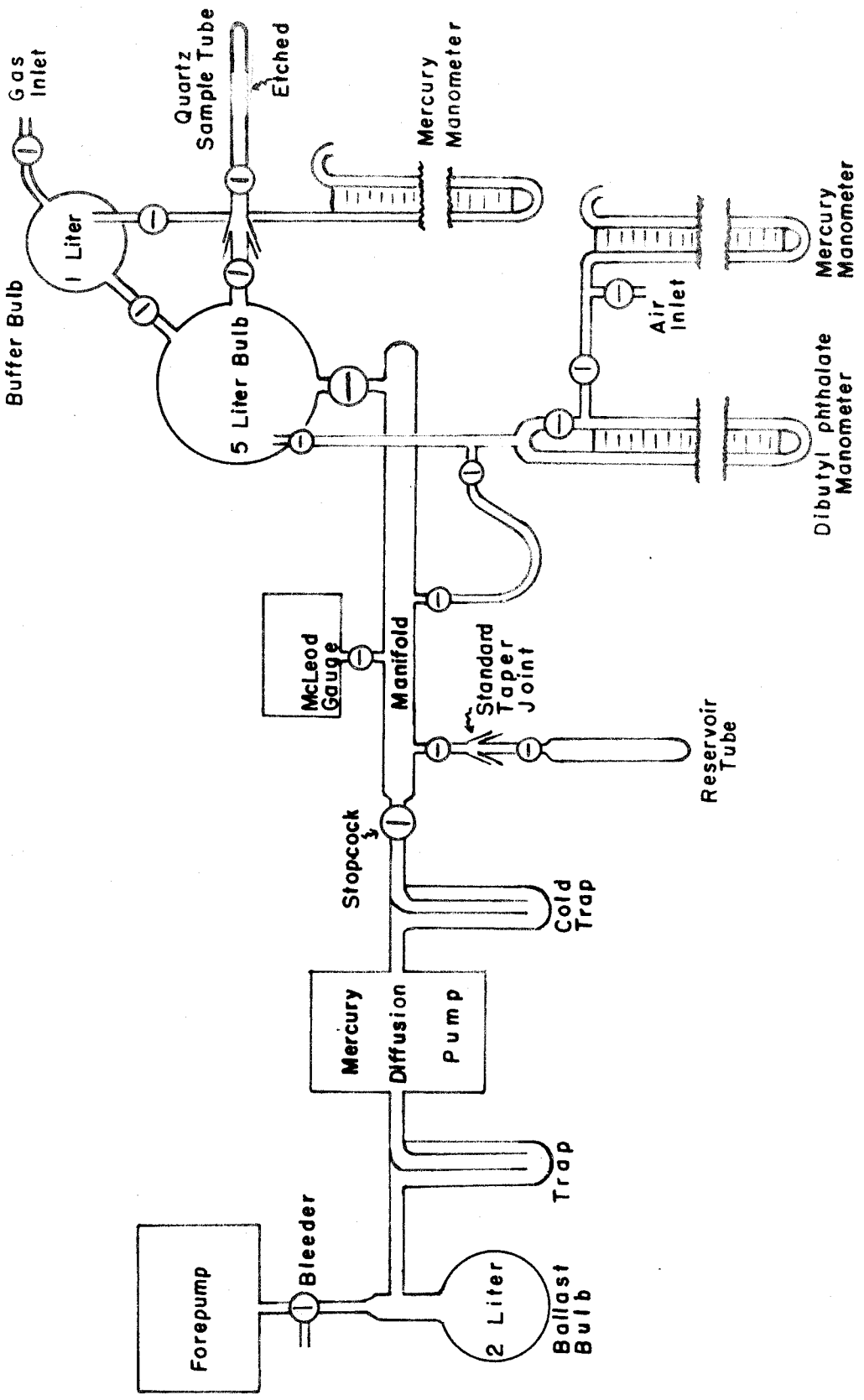

Figure B. Diagram of sample preparation apparatus.

The high vacuum line was of standard design. It had the usual accoutrements of forepump, line bleeder, ballast bulb, mercury trap, mercury diffusion pumps (2 stages), cold trap, manifold and low pressure gauge (McLeod type). The special components which were provided for the preparation of samples were centered about a five liter bulb which was connected through a large bore stopcock to the manifold. A tube led from this bulb to a smaller bulb which had an inlet for a gas from a cylinder and a u-tube mercury manometer for measuring that gas' pressure connected to it. Another tube led from the large bulb through a 10 millimeter bore stopcock to a detachable sample tube (described below). A third tube led to an isolatable manometer system. This manometer system was comprised of two manometers. The first in line from the bulb was a low density fluid u-tube manometer. The fluid used was dibutyl phthalate which was chosen because it is essentially inert to NO_2, it is fairly easy to handle, and it has a very low vapor pressure. The two arms of this manometer were connected by a stopcock. A tube situated on the bulb side was connected through a stopcock to the manifold. This was provided so that the manometer fluid could be degassed. The degassing took place at a temperature for which the vapor pressure of the fluid was fairly high. No trouble was encountered in the measurement of pressures when this precaution was observed.

A tube, attached on the side away from the bulb, led through a stopcock to a "tee" joint. One arm of the joint was connected to a mercury manometer and the other was isolated from the atmosphere by a stopcock. One may see that by this scheme the NO_2 need not come into contact with the mercury. For low pressure samples, the first manometer was used alone. For those pressures higher than the low density manometer could handle, the two were used jointly. This involved leaking air into the section between the manometers and reading the resultant pressure differences on both. By the appropriate normalization to mercury density and subsequent combination of the differences one obtained the pressure.

The preparation of samples proceeded as follows. The first method was that of direct pressure adjustment. The other method, which was faster, involved the isolating of a known pressure of NO_2 in the sample tube (also used as a sample). Then the large bulb was filled with nitrogen to the desired sample pressure, which was lower than that of the sample tube, and finally the sample tube was opened for a very short length of time. The time allowed was felt long enough for pressure equalization but short enough so that back diffusion would be of no consequence. Since the volume of the sample tube was only 20 millileters, the amount of NO_2 released into the bulb was negligible. The samples containing a diluent gas were prepared in an analogous way to this latter procedure. Instead of using nitrogen, any gas of

interest was used. Also, the pressure of this gas was adjusted to be greater than the NO_2 pressure in the sample tube. A small correction had to be applied to the pressure of the NO_2, since the NO_2 gas in the stopcock bore was added to the NO_2 gas in the sample tube when the diluent gas was added. The pressure of the diluent gas was just the difference between the gas pressure before addition less the corrected NO_2 pressure.

The sample tube consisted of an 8-inch section of 12-millimeter inside diameter quartz tubing that was sealed off at one end, etched for 2 inches length on the inside diameter and connected through a graded seal to an 8-millimeter bore high vacuum stopcock. The wall thickness of the etched section was 0.65 millimeters in comparison to an initial 1.4 millimeters wall thickness. This treatment increased the volume in the etched portion by 26% and decreased the amount of dielectric container material by about a factor of 2. There are three reasons to use quartz instead of pyrex. First, pyrex is of poor homogeneity in constitution which would produce an uneven etch and perhaps even result in the formation of pinholes. Secondly, pyrex has a higher dielectric constant than quartz and would cause the microwave cavity to exhibit a lower Q than would the quartz. The Q-factor (quality factor or figure of merit) is defined as 2π times the incident electromagnetic energy divided by the energy lost. This Q-factor lowering would produce a decrease in the absolute sensitivity. Finally, pyrex

is paramagnetic by virtue of impurities. It exhibits a magnetic resonance absorption at $g \approx 4$ which has a very large line width. This would produce a skewed base line which would make the analysis of the line shape more difficult.

The stopcock grease that was used in this research was Kel-F. This proved a good choice since it is sufficiently inert to NO_2. However, it is necessary to observe the precaution of periodically refurbishing the grease, since it has the undesirable property of flowing.

The E.P.R. spectra were obtained using a Varian Associates V-4500 X-band E.P.R. spectrometer (with modifications as noted below) in conjunction with a Varian Associates 6-inch magnet and its associated power supply. Part of the research was carried out using the standard Varian setup with 400 cps modulation. A rectangular TE_{102} mode cavity with the dimensions: a = 0.900 inch, b = 0.750 inch, and c = 1.700 inch was employed. The remainder of the spectra were observed using 100 kcps modulation. The equipment necessary was homemade and of standard design. The crystal current was fed into a tuned preamplifier which then was sent through a tuned phase sensitive detector with a cathode follower output. The resultant signal was recorded on a commercial Brown Recording Potentiometer. The cavity used for this work was a cylindrical TE_{011} mode type with an inner diameter of 1.843 inch and a length of 1.010 inch. The sample tube was axially situated and the coupling into the cavity was through

a centrally located hole in the surface of the cylinder. Both cavities were furnished with 16-millimeter inside diameter side arms to support the sample tube.

The spectra of NO_2 at a pressure greater than about 3 millimeters mercury were recorded with a time constant of no greater than 1 second and scan rates of approximately 50 gauss per minute and 80 gauss per minute. The spectra of the lower pressure NO_2 were observed at a maximum time constant of three seconds and scan rates four times slower than the above.

The calibration of the magnetic field scan was effected through the observation, before and after a group of NO_2 spectra, of the spectrum arising from the absorption of radiation by the electron spin system of $^{55}Mn^{++}$. The sample used was a dilute solution in water of $MnSO_4$. For this isotope of Mn, $I = 5/2$. Since the ground state of Mn^{++} is ^6S, there is no first order orbital contribution. With these considerations, one would predict that a six line spectrum with $g = 2$ would be produced. The splittings may be calculated according to the equation supplied in the work of Bleaney and Ingram (32):

$$(49) \qquad H^* = H_o - Am - A^2/(2H_o)[I(I+1) - m^2 - 2m(2M-1)] .$$

H^* is the value of the magnetic field at the center of a line; H_o is the unperturbed magnetic field value for $g = 2$; $A = -95$ gauss is the coupling

parameter (other values for A exist, for example, A = -96.5 gauss (33), the error introduced is small and essentially constant); m and M are the nuclear magnetic and electron magnetic (respectively) quantum numbers in the external field direction. The values of M and m are:

(50) $M = -3/2, \ldots, 5/2 \; ; \quad m = -5/2, \ldots, 5/2 \; .$

The term in (2M-1) produces a broadening but no displacement of each of the six lines. For H_o = 3400 gauss, the values of $\Delta H_m = H^*_m - H^*_{m-1}$ are:

(51)
$$\begin{aligned} \Delta H_{5/2} &= 100.5 \text{ gauss} \\ \Delta H_{3/2} &= 97.5 \quad '' \\ \Delta H_{1/2} &= 95 \quad '' \\ \Delta H_{-1/2} &= 92.5 \quad '' \\ \Delta H_{-3/2} &= 89.5 \quad '' \end{aligned}$$

D. RESULTS

The E.P.R. spectrum of NO_2 in the gas phase exhibits a marked pressure dependence. Qualitatively, one notes at pressures of three millimeters of mercury and less, the many lines which are expected from considerations discussed in Section IIA. An increase in pressure results in the broadening of the component lines. As this broadening increases, an increased intensity is observed in the central portion of the spectrum, especially in three specific spectral regions. With further increase in pressure, the outer spectral components fade and a triplet emerges in the central portion at the positions of the above described intensity enhancement. The components of the triplet continue to broaden with pressure increase. At about 40 millimeters of mercury, the last evidence of the triplet structure fast disappears and a single line remains at the position previously occupied by the central line of the triplet. The singlet continues to broaden with further increase in pressure.

Before considering the data in detail, a digression shall be made in order to explain the calculation of the partial pressures of NO_2 and N_2O_4 which are in equilibrium with each other. Verhoek and Daniels (34) have investigated the NO_2-N_2O_4 equilibrium. They arrived at the

following expression for the gas phase equilibrium constant:

$$(52) \qquad K_e = a + b\, C^{o}_{N_2O_4} = P^{2}_{NO_2}/P_{N_2O_4} \,.$$

$C^{o}_{N_2O_4}$ is equal to the total number of moles per liter of N(IV) oxides present expressed as N_2O_4. In solving equation 52 for P_{NO_2} in terms of experimentally measurable or known quantities, the following relations are used:

$$(53) \quad (a) \qquad P_T = P_{NO_2} + P_{N_2O_4}$$

$$(b) \qquad C^{o}_{N_2O_4} = C_{N_2O_4} + \frac{1}{2}\, C_{NO_2} = (2\,P_T - P_{NO_2})/2\,RT \,.$$

Rearranging equation 52 and solving for NO_2 by use of the binomial theorem:

$$(54) \qquad P_{NO_2} = (2 - b/RT)^{-1}\left(-[a+(3bP_T/2RT)] + [\,(a+[3bP_T/2RT])^2 + 4(1-[b/2RT])\times(a+[bP_T/RT])P_T\,]^{1/2} \right).$$

Verhoek and Daniels obtained an average value for $\Delta H = 14.6$ kilocalories/mole. K_e is rewritten:

$$(55) \qquad K_e = (a_o + b_o\, C^{o}_{N_2O_4})\, \exp(-\Delta H/RT).$$

Substituting known values for a and b at T, one calculates:

(56) $a_o = 8.54 \times 10^9$ atm ; $b_o = 1.58 \times 10^{10}$ atm/mole/liter .

By using equations 55 and 52 along with the values for the temperature independent constants, the values of a and b may be computed for the experimental temperature, namely, T = 300°K. The partial pressure of NO_2 may now be calculated for a given P_T from equation 54. Likewise, the partial pressure of N_2O_4 may be obtained from equation 53a.

The data of interest include the various pressures, the difference in frequency between the points of maximum and minimum deflection of the first derivative of the absorption spectrum which is designated as $\Delta\nu_e$, the absolute value of the ratio of the maximum slope of the first derivative curve between the maximum and minimum deflection to the maximum slope external of the extrema which is designated as R and the number and, where possible, the separation of the lines. The data for NO_2 in the absence of a diluent gas (N_2O_4 is always present in these investigations) is presented in Table I. Likewise, tabulated in Table II are the results of the series of experiments on NO_2 in the presence of a diluent gas. The gases chosen as diluents are He, A, N_2 and O_2. Included in the presentation of data in Tables I and II is the number of spectra averaged.

The merging of the spectral lines into a singlet causes one to question the possibility of interpretation. However, the values of R

TABLE I

Pressure		Number of Spectra	Average $\Delta\nu_e$	Average R	Number of Lines Observed
Total (mm Hg)	NO_2 (mm Hg)	Averaged	(Mcps)		
0.65	0.65				many
1.00	1.0				"
1.38	≈ 1.3				"
1.68	≈ 1.6				"
1.99	≈ 1.9				"
2.30	≈ 2.3				"
2.51	≈ 2.5				"
3.86	≈ 3.8				3 main, many small
6.83	6.5	11	348	3.72	3+
7.30	6.8				3+
12.8	11.5	11	354	2.32	3
19.4	16.9	10	385	2.66	3
32.4	26.6	9	401	2.38	3 ⇉ 1
40.0	31.9	13	405	2.19	3 ⇉ 1
42.4	33.9	14	413	2.31	≈ 1
45.3	35.4	25	412	2.42	≈ 1
55.5	42.2	11	427	2.03	1
77.4	54.0	14	459	2.48	1
90.5	61.0	7	450	2.73	1
95.5	63.6	10	460	2.87	1
103.3	68.5	7	435(?)	2.23	1
108.3	70.0	7	465	3.05	1
133.4	81.9	7	486	3.01	1
143.1	86.1	10	503	3.16	1
171.3	99.7	7	523	3.34	1
182.9	102.7	10	528	3.34	1
256.5	128.9	10	567	3.52	1
302.2	144.4	10	591	3.52	1
384.7	170.2	11	629	3.55	1
525.8	212.0	10	682	3.72	1
990	372	2	875	3.82	1

TABLE IIa

NO_2-N_2O_4	Pressure Total (mm Hg)	Pressure A	Number of Spectra Averaged	Average $\Delta\nu_e$ (Mcps)	Average R
94.8	129.3	34.5	7	476	2.97
↓	149.1	54.3	8	484	3.01
	166.6	71.8	7	491	3.10
	187.4	92.6	7	500	3.02
	208.6	113.8	7	507	3.41
	246.8	152.0	7	522	3.31
	287.1	192.3	7	529	3.42
	326.3	231.5	7	554	3.17
	364.9	270.1	7	560	3.22
	404.5	309.7	7	565	3.18
	451.2	356.4	7	570	3.35
	500.6	405.8	7	577	3.32
	548.7	453.9	7	585	3.33
	599.7	504.9	7	583	3.48
	647.9	553.1	7	595	3.51
	695.9	611.1	7	602	3.58
	745.7	650.9	7	613	3.68
113.4	129.2	15.8	7	477	3.09
↓	148.6	35.2	7	482	3.16
	168.8	55.4	7	489	3.23
	187.9	74.5	7	506	3.23
	208.6	95.2	7	522	4.03(?)
	247.3	133.9	7	526	3.24
	286.9	173.5	10	543	3.20
	325.7	212.3	7	559	3.15
	364.9	251.5	7	565	3.37
	403.8	290.4	7	570	3.63
	452.3	338.9	7	577	3.19
	501.1	387.7	7	-	3.24
	549.8	436.4	7	568	3.55
	597.5	484.1	7	585	3.26
	645.0	531.6	7	610	3.72
	694.5	581.1	7	620	3.50
	745.0	631.6	7	630	3.42

TABLE IIb

NO_2-N_2O_4	Pressure Total (mm Hg)	Pressure Argon	Number of Spectra Averaged	Average $\Delta\nu_e$ (Mcps)	Average R
36.7	81.0	33.6	7	424	2.24
↓	129.8	82.4	8	447	2.43
	176.7	129.3	7	477	2.80
	217.7	170.3	6	530	2.77
	294.9	247.5	7	518	3.05
	373.5	326.1	7	549	2.38
	452.5	405.1	7	542	3.30
	556.6	509.2	6	578	2.67
	643.5	596.1	7	605	2.65
	742.0	694.6	7	613	2.92
69.8	116.7	8.6	7	452	2.69
↓	170.4	62.3	6	478	2.77
	217.3	109.2	7	508	2.87
	296.4	188.3	7	534	3.01
	374.1	266.0	6	553	2.50
	451.4	343.3	7	598	3.08
	564.8	456.7	7	597	3.02
	643.5	535.4	7	588	3.08
	742.9	634.8	7	625	3.06
84.5	536.5	396.7	7	589	3.43
↓	740.6	600.8	8	611	3.10
101.4	540.3	360.6	5	602	3.60
↓	739.8	560.1	8	624	3.04

TABLE IIc

Pressure(mm Hg) NO_2-N_2O_4	Total	Helium	Number of Spectra Averaged	Average $\Delta\nu_e$ (Mcps)	Average R
33.3	70.7	28.8	7	413	2.12
↓	129.7	87.8	7	468	2.24
	179.0	137.1	7	452	2.28
	251.5	209.6	6	450	2.70
	328.4	286.5	6	483	2.81
	396.4	354.3	6	485	2.66
	497.2	455.4	7	489	3.05
	642.3	600.5	7	520	3.12
	744.1	702.3	8	545	3.36
	945.1	903.9	7	547	3.21
		Oxygen			
33.4	87.6	45.5	7	453	2.35
↓	134.5	92.4	11	492	2.68
	251.2	209.1	7	585	2.81(?)
	490.2	448.1	-	672(?)	(4.41)(?)
	753.8	711.7	-	?	?
		Nitrogen			
36.8	74.8	27.1	7	430	2.28
↓	124.4	76.7	8	455	2.39
	202.8	155.1	7	497	2.64
	310.6	262.9	7	531	2.99
	494.7	447.0	7	594	3.35
	750.2	702.5	7	608	2.88
	958.2	910.5		695	3.66

at low pressures and very high pressures indicate almost a "pure" Lorentzian line shape. This is true since it may be shown that for a Lorentzian line shape, R = 4.0; while for a Gaussian line shape, R = 2.2. It was therefore assumed that the discrepancy in the values of R is the result of the overlap of the spectral lines. Appendix A contains a theoretical treatment of the progressive overlap of three Lorentzian lines. The equation used in the analysis was (29):

$$(57)\quad \frac{d\alpha}{d\nu} = \frac{8\pi^3 N}{18\, ckT}\,|\mu|^2\left(2\nu\,\Delta\nu\,\Sigma_i\left[\frac{1}{(\nu_i-\nu)^2+\Delta\nu^2}+\frac{\nu(\nu_i-\nu)}{((\nu_i-\nu)^2+\Delta\nu^2)^2}\right]\right).$$

Figure 3 contains a plot of $\Delta\nu_e$ derived from the calculated spectra versus the half line width, $\Delta\nu$. By a comparison of the experimentally derived values of $\Delta\nu_e$ with the calculated values of $\Delta\nu_e$, the value of $\Delta\nu$ for the experimental conditions was obtained. Figure 4 shows the dependence of $\Delta\nu$ on the total pressure.

In order to justify the use of the combination of three Lorentzian lines, a plot of $\Delta\nu$ as a function of R, the calculated spectra is presented in Figure 5. Included on the graph are the experimental values of the no diluent series. The agreement appears poor, however the general contour is well preserved. An unfortunate experimental circumstance has caused the apparent disagreement. Namely, the presence of oxygen in the microwave cavity as a constituent of air and at atmospheric pressure produces a baseline which is not constant. The effect

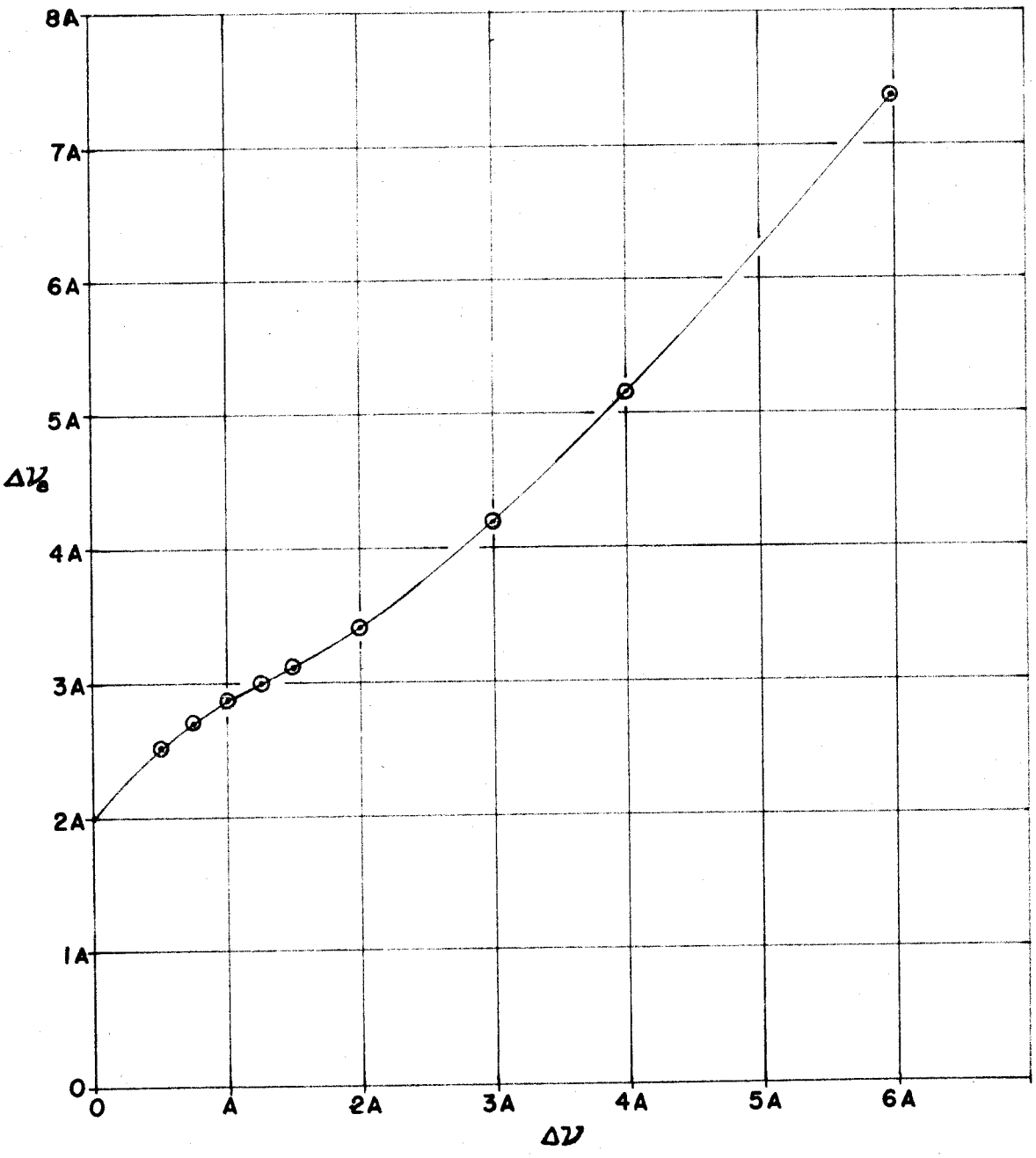

Fig. 3. - The calculated frequency difference between the maximum and minimum deflections of the first derivative of the absorption, $\Delta\nu_e$, as a function of the half line width, $\Delta\nu$, each measured in terms of an adjustable parameter, A, which is equal to the line separation between adjacent lines of the triplet.

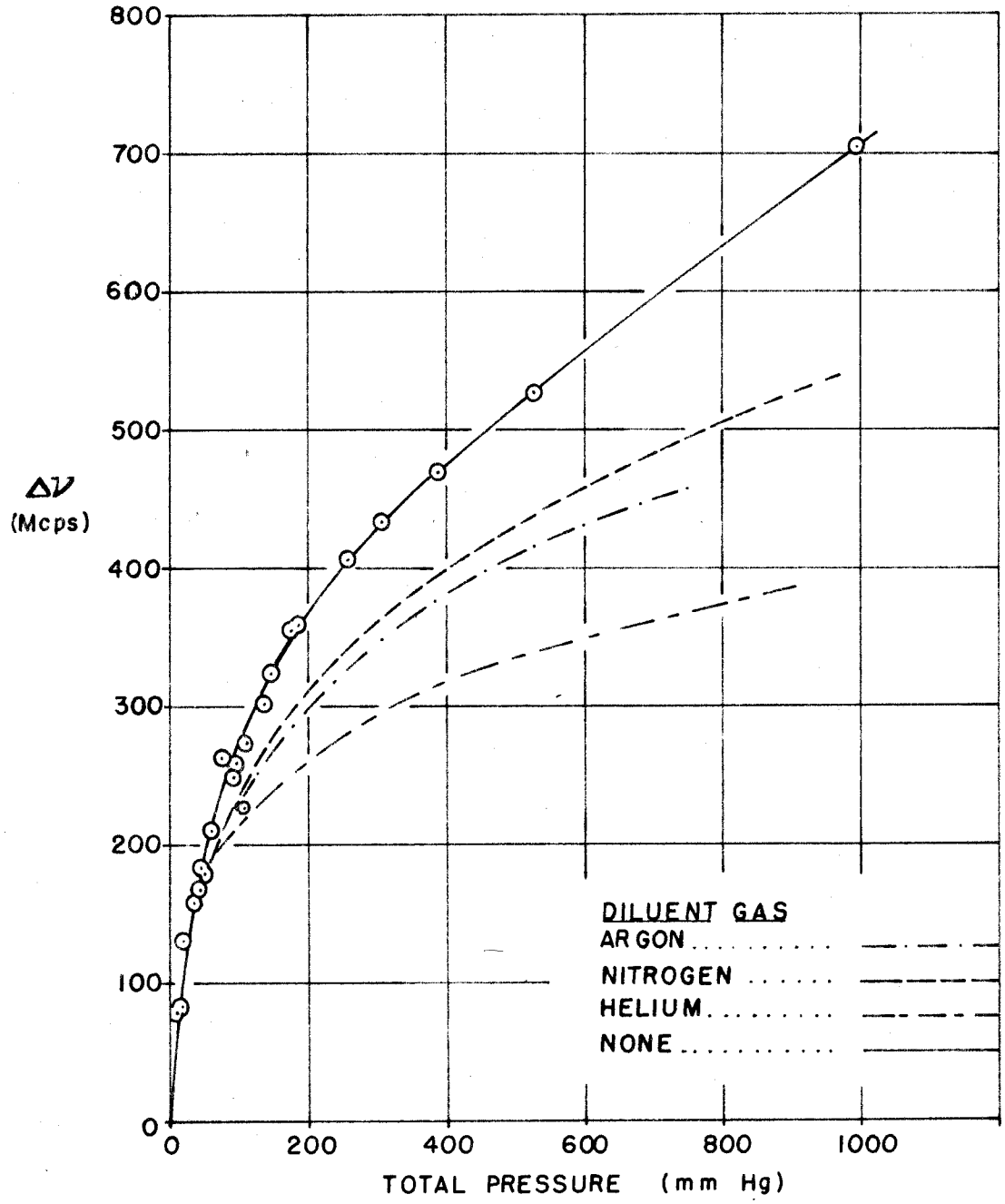

Fig. 4. - Plot of the dependence of the half line width, $\Delta\nu$, as a function of the total pressure of NO_2, N_2O_4 and diluent gas.

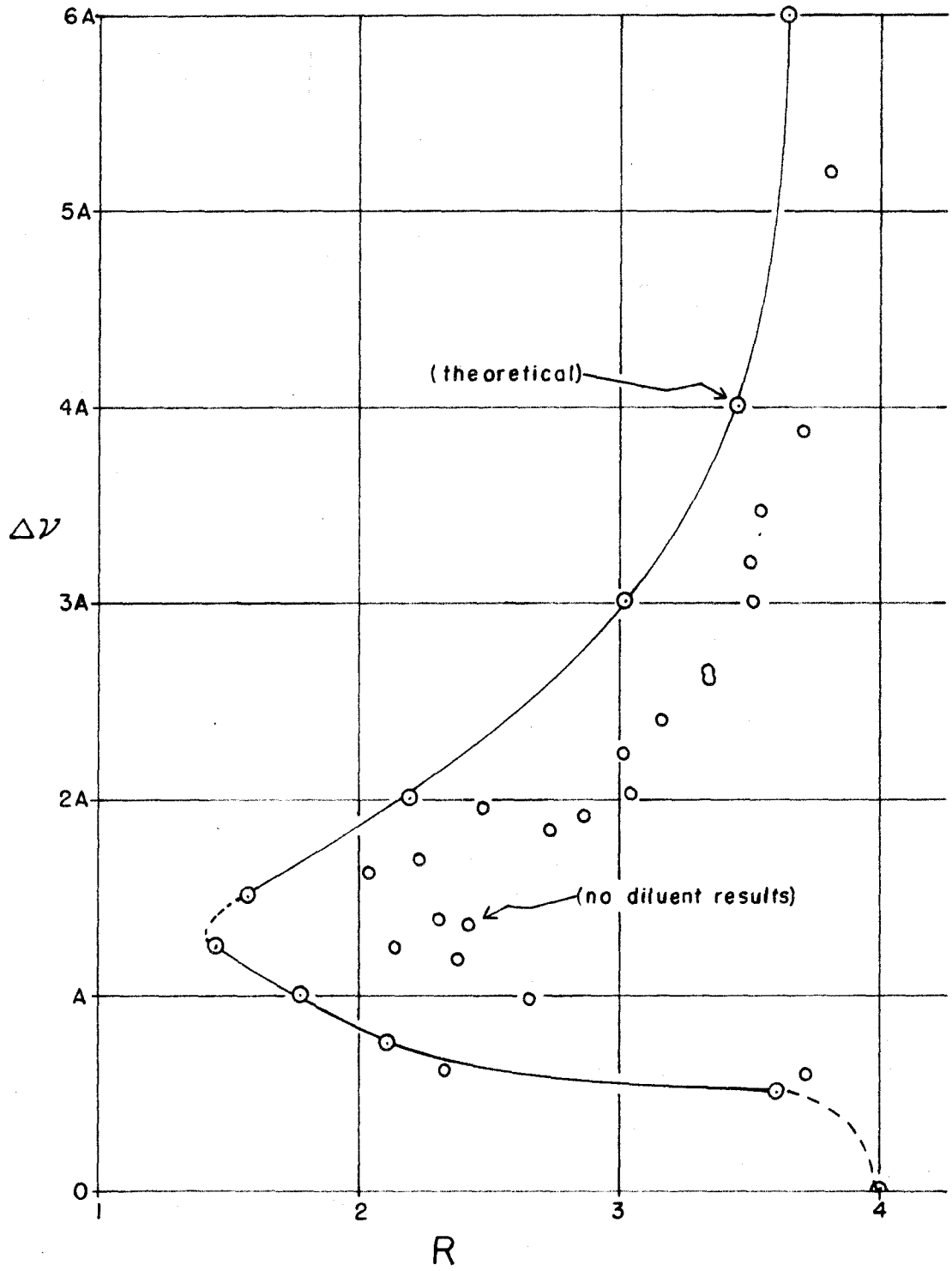

Fig. 5. - Plot of the relation between the half line width, $\Delta\nu$, expressed in terms of the line separation, A, and the slope ratio, R.

of the oxygen absorption on the NO_2 spectrum is dramatically demonstrated by the spectrum of NO_2 at a partial pressure of 42 millimeters of mercury and diluted by oxygen with a partial pressure of 711 millimeters of mercury as shown in Figure 6. It is not obvious from the spectrum that two absorptions are present, but a faster and more extended sweep would indicate that the two absorptions were superimposed. The oxygen absorption is much broader than that of NO_2. One can readily surmise from Figure 6 that the presence of oxygen will produce a baseline that will change the magnitude of R towards larger values. Returning to Figure 5, one notes that all of the experimental points lie towards higher R just as is expected for the explanation that is offered. The conclusion is, therefore, that the method presented here, namely, that of the coalescing of three Lorentzian lines with increasing half line width, is a logical and satisfactory choice.

For one's edification, sample spectra are presented in Figures 7, 9, 10, 12, 16, 18. Accompanying these figures are spectra calculated according to the above procedure (see Figures 8, 11, 13, 14, 15, 17). Figures 7-18 are ordered in a manner which facilitates the comparison between experiment and theory. Figure 19 contains two spectra which show various stages of resolution of the many lines present in Figure 20 due to the discussed interactions. Figure 20 also contains a calculated spectrum which will be discussed later.

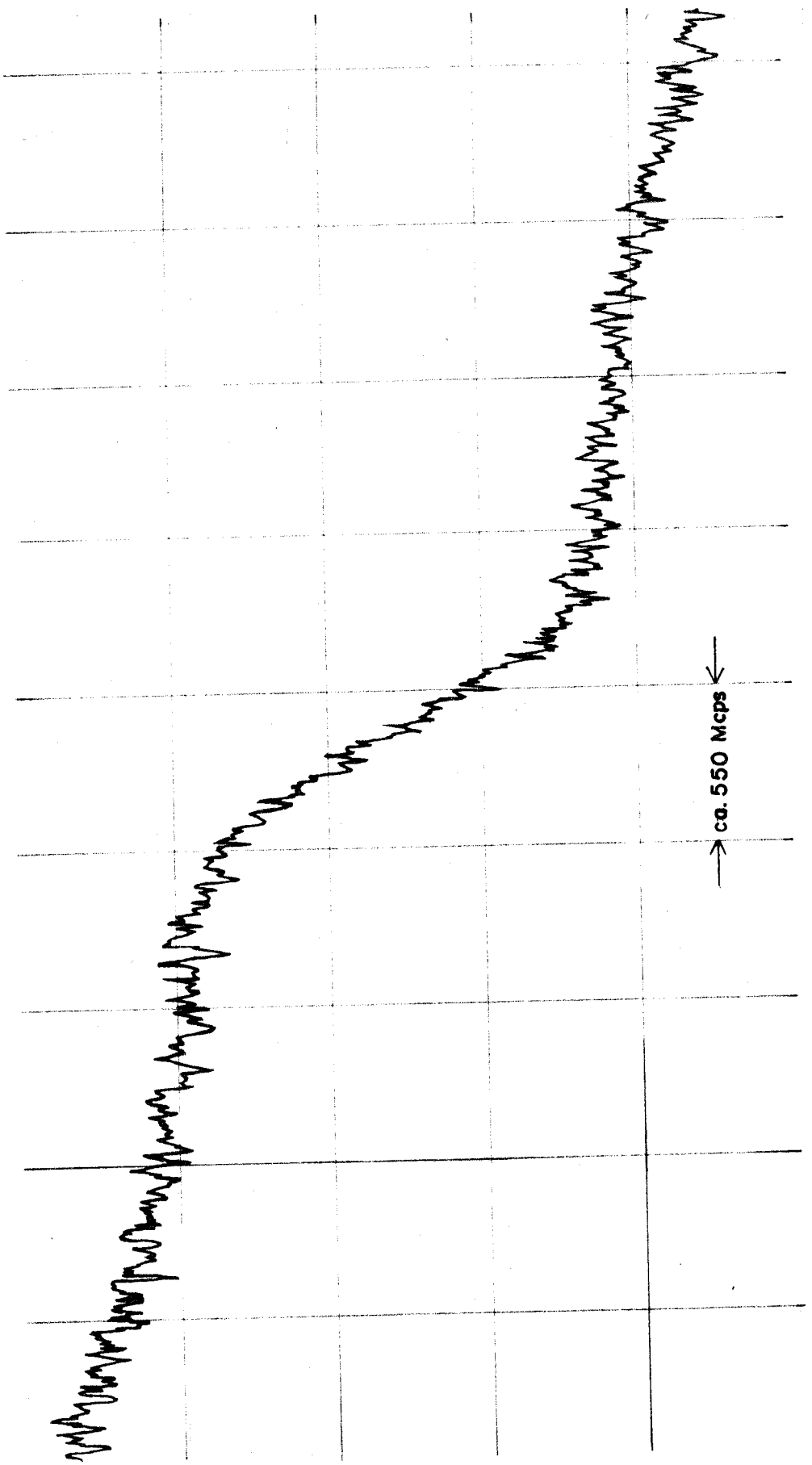

Fig. 6.- Trace of the E.P.R. spectrum obtained from a sample containing 42 mm Hg pressure of NO_2 and N_2O_4 and 711 mm Hg pressure of O_2.

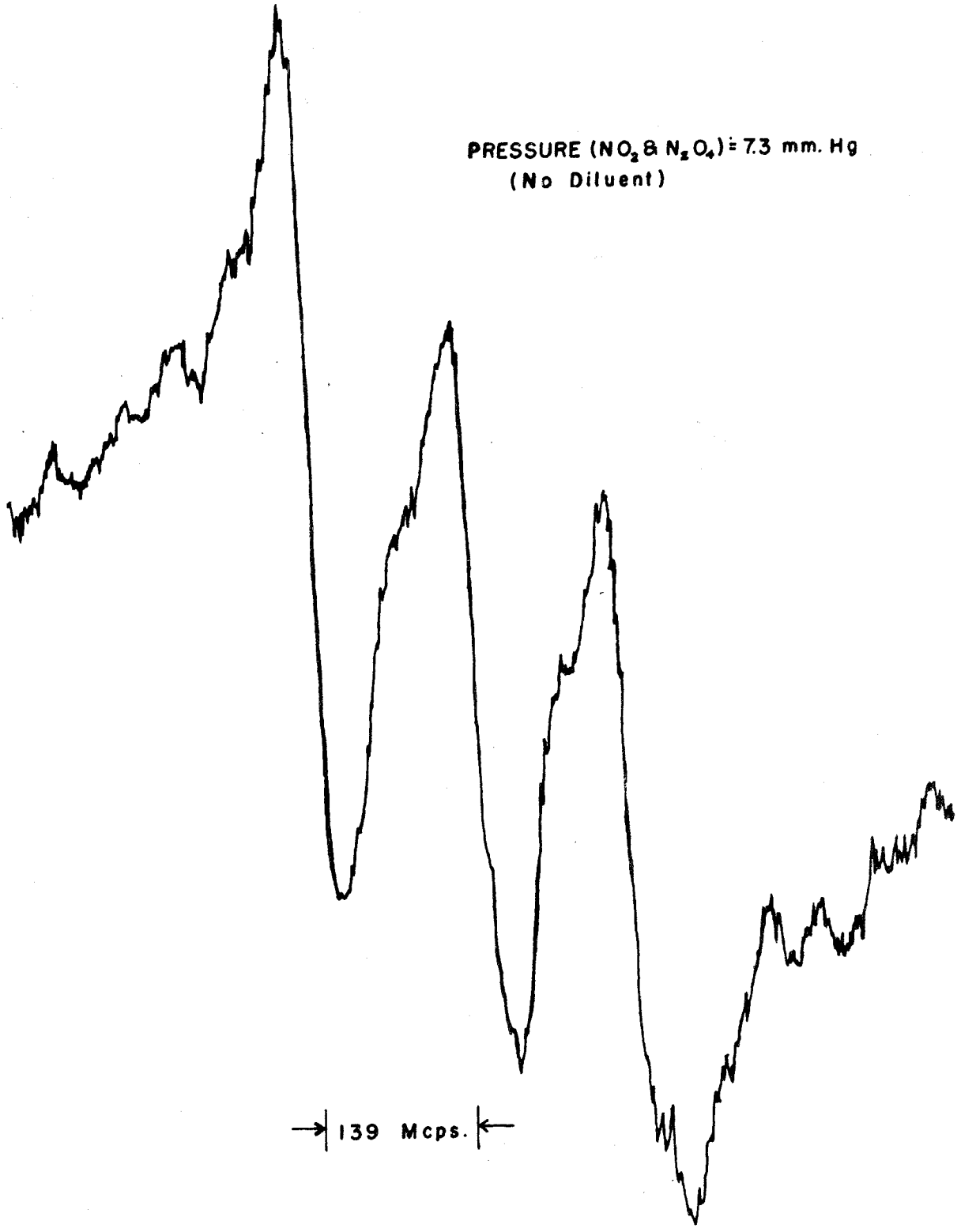

Fig. 7.- Trace of the E.P.R. spectrum of NO_2 (first derivative).

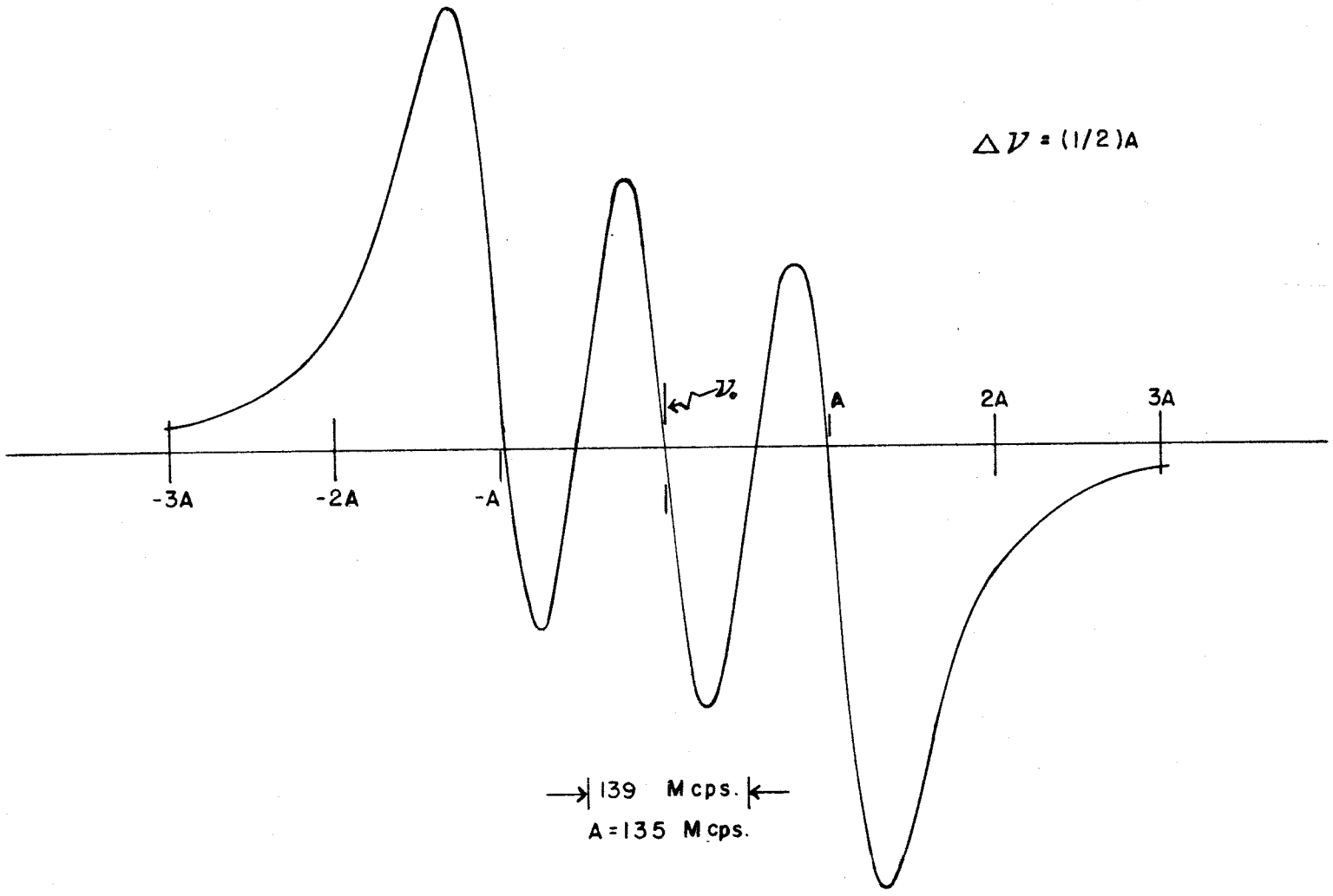

Fig. 8. - Graph of the calculated first derivative of the absorption spectrum with a triplet separated by A.

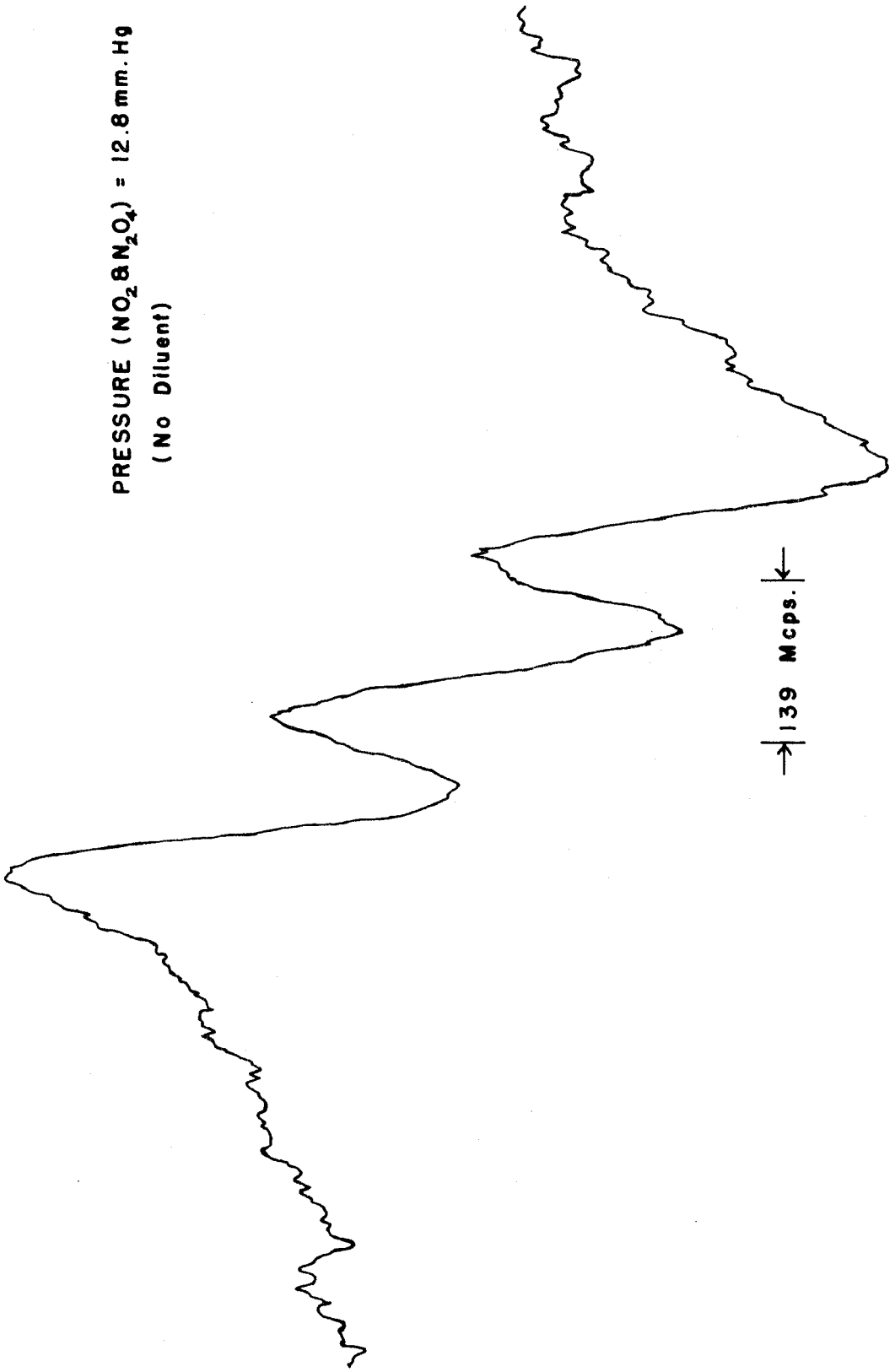

Fig. 9.- Trace of the E.P.R. spectrum of NO_2 (first derivative).

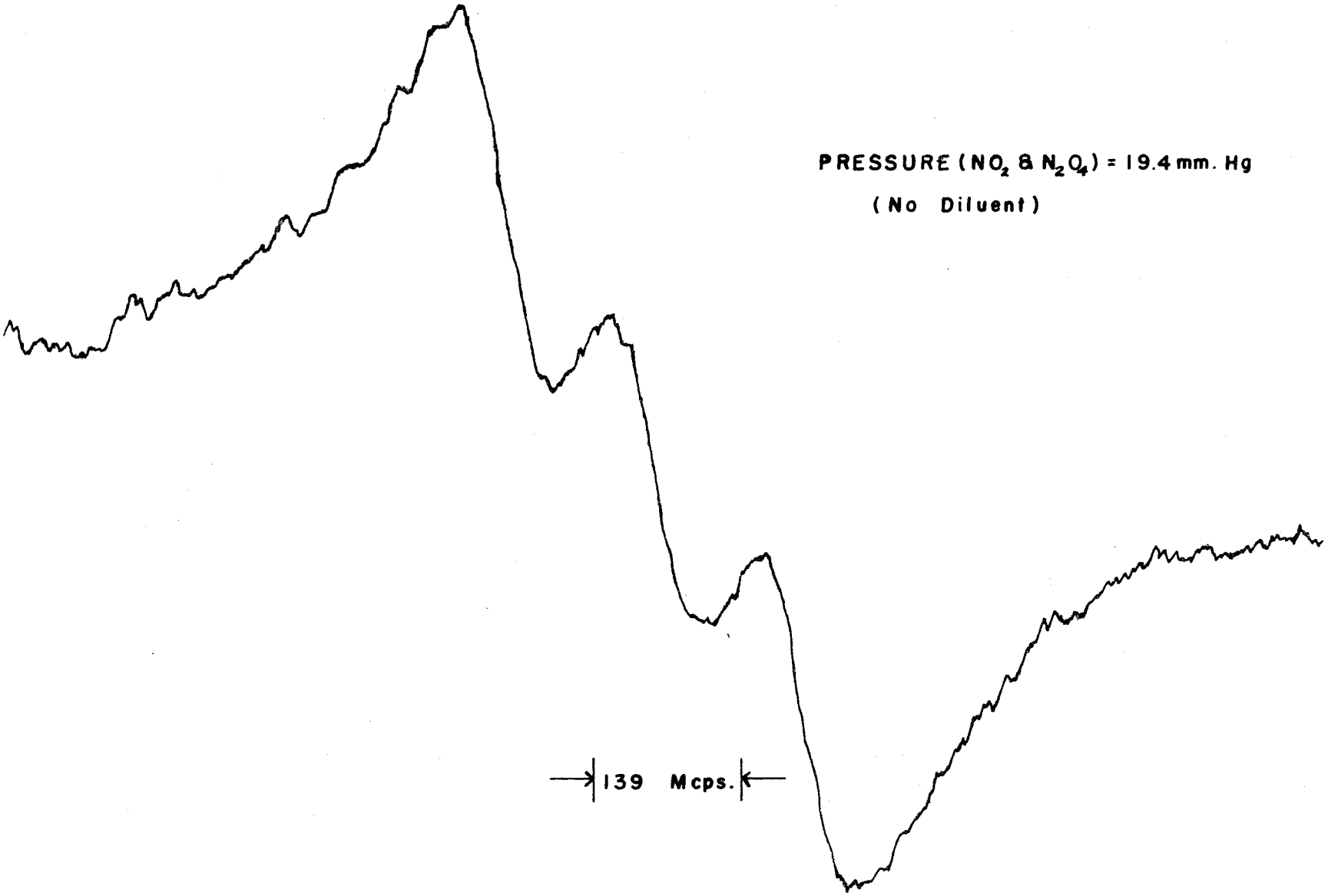

Fig. 10. - Trace of the E.P.R. spectrum of NO_2 (first derivative).

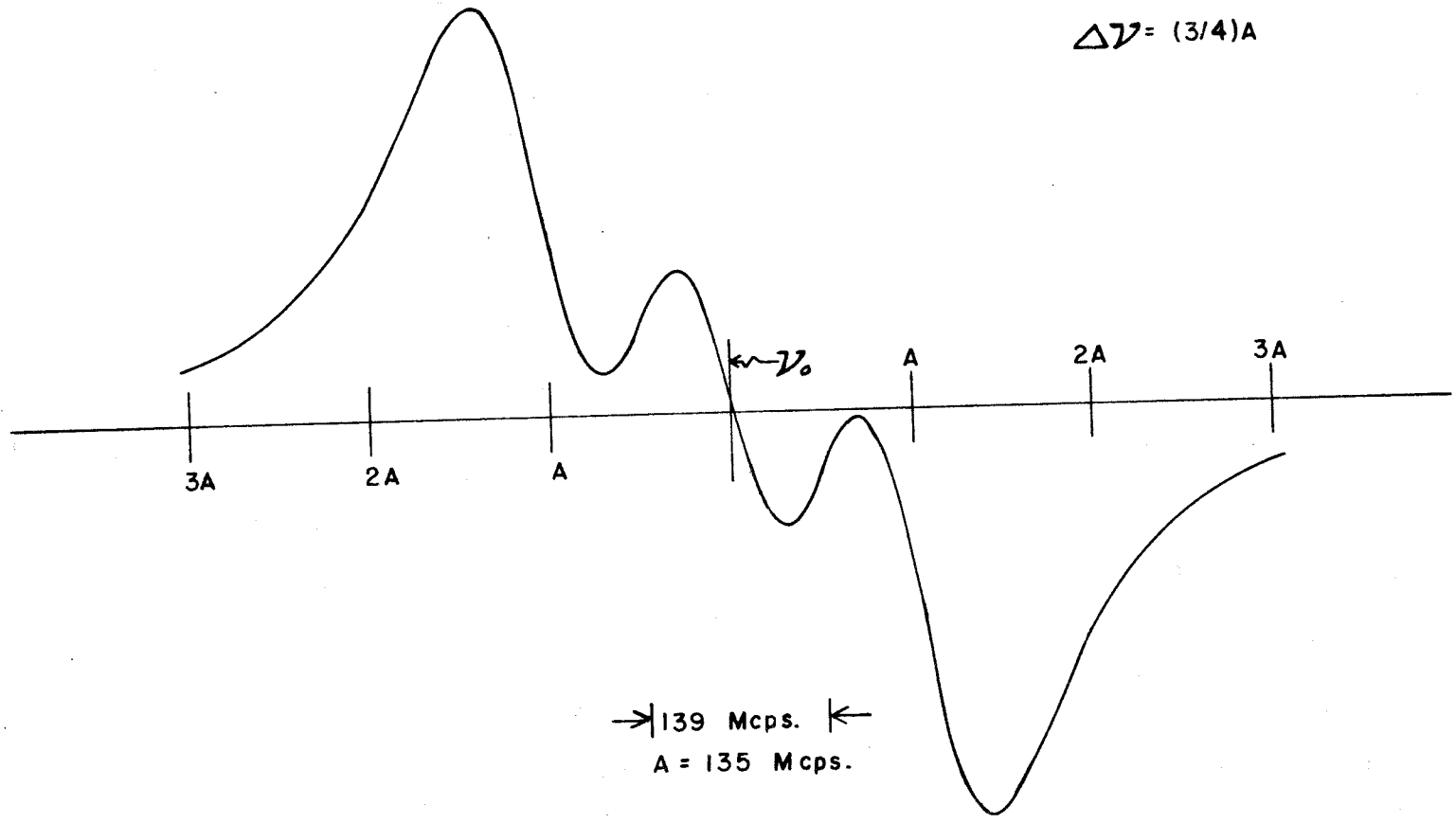

Fig. 11. - Graph of the calculated first derivative of the absorption spectrum with a triplet separated by A.

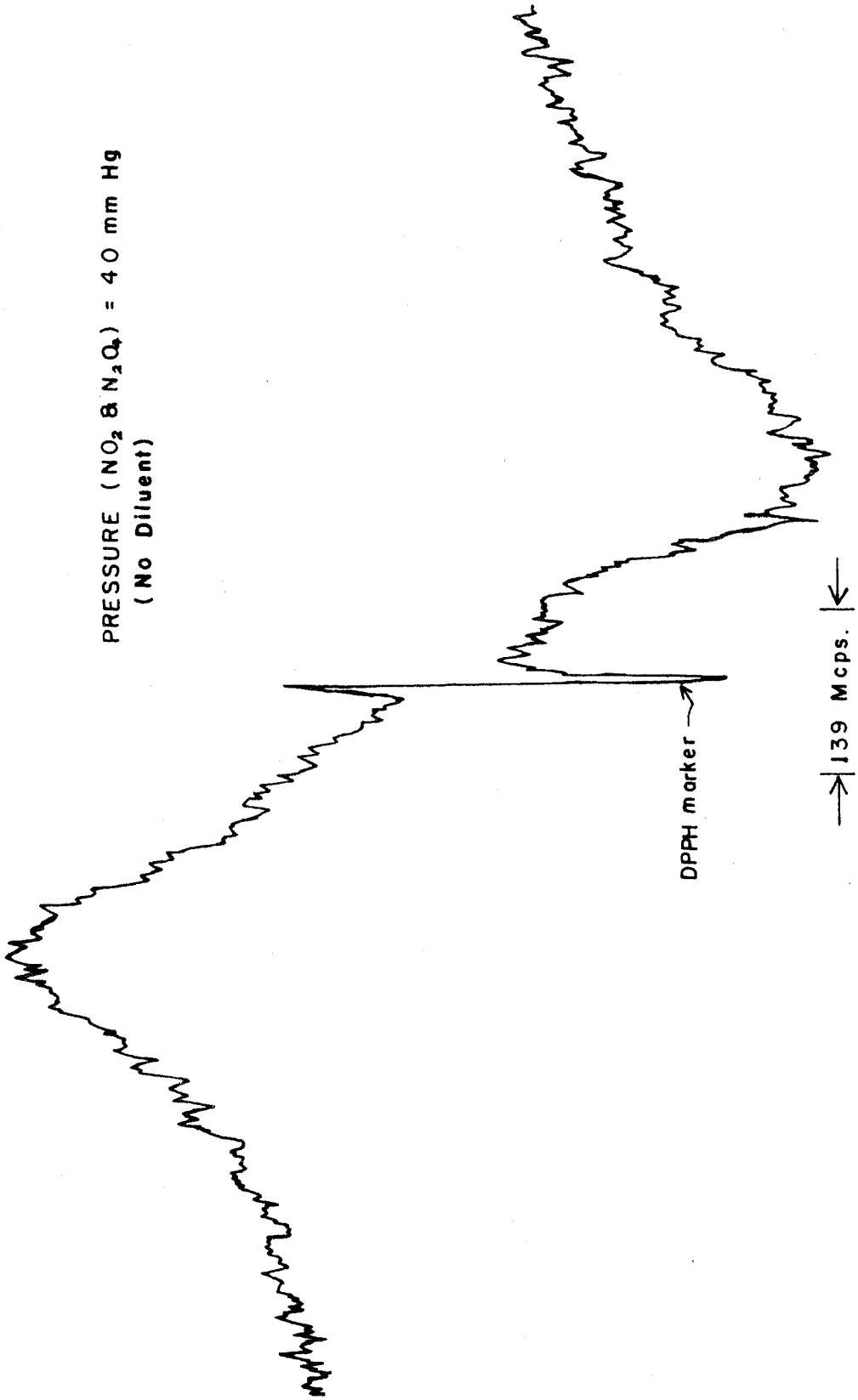

Fig. 12.- Trace of the E.P.R. spectrum of NO_2 with a diphenylpicryl hydrazyl (DPPH) marker (first derivative).

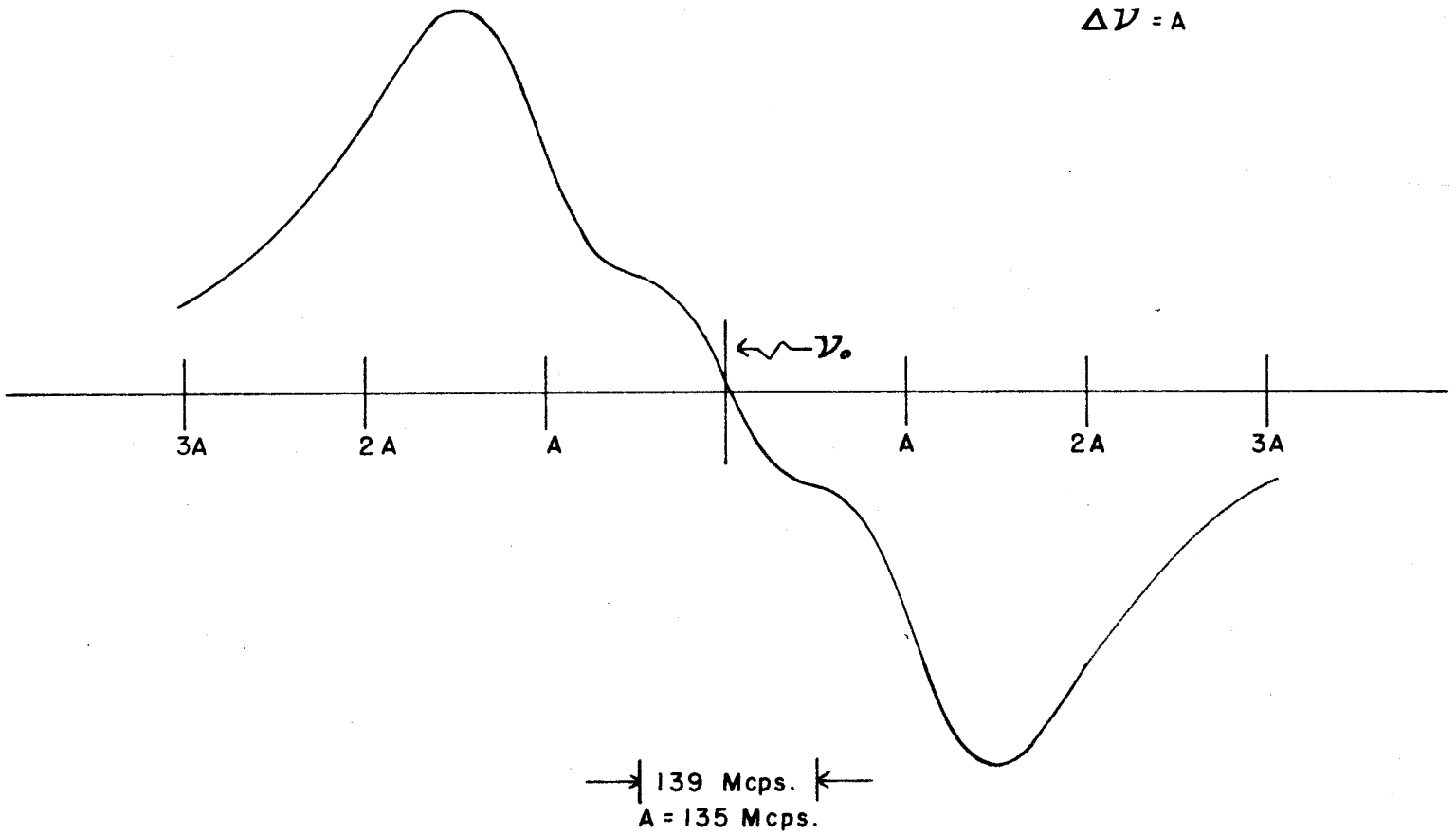

Fig. 13. - Graph of the calculated first derivative of the absorption spectrum with a triplet separated by A.

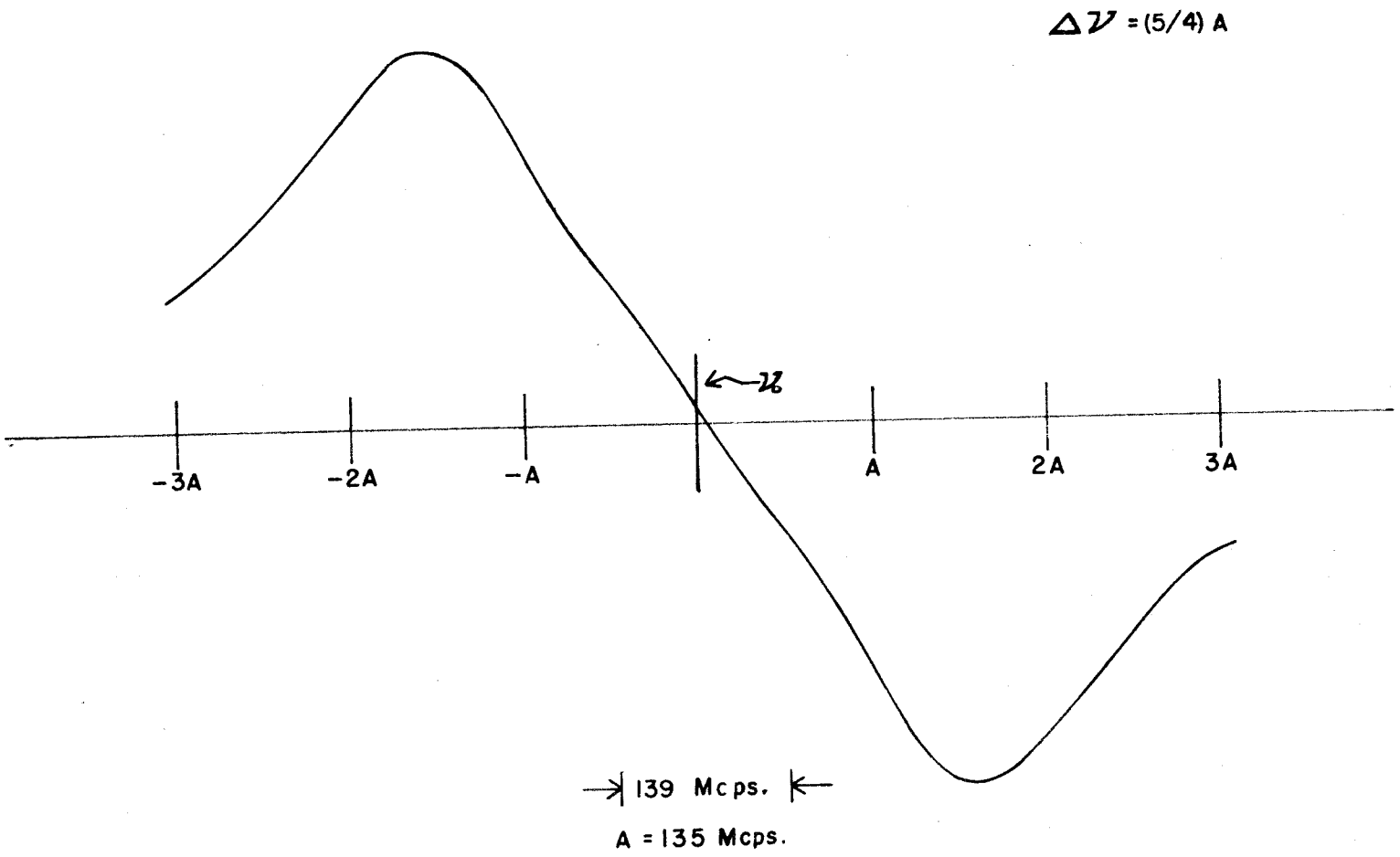

Fig. 14. - Graph of the calculated first derivative of the absorption spectrum with a triplet separated by A.

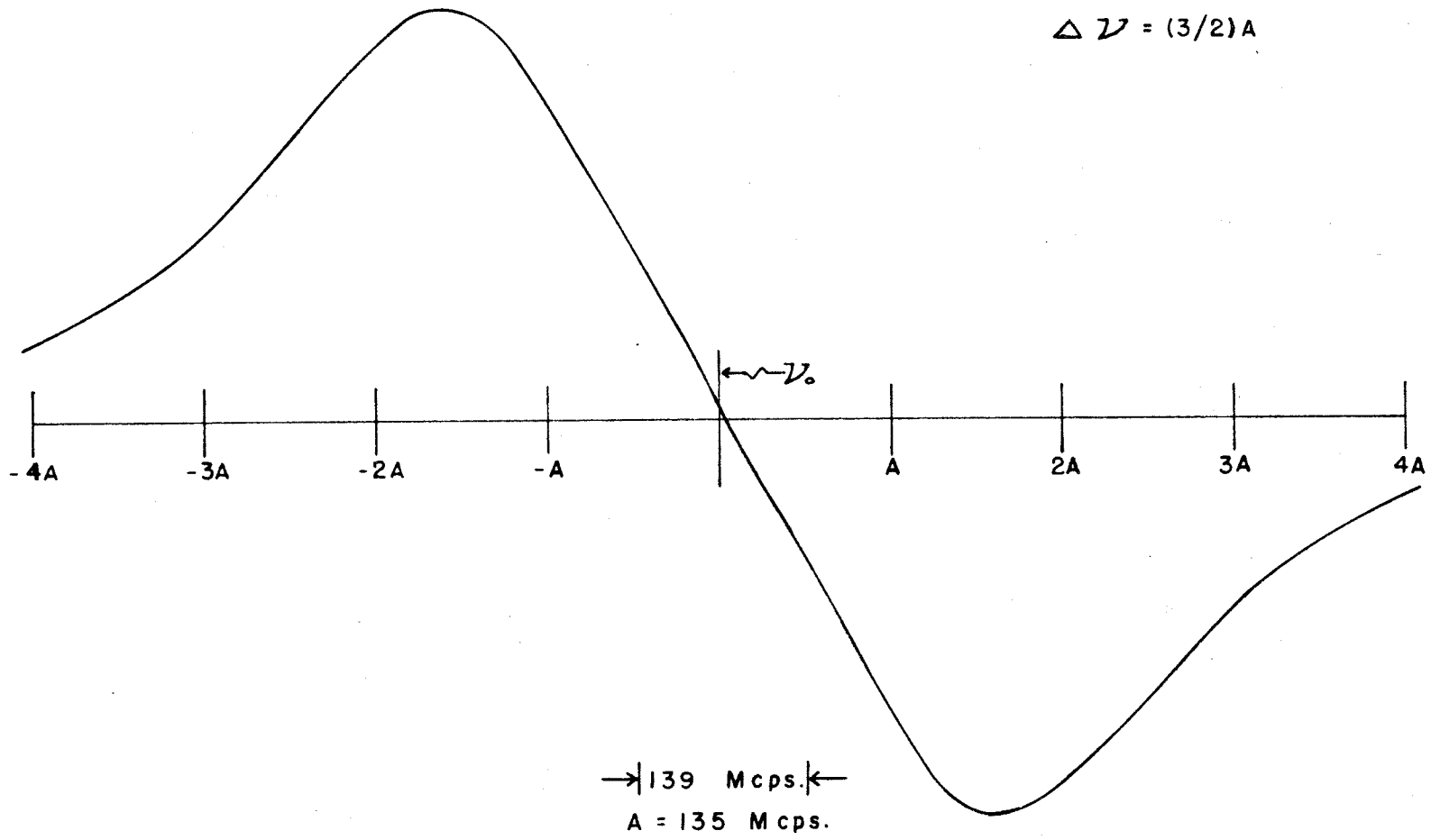

Fig. 15.- Graph of the calculated first derivative of the absorption spectrum with a triplet separated by A.

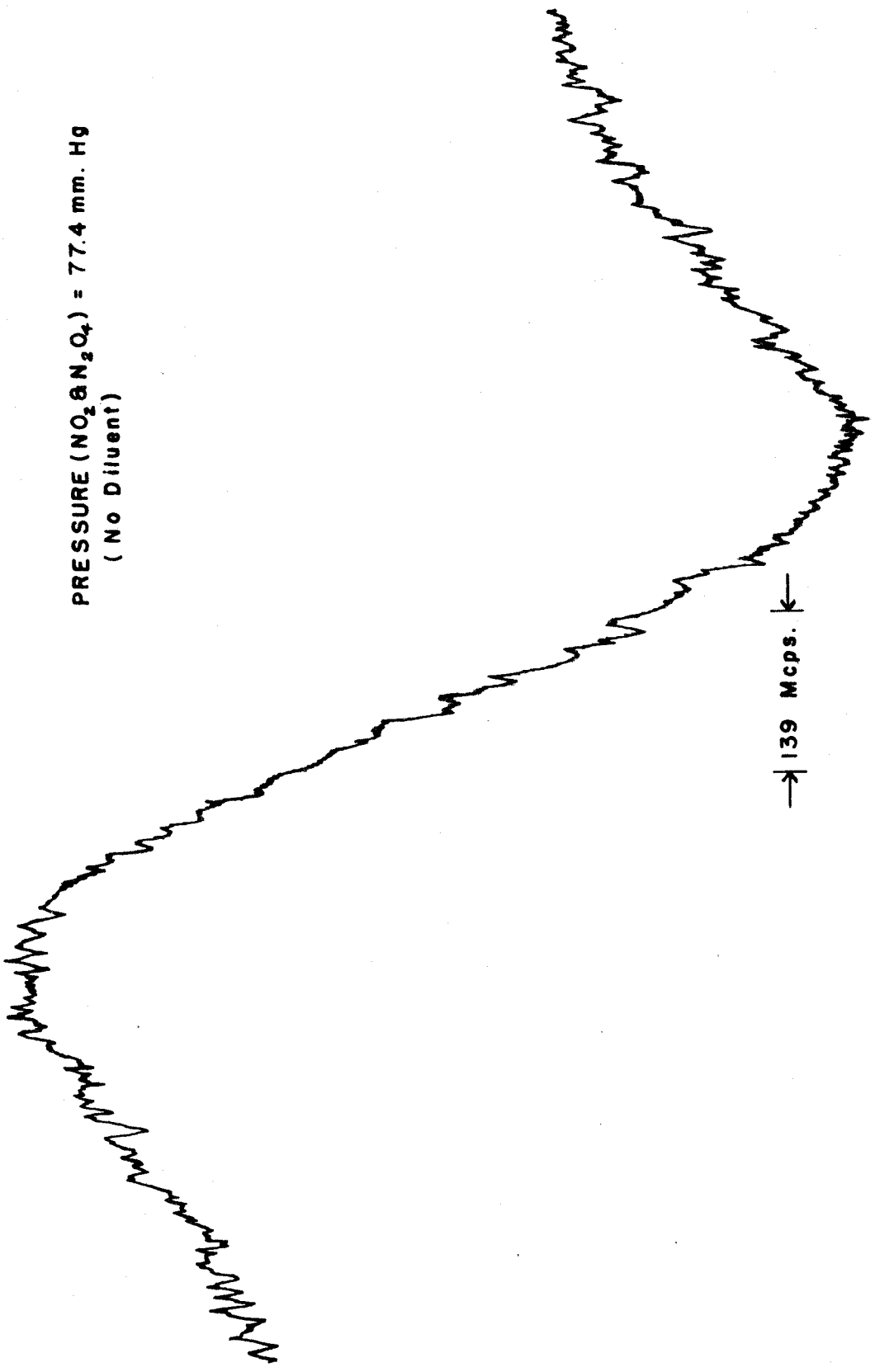

Fig. 16.- Trace of the E.P.R. spectrum of NO_2 (first derivative).

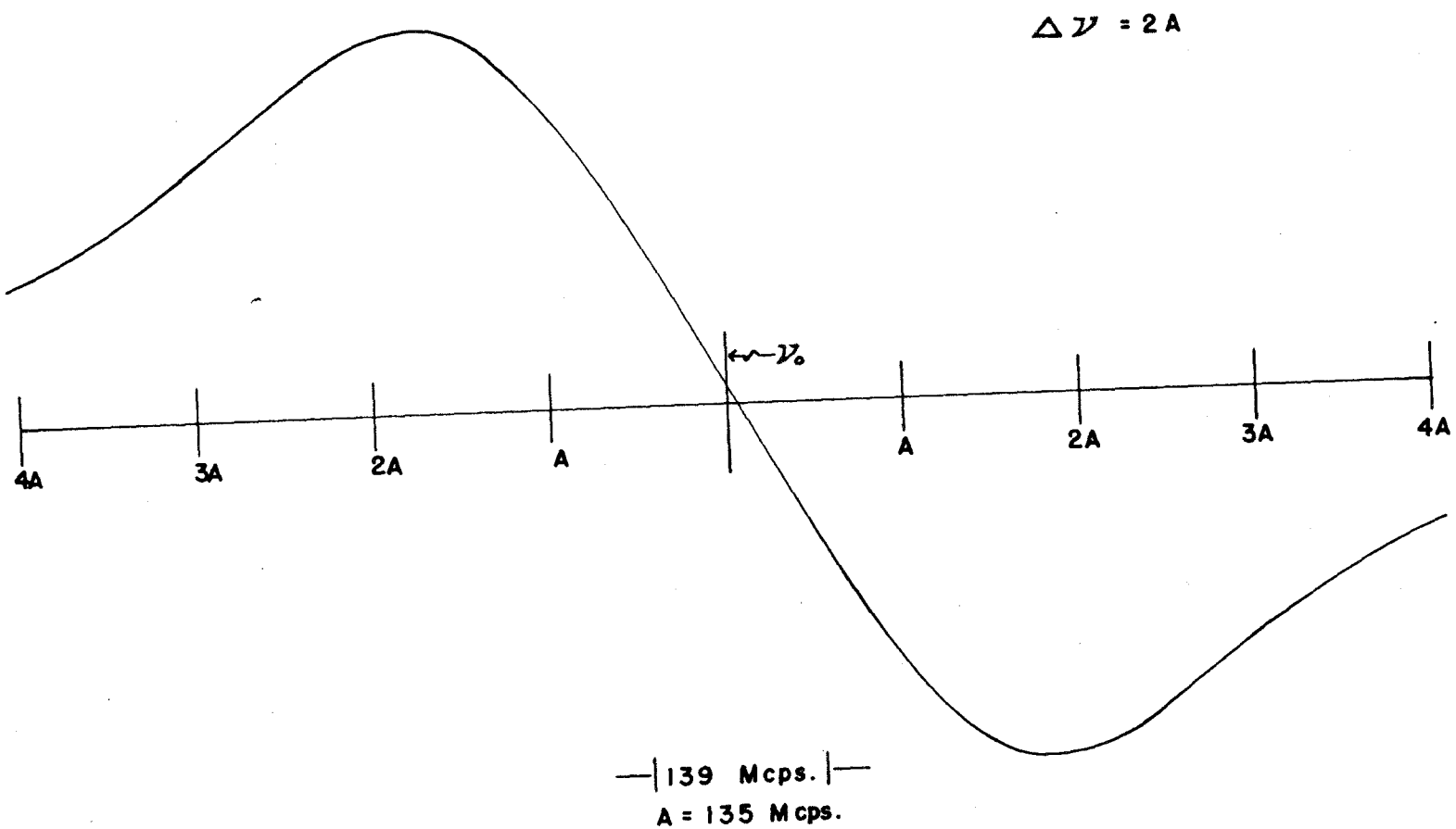

Fig. 17.- Graph of the calculated first derivative of the absorption spectrum with a triplet separated by A.

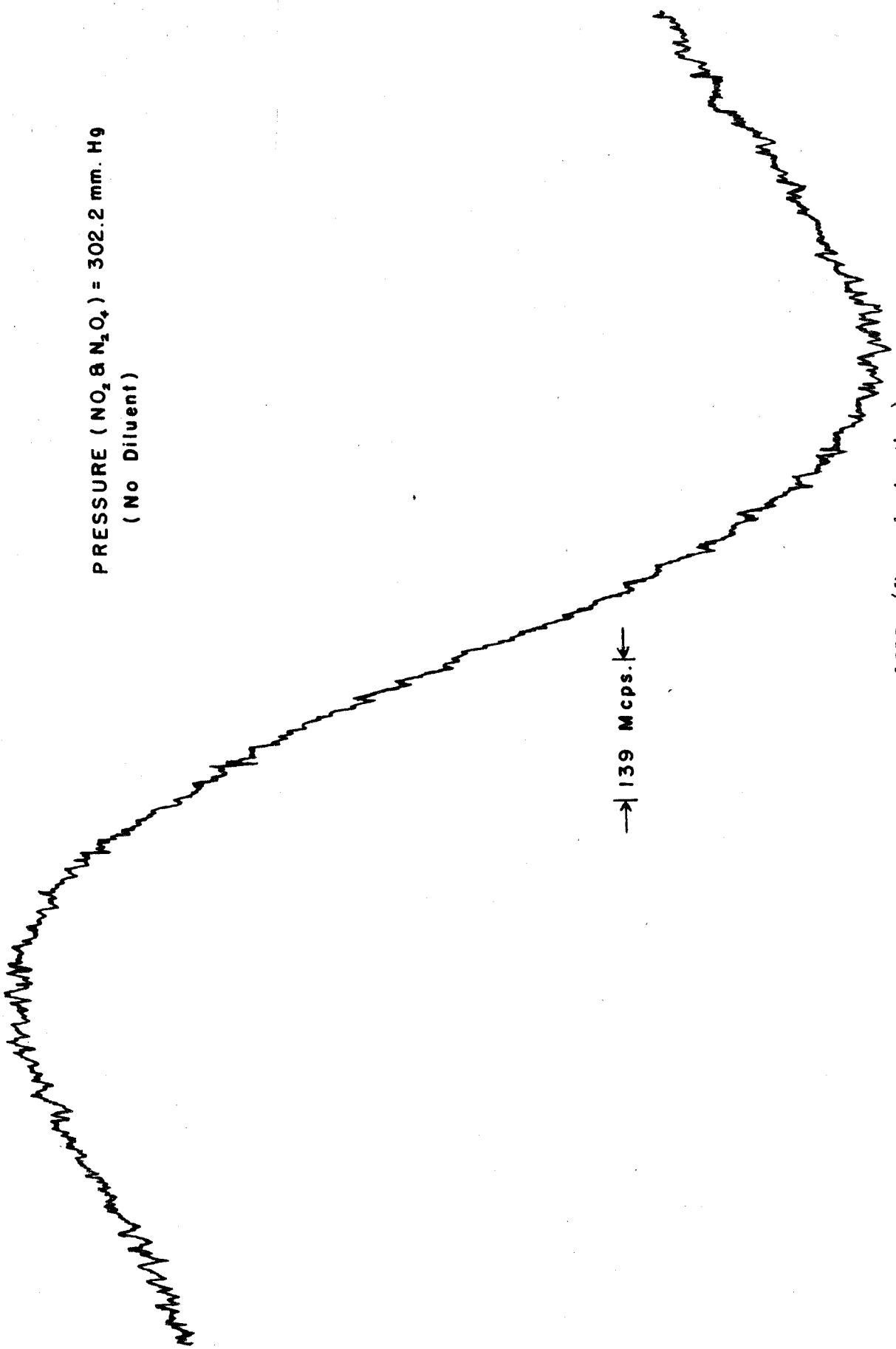

Fig. 18.- Trace of the E.P.R. spectrum of NO_2 (first derivative).

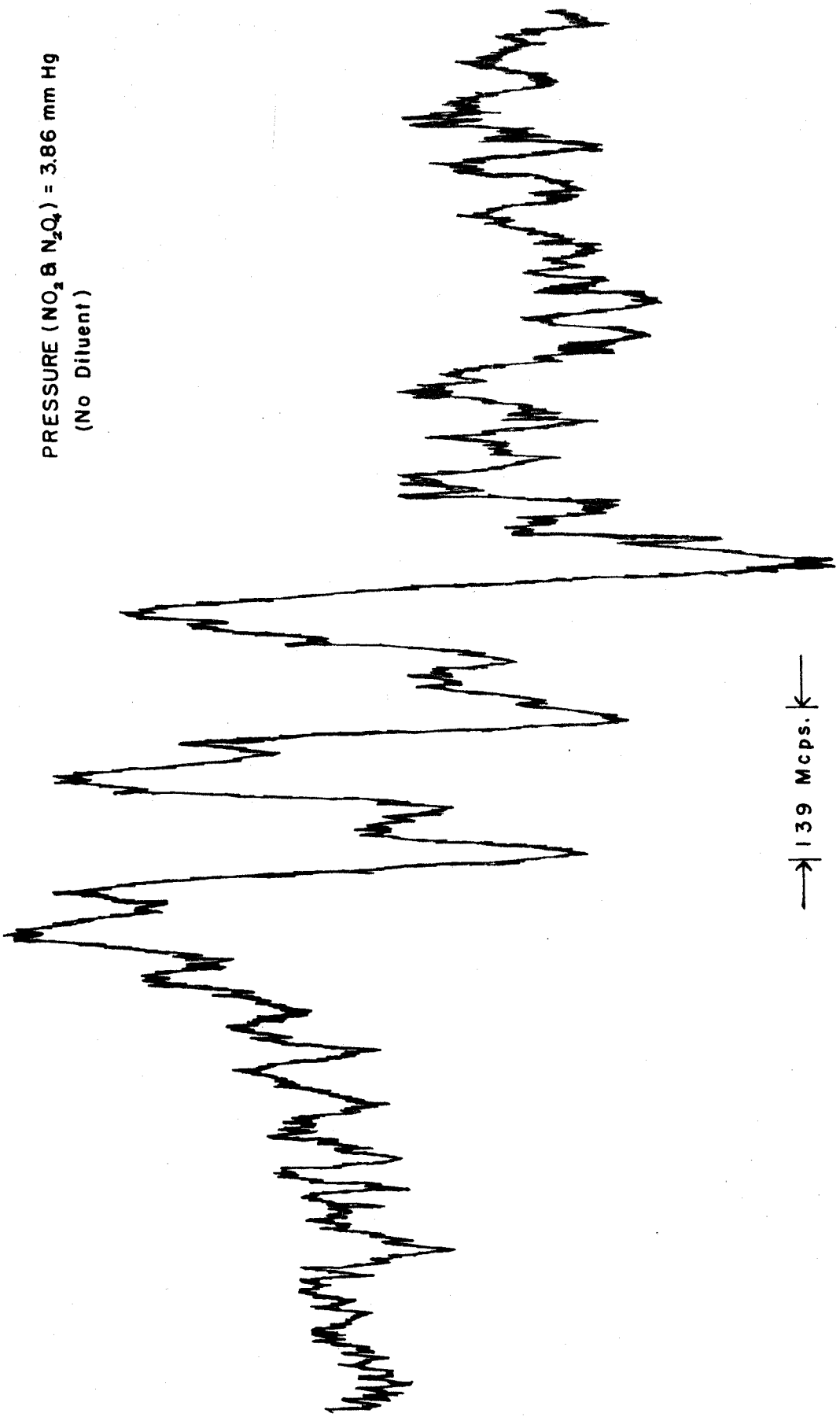

Fig. 19.- Traces of gas phase NO_2 spectra at two pressures showing two stages in the progression from a many lined spectrum to a three lined spectrum.

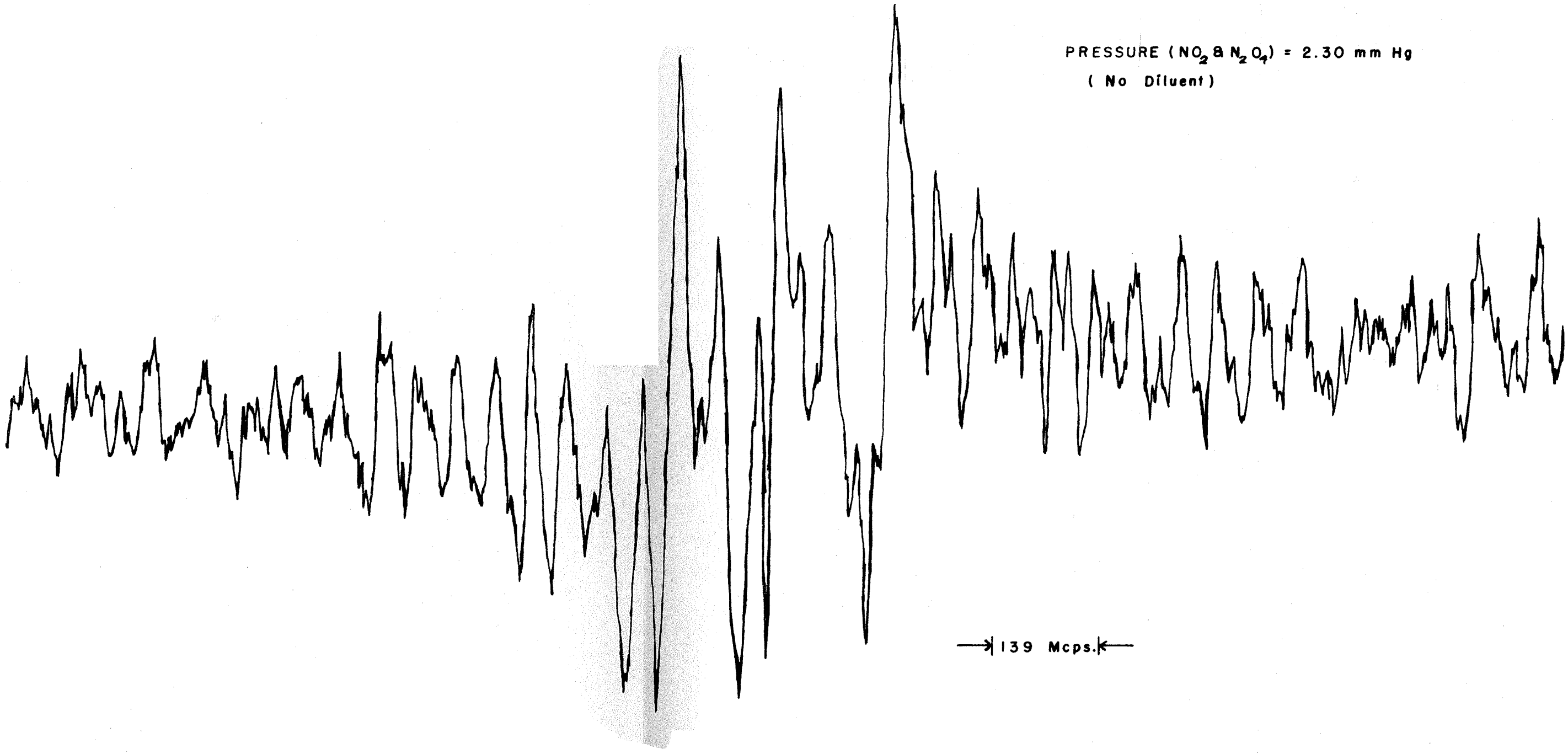

Fig. 19. (continued)

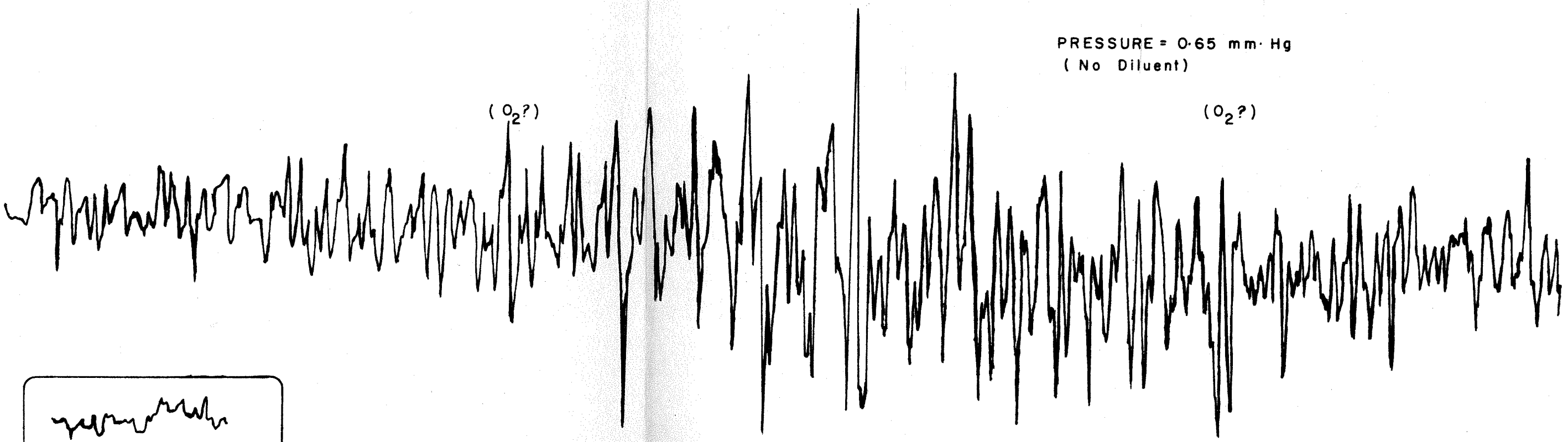

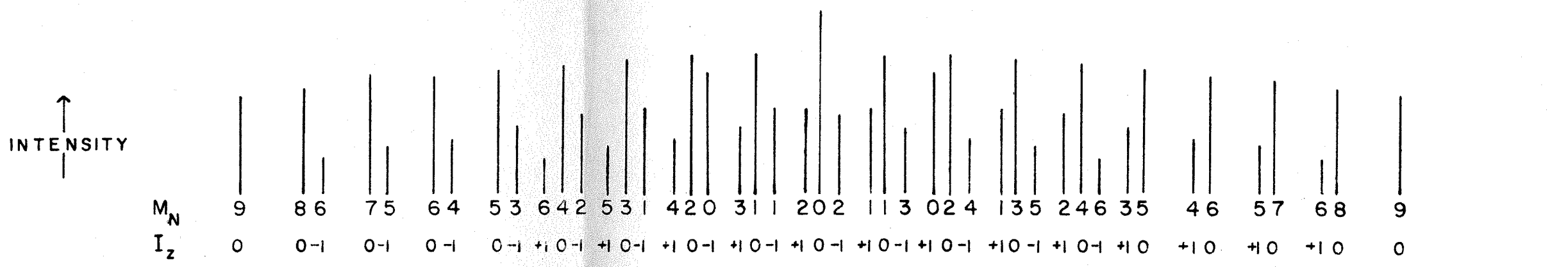

Fig. 20. - (Top) Trace of the E.P.R. spectrum of gas phase NO_2 at 0.65 mm Hg pressure.

(Bottom) Theoretical assignment of the main components assuming $\sigma - \bar{f}_\lambda \lambda$ = 127 Mcps and = 73 Mcps.

Before attempting an interpretation of the results, a consideration of the errors involved is desirable. With respect to the pressure measurement, the error produced is totally negligible, since the manometric measurement can be reproduced to within a millimeter for both the mercury and the dibutyl phthalate manometers. The temperature during the experiment varied between 27° and 30° C. This variation produces an error in the pressure, the NO_2-N_2O_4 equilibrium constant and the molecular velocity. The effect on the first and last parameter is negligible through obvious considerations. Namely, the pressure depends directly on the absolute temperature to a first approximation (Perfect Gas Law) and the relative change in absolute temperature is 1% referred to 27° C. Similarly, the molecular velocity depends upon the absolute temperature to the $\frac{1}{2}$ power and the relative change in molecular velocity due to temperature variation is about 0.5% under the experimental conditions. Through computation of the partial pressure of NO_2 by use of the temperature dependent equilibrium constant (see equation 55) one finds a maximum error of about 9% at one atmosphere and 7% at one-tenth of an atmosphere pressure of NO_2 and N_2O_4 due to temperature variation (the reference temperature is 27° C). This error is fairly large, however, the error inherent in the measurement of $\Delta\nu$ and R are likewise as large or larger. The effect of this error is not thought serious since the curves obtained were fairly regular (see Fig. 4). Part of the problem in the $\Delta\nu$ measurement

arises from the random noise of the instrumentation and part from the fairly flat extrema observed empirically. The instrument was likewise very sensitive to external influences (such as microphonics) and these obverse effects occurred many times, especially when least propitious. For reasons mentioned above, the oxygen data is felt to be of limited reliability. In this case, the measurement of R is felt to be of little meaning and it is expected that the measurement of $\Delta\nu_e$ is affected also. It is pointed out that the measurement of $\Delta\nu_e$ is much less sensitive than is the measurement of R to the presence of oxygen.

E. DISCUSSION

In order to simplify the interpretation of the observed E.P.R. spectrum of NO_2 in the gas phase as a function of pressure, it is necessary to understand the effect of the various energy terms. With this object in mind, two abbreviations of the Hamiltonian,

$$\mathcal{H} = \mathcal{H}_o + \mathcal{H}_{SI} + \mathcal{H}_F + \mathcal{H}_{SR} , \tag{58}$$

(the terms of which were considered in Section B1) will be considered:

$$\text{Case I} \quad : \quad 0 \approx \mathcal{H}_{SR} \ll \mathcal{H}_F + \mathcal{H}_{SI}$$

$$\text{Case II} \quad : \quad \mathcal{H}_F = \mathcal{H}_{SI} = 0$$

Case I. For convenience, since it is compatible with the theoretical predictions that have been made in Section B1, the Fermi contact term, σ, will be considered much larger than λ. It is to be remembered that $\mathcal{H}_{SI}$ is rotational energy state dependent. At low pressures, the effect of collisions will be minimal and one would expect to be able to resolve many lines. The extent of resolution, of course, depends on the density of energy states. For pressures low enough so as to permit M_N to be considered a good quantum number, one would expect to find a single and sharp, strong absorption at ν_o and a series of lines symmetrically displaced from ν_o whose distribution may be surmised from the Hamiltonian (eq. 25) and Figure 2. In this discussion, the

effect of second order terms is neglected. The central line at ν_o corresponds to a transition with $I_z = 0$ of the type $\Delta S_z = 1$. The lines symmetrically displaced from ν_o correspond to transitions with $I_z = \pm 1$ of the type $\Delta S_z = 1$. The integrated intensity of the central absorption line is expected to be equal to one half of the total sum of the integrated intensity of the lines on either side of ν_o. Furthermore, the spectral density about $\nu_o \pm \sigma$ is expected to be high.

With an increase in pressure, the collision frequency of the molecules increases. This increase in collision frequency will produce increased relaxation with the result that the more closely spaced lines will begin to overlap. Further increase in pressure will continue this process of overlapping with the result that a triplet will emerge. The line separation of the triplet will be $\sigma - \bar{f}_\lambda \lambda$; where $\bar{f}_\lambda \lambda$ is the collision averaged dipole-dipole interaction energy. The three lines will be of approximately the same width since collisions will mix I_z states. Finally, when the collisions become sufficiently frequent, the three lines will merge into a single absorption whose line width will be pressure dependent. It should be noted as a point of interest that if λ were larger than has been assumed, there would arise a marked difference in the relaxation of the $I_z = 0$ state as compared to the relaxation of the $I_z = \pm 1$ states. This phenomenon arises from the fact that some collisions are not effective in mixing spin states but are effective in mixing rotational energy states.

Case II. This case represents another extreme and is included to afford the reader a clearer understanding with respect to the $I_z = 0$, $\Delta S_z = 1$ absorption pattern. Since so little is known about the rotational magnetic terms, some limitations will be imposed on the components of $\mathcal{H}_{SR}$ in order to facilitate analysis.

Consider the first term of $\mathcal{K}$ in equation 22, $\frac{1}{2}(\epsilon_{AA} + \epsilon_{CC}) = \eta$, large in comparison to $\epsilon_{AA} - \frac{1}{2}(\epsilon_{BB} + \epsilon_{CC}) \frac{\mathcal{K}^2}{N(N+1)} = \rho$. Under these conditions, one would observe a strong central absorption for $M_N = 0$ with a set of lines symmetrically displaced and of equal interval. The intensity would slowly diminish as $|M_N|$ increases, since $M_N = -N, \ldots, N$. The effect of ρ is to split the individual M_N levels. The extent of splitting is linearly dependent on M_N. The net effect of the splitting of the M_N states by the ρ term and the decrease in the number of energy states with the increase in M_N is to decrease the degeneracy of the energy states and, therefore, to increasingly decrease the intensity of the absorption lines with the greater value of M_N. In addition, the lines corresponding to equal M_N will be displaced from $M_N\eta$ in a manner which increases the separation with increasing K for a given value of N and which decreases in intensity with increasing K (NO_2 is a near prolate symmetric top). The effect of collisions would be to average the ρ contribution to the energy and to produce a mixing of M_N states. In other words, the collisions enhance the effect of the off-diagonal

magnetic moment matrix elements as well as cause a loss of coherence in the rotational motion. One would expect the effect of collisions to be such that the absorption of states of high $|M_N|$ would decrease in intensity with an attendant increase of intensity in the lines of low $|M_N|$. The lines of different M_N would eventually coalesce into a single broad line which would exhibit a further pressure dependence.

On the other hand, if ρ were much larger than η a very much more complicated situation would arise. The very intense central line would still be present corresponding to: $\Delta S_z = 1$; $M_N = 0$. However, one would now observe a series of lines symmetrically displaced about the central absorption line which would exhibit a complex intensity relation and an increasing separation for each value of M_N. Also since η is so small the series will repeat itself at regular intervals with lines of different M_N mixed together. One can see that the resolution of the great number of lines will be difficult ($\frac{K^2}{N(N+1)}$ is small for most lines). If this situation was operative, it is not unreasonable to expect a broadened spectrum even at very low pressures. For a ρ of sufficient magnitude to produce sharp and well resolved lines, the strong field case defined above is not expected to be valid. One then expects a singlet with a line shape that is symmetrical about ν_o but of doubtful predictability with some low intensity, symmetrically displaced lines with respect to ν_o. An increase in pressure is expected to cause the line shape to become more Lorentzian.

Clearly, the latter consideration ($\rho \gg \eta$) is unimportant for NO_2. A combination of Cases I and II (with $\eta > \rho$) will, however, prove very satisfactory. It should be noted that the available signal to noise ratio was such as to exclude a complete systematic analysis of the NO_2 spectrum. Many lines of the spectrum are indistinguishable from the noise and are not separable unless a very tedious and sophisticated analysis method were applied. This treatment is beyond the scope of this research.

It is reiterated that in the spectral analysis, the contributions of ρ have been neglected due to their small magnitude for the M_N values considered. The same is true for λ contributions. The sagacity of the latter approximation is easily justified. Theoretically, λ is predicted to be 10.9 Mcps (see Section B1). τ, likewise, is predicted to be -8.7 Mcps. From equation 13, one recalls the rotational state dependence of the contributions of these anisotropic coupling parameters. From Figure 2, the dependence of f_λ (from equation 26a) on the rotational energy levels is noted. It is seen that the main contributions to the spectrum (on the basis of intensity) will result from energy states with f_λ values between 0.3 and 0.5 for $M_N = 0$; see, for example, Figure 2, $M_N = 0$. The difference between these values of f_λ is 0.2, which corresponds to a spread of 2.2 Mcps for the anisotropic term. This value is approximately the magnitude of the line width that is observed. One concludes that the $M_N = 0$ line of

$I_z = \pm 1$ will be shifted from σ, the contact interaction contribution, by approximately $0.4\,\lambda$ or 4.4 Mcps. The argument used for the $M_N = 0$ energy states may be extended to the other M_N levels. Since this discussion is also appropriate for f_τ, the value for the average f_τ will be quoted without proof. The contribution for $K = \pm 1$ levels from the anisotropic coupling is $0.4\,\lambda \pm 0.25\,\tau$ or 4.4 ± 2.2 Mcps. This is perhaps resolvable, but must be considered marginal.

To justify the treatment of ρ, one cites the fact that $K^2/N(N+1)$ is small for most of the more populous energy levels (near prolate symmetric top). Another reason for the validity of the assertion that the effect of ρ is negligible is the apparent resolvability of high $|M_N|$ values for $I_z = 0$; see Figure 20.

Table III contains an estimate of the intensities expected for the various values of M_N and I_z and for the $K = \pm 1$ states. The values are referred to an arbitrary scale. The intensities were computed by the summation of the individual state intensities according to:

$$(59) \qquad I_{NKM_N} = \exp\left(\left[(B+C)\,\frac{N(N+1)}{2} + \left(A - \frac{B+C}{2}\right)K^2\right]/kT\right) ;$$

where A, B, C are the reciprocal moments of inertia as given by Bird (8). Using the calculated intensities coupled with the expectation that the spin-spin coupling should be approximately 135 Mcps on the basis of the observed broadening pattern:

TABLE III

$\|M_N\|$	$I_z = 0$	$I_z = \pm 1$	
		$\|K\| \neq 1$	$\|K\| = 1$
0	75	~ 50	~ 8.2
1	57.0	~ 35	~ 7.5
2	57.0	~ 33	~ 6.7
3	55.2	~ 28	~ 5.0
4	53.6	~ 23	~ 3.7
5	50.7	~ 20	~ 2.5
6	48.3	~ 15	?*
7	46.5	?*	
8	43.9		
9	40.5		
10	38.0		
11	34.8		
12	32.5		
13	29.5		
14	27.5		
15	24.9		
16	23.0		
17	20.7		
18	19.1		
19	17.1		
20	15.8		
21	14.1		
22	13.0		
23	11.6		
24	10.6		
25	9.5		

*Not estimable.

$$\sigma + \bar{f}_{\lambda}^{M_N=0} \lambda = 127.3 \pm 2 \text{ Mcps} \tag{60}$$

$$\eta = 73.5 \pm 2 \text{ Mcps} \tag{61}$$

The lines corresponding to $K = \pm 1$ are of low intensity and are closely spaced about $\sigma - \bar{f}_{\lambda}\lambda$. Their contribution to the spectrum has not been analyzed. If η were larger than σ, one would not expect to find lines of great intensity appearing between $\nu_o \pm \sigma$ and ν_o. There are lines in these positions. In addition, since the line intensity drops off so slowly for $I_z = 0$ with increasing M_N, the spectrum would be expected to be of greater frequency range. The conclusion is that $\sigma > \eta$. The present assignment is further justified by the spectral intensity enhancement of the central portion of the spectrum. The assignment is necessarily a rough one. It is pointed out that the terms which have been neglected in attaining the values in equations 60 and 61 will produce a discrepancy between the theoretical lines and the empirically observed lines. The slight asymmetry noted can be attributed to second order effects which are of order of $\frac{\sigma^2}{2\nu_o}$ or 0.8 Mcps. The conclusion reached is that the restrictions which have been imposed on the magnitude of the energy terms in order to interpret the spectrum are justified.

From the value of $\sigma - \bar{f}_{\lambda}^{M_N=0} \lambda$ and the value of λ calculated from theory, one may estimate σ. Since the orbitals involved have the same electron spin polarization, is is expected that σ and λ be

of the same sign. Therefore:

(62) $\sigma = 127.2 + 4.4 = 131.6$ Mcps.

No additional conclusions concerning the various energy contributions are felt to be legitimate.

The value of σ is of special interest for two reasons. First, it closely approximates the theoretically predicted value derived in Section B1; $\sigma = 177$ Mcps. The value of 131 Mcps corresponds to 8.1% s-character on the nitrogen atom. The other feature of interest is the difference between the magnitude of σ herein obtained and that value gleaned from the dilute NO_2 solution E.P.R. data by Bird, Baird and Williams (12) of 300 Mcps. This latter value can in no way be fitted to the NO_2 gas phase E.P.R. data. As pointed out earlier (Section A), the values obtained for F (now called σ) by Bird et al. were almost equal for the CCl_4 solution and the CS_2 solution of NO_2, but were not shown to be equal. It is asserted that the difference is real and to be expected. Upon further consideration, one realizes that the very low pressure gas phase corresponds closely to an unperturbed molecular system or "free state." More specifically, it is a situation in which a molecule sees a very small potential from the environment. The solutions do not so behave, for there exists an almost intimate contact with the surrounding molecules. The NO_2 molecule, therefore, sits in an environmental potential which is expected to perturb the electronic

distribution. The origin of the forces may be attributed to a permanent dipole, induced dipole, quadrupole moment, etc. These forces are generally classified as polarization or Van der Waals forces. CCl_4 and CS_2 are both nonpolar, of about the same polarizability (31b) but of slightly different density (35a) (the density of CCl_4 is 1.595 and of CS_2 is 1.263 gram/cm^3 at 20° C). This latter factor leads one to wonder if the CCl_4 molecules can distort the NO_2 molecule more than CS_2 can. The distortion, which could result in a lowering of the moment of inertia slightly with attendant lessening of the bond angle for O-N-O, could necessitate more s-character about the nitrogen. This effect is seen in the diagram of Walsh (24).

The marked effect which is noted is expected since NO_2 has an unpaired electron which is very sensitive to external forces. One is, nevertheless, limited in the variety of molecules which may be used as a solvent for NO_2, since the reactivity of NO_2 is in general great. This fact restricts the study of the interaction of molecules with NO_2 to a small class of compounds which are in general of zero or very small dipole moment. As a further proof of this explanation, the data of Jen, et al. (36) is presented. These researchers investigated the E.P.R. spectrum of NO_2 trapped in an argon matrix at liquid helium temperature. They found a triplet which showed a line separation of 162 Mcps. This splitting is attributed to the isotropic contact interaction, $\mathcal{H}_F$. The value obtained in the study of Jen et al. is

intermediate to that obtained from the gas phase data and the solution phase data. This situation is considered reasonable on the grounds that the polarizability of argon is expected to be much less than that of CS_2 or CCl_4. In addition, since the matrix is an almost rigid system as compared to the highly mobile liquid, the instantaneous electric field gradient is greater in the case of the liquid as compared to the solid.

The final feature of the E.P.R. spectra of NO_2 that is of interest is the attendant broadening with the increase of pressure. As noted in Section B2, the natural line width and the Doppler effect line width are of negligible consequence. The best resolution obtained in this research was of such a nature as to exclude the observation of individual lines. This statement should be qualified to include only those transitions which are not highly degenerate (such as the $M_N = 0$, $I_z = 0$ state). The mechanism of pressure broadening has been discussed. The observed broadening is the result of the mixing of the rotational and the spin states. As discussed under saturation, some of the spin state mixing results in relaxation which maintains the thermal equilibrium of the spin system. For example, terms of the type: $S_y \pm iS_x$, produce this effect.

With continued increase in broadening, the three lines are expected to coalesce into a singlet. This is observed. The singlet continues to broaden with increase in pressure until the collisions are

numerous enough to produce $\Delta I_z = \pm 2$ transitions. The line would then be expected to narrow. This is not observed, since the pressure is not sufficiently high.

Turning now to Figure 4, which shows the increase of line width with increase of pressure, one notes a very steep slope at low pressures and a relatively gentle slope at high pressures. The explanation of this lies in the fact that the mixing of the rotational levels causes the value of M_N to be averaged to zero. This results in an increase in intensity in the central section of the spectrum relative to the wings. In addition, high N states relax faster than low N states, and hence the same is true for M_N. At that pressure when the averaging of M_N is about complete ($M_N = 0$, also M_N ceases to be a good quantum number), the change in half line width becomes linear with respect to pressure increase. Since all the diluent molecules have the same effect as an NO_2 molecule does on an NO_2 molecule (only varying in degree), one would expect a linear dependence of the half line width at high pressures in all cases. This is observed. (See Figure 4.)

One may calculate the values of T_1 from the relation:

$$\Delta\nu = [4\pi T_1]^{-1}; \tag{63}$$

where the symbols have been defined in Section B2. As one may note from Figure 4, the magnitude of $\frac{1}{T_1}$ is not a constant, but, rather seems to approach a linear behavior with respect to the total pressure at

moderate pressures. That this behavior is expected may be shown by considering $b = 6$ Å (see Section B2c), $v = 4 \times 10^4$ cm/sec and $\tau \geq 10 \frac{1}{2\pi\nu_o}$. Using the relation between the pressure and the mean time between collisions:

$$\tau = \frac{1}{2\pi N v b^2} \quad ;$$

and the perfect gas law:

$$N = \frac{N_o P}{RT} \quad ;$$

at $T = 300°$ K, one finds that in order that the inequality above concerning τ be true, $P \leq 0.28$ atm. Since τ^2 is involved in the denominator of the T_1 expression (see equation 47), the inequality is a little more restrictive than need be. In view of the large errors involved in the experiment, a 10 to 15% contribution from the number one in the denominator of equation 47 can be neglected. Taking this factor into consideration, allows the pressure to be about 4 times as large as already stated, namely $p \leq 1.1$ atm. The condition, $\tau = 10 \times \frac{1}{2\pi\nu_o}$, is chosen such that $(2\pi \nu_o \tau)^2 >> 1$ for which $T_1 \propto \tau$. For these conditions it is easily seen that $\frac{1}{2T_1} \propto P$. That this behavior as observed is to be expected may be understood by recalling that, at most, the pressure of 1.1. atmospheres was barely exceeded.

From Figure 4 one may get an idea of the magnitude of the interaction energy, E_{SR}, involved:

$$(64) \qquad \frac{1}{2T_1} = E_{SR} \frac{2\pi N_o b^2 v}{4\omega_o^2 RT} P ;$$

where the symbols have been defined earlier with the exception of $\omega_o = 2\pi\nu_o$ and N_o = Avogadro's number. With b = 6 Å, $v = 4 \times 10^4$ cm/sec and T = 300° K:

$$(65) \qquad \Delta\nu = 2.2 \times 10^{-13} E_{SR} \text{ (in cps) } P .$$

For a pressure of 0.69 atm (ca. 525 mm Hg) one obtains a value of 3.46 KMcps for E_{SR}. This value represents an average interaction energy. Using this value, one may calculate the value of b for the other gases. The assumptions that are made are that the mean collision diameter calculated is equal to the average of that for NO_2 and the colliding molecule and that the mean collision diameter for NO_2 and N_2O_4 are the same. It is felt that the latter is a fair assumption in that the lifetime of an N_2O_4 molecule with respect to splitting to form 2 NO_2 is short and that the N_2O_4 molecule has a hard sphere diameter about that which is used for the NO_2-NO_2 collision diameter. The values of the collision diameter for the various gases used in the experiments are tabulated in Table IV. In addition, values of the collision diameter obtained from the van der Waals equation as tabulated in the Handbook of Chemistry and Physics (35b) are included in Table IV. The values of the collision diameter for A and N_2 from this

TABLE IV

Gas	b (collision diameter) this experiment	b ref. (35b)
NO_2	6 Å calculated	
N_2O_4	6 Å assumed	
A	4.0 Å	2.94 Å
N_2	4.4 Å	3.15 Å
He	2.1 Å	2.65 Å

experiment are seen to be larger than the corresponding mean diameters from kinetic theory. This is explicable on the basis of the polarizability of these diluent gases. Helium is seen to give a value of the collision diameter from this experiment which is small in comparison with the kinetic theory value from the van der Waals equation. This is not unreasonable since helium is not easily polarized and in order to produce a strong collision of the type necessary for relaxation, the molecules would have to be at close approach.

In conclusion, the fruits of this research will be concisely recorded. Experimentally, at low pressures one observes a many-lined spectrum which is the result of a large number of transitions. Many of these transitions are of the same or nearly the same energy and therefore their lines are superimposed. With increase in pressure, the lines away from the center of the spectrum decrease in intensity with respect to the central lines and a triplet emerges in the center. The triplet broadens upon further increase in pressure until it forms a broad singlet whose line width increases linearly with an increase in pressure up to the maximum pressure investigated, namely 1.3 atmospheres. The broadening due to nitrogen, argon and helium is less effective than that due to NO_2 and N_2O_4, and their effectiveness decreases in their respective order. The collision diameters for the relaxation process are about equal to those collision diameters obtained from the van der Waal's equation (kinetic theory). These collision diameters

were obtained on the assumptions (1) that the collision diameters for NO_2 and N_2O_4 are identical; (2) that the collision diameter for NO_2 is obtained through calculation by Anderson's theory (30). The observed spectrum can be accounted for by values for the Fermi contact interaction constant of 131 Mcps corresponding to 8.1% nitrogen 2-s character and for the spin rotation interaction constant of 73 Mcps. The Fermi contact interaction constant corresponds favorably to the amount of nitrogen 2-s character predicted by McEwen's theoretical treatment (15). Values for the anisotropic nuclear spin-electron spin coupling parameters are calculated on the basis of the works of McEwen (15) and Lin (6, 7).

In summary, the E.P.R. spectrum of gas phase $^{14}N\,^{16}O_2$ has been recorded in the pressure interval between 10^{-3} and 1.3 atmospheres. The observations are consistent with an assignment of approximately 131 Mcps for the Fermi contact interaction. The Fermi contact interaction is a virtual measure of the nitrogen 2s-orbital character of the unpaired electron for the present case and allows the assignment of approximately 8% nitrogen 2s-character. This value is consistent with the 10.6% predicted in McEwen's theoretical treatment. Using the 21.2% nitrogen 2p-orbital character predicted by McEwen in conjunction with Dousmanis' nitrogen 2p-orbital value for $\left\langle \frac{1}{r^3} \right\rangle_{ave}$, the magnitude of the anisotropic electron spin-nuclear spin interaction should be approximately 10 Mcps neglecting the rotational energy state dependence. The data is in concordance with the assignment of approximately 73 Mcps for the spin-rotation coupling constant. This latter assignment neglects the terms which depend on the rotational angular momentum motional constant and its projection on the molecular symmetry axis.

The E.P.R. spectrum at the lowest pressures investigated consisted of many lines. The individual lines result from the superposition of transitions from molecules in many rotational states. The energy difference between the unperturbed electron spin states is a function of the electron magnetic moment-rotational magnetic moment interaction and the electron spin-nuclear spin interaction which can be divided into two parts, namely, rotational energy state dependent and independent components.

The molecular polarization along the magnetic field direction, which results from the electron spin-rotation coupling, is destroyed when the pressure is increased, due to the frequent molecular collisions. The E.P.R. spectrum changes accordingly, showing a decrease in spectral intensity arising from the transitions of the more highly polarized molecules and an increase in spectral intensity of transitions of more randomly oriented molecules. A three line spectrum emerges when the intermolecular collisions have become sufficiently frequent so that the molecular polarization is almost random and the collision induced transitions between nuclear spin states are not frequent. With further increase in pressure, the collision induced transitions between nuclear spin states progressively destroy the constancy of motion of the nuclear angular motion. As a result, the E.P.R. spectrum exhibits a broadening of the triplet into a pressure dependent singlet.

APPENDIX A

Application of the Damped Harmonic Oscillator Equation for Three Spectral Lines.

The equation herein involved is that given by Van Vleck and Weisskopf (29):

$$(A1) \quad \alpha = \frac{4\pi^3 \nu N}{3ckT} \quad \frac{\Sigma_j \Sigma_i |\mu_{ij}|^2 \nu_{ij} f(\nu_{ij}, \nu) e^{-W_j/kT}}{\Sigma_j e^{-W_j/kT}} \quad ;$$

where:

$$(A2) \quad f(\nu_{ij}, \nu) = \frac{1}{\pi} \quad \frac{\nu}{\nu_{ij}} \quad \frac{\Delta\nu_j}{(\nu_{ij}-\nu)^2 + \Delta\nu_j)^2}$$

The equation is appropriate for the microwave region (since $h\nu_{ij} << kT$) up to moderate pressures when the term which has been excluded becomes more important. Moderate pressures, though loosely defined, includes all pressures of interest in this research. As noted in the text, due to different assumptions, this is not the same equation as obtained by Lorentz. This equation is the result of the requirement of adiabatic collisions, namely, those collisions which do not result in a transfer of energy to or from the internal energy (rotation, magnetic, etc.). The parameters are defined as: α is the absorption; $|\mu_{ij}|^2$ is the square of the dipole

matrix element; ν_{ij} is the transition frequency; W_j is the energy of state j.

For the present case, the dipole matrix elements refer to an electron spin jump and are therefore the same, $|\mu|^2$. The summations are likewise redundant. For the strong field case $\Delta I_z = 0$, $\Delta S_z = \pm 1$. Furthermore, the difference in energy between the three I_z states is so small that the exponential may be removed from the summation. This maneuver results in a summation over states in the denominator which is equal to 3. Therefore:

$$\text{(A3)} \qquad \alpha = \frac{4\pi^3 \nu N |\mu|^2}{9\, ckT} \sum_j \nu_o f(\nu_j, \nu) .$$

The relaxation parameter for each energy state $\Delta\nu_j$ is not in general the same, but for the present case they are considered as such. This can be justified by consideration of Figure 7, and by arguments in Section E. Since the absolute intensity is not of interest, the presummation term of equation A3 is neglected, save the frequency dependence:

$$\text{(A4)} \qquad \alpha' = \nu \sum_j \nu_j f(\nu_j, \nu) .$$

Taking the first derivative:

$$\text{(A5)} \qquad \frac{d\alpha'}{d\nu} = 2 \sum \nu_j \left[f(\nu_j, \nu) + \frac{\nu(\nu_j - \nu)}{(\nu_j - \nu)^2 + \Delta\nu^2} f(\nu_j, \nu) \right] .$$

From equation A5, spectra were constructed using the separation of the outer to central line as the variable parameter. In other words, $\Delta\nu$ was expressed as a function of the line separation called A. Likewise, the frequency difference $(\nu_{ij}-\nu)$ was expressed in terms of A. From the spectra derived in this manner, the dependence of $\Delta\nu_e$, the frequency difference between the farthest separated extrema of the derivative curve of the absorption, on $\Delta\nu$ was obtained. The result is shown in Figure 3. The value of R for the theoretical spectra is shown in Figure 5.

Bibliography

1. F. A. Lindemann, Trans. Faraday Soc., 17, 598-599 (1922).

2. T. Carrington and N. Davidson, J. Phys. Chem., 57, 418-427 (1953).

3. C. H. Townes and A. L. Schawlow, Microwave Spectroscopy, McGraw-Hill, New York (1955);
   (a) pages 60-62,
   (b) page 96,
   (c) pages 336-337,
   (d) pages 337-338,
   (e) pages 355-361,
   (f) pages 371-373.

4. J. G. Castle, Jr. and R. Beringer, Phys. Rev., 80, 114-115 (1950).

5. R. Beringer, Ann. N. Y. Acad. Sci., 55, 814-822 (1952).

6. C. C. Lin, Ph. D. Thesis, Harvard University, Cambridge, Mass. (1955).

7. C. C. Lin, Phys. Rev., 116, 903-911 (1959).

8. G. R. Bird, J. Chem. Phys., 25, 1040-1043 (1956).

9. E. T. Arakawa and A. H. Nielsen, J. Mol. Spect., 2, 413-427 (1958).

10. G. R. Bird, private communication.

11. G. R. Bird and J. C. Baird, Bull. Am. Phys. Soc., 4, 68 (1959).

12. G. R. Bird, J. C. Baird and R. B. Williams, J. Chem. Phys., 28, 738-739 (1958).

13. E. Fermi, Z. Physik., 60, 320-323 (1930).

14. H. M. McConnell, private communication.

15. K. L. McEwen, J. Chem. Phys., 32, 1801-1814 (1960).

16. H. Goldstein, Classical Mechanics, Addison-Wesley, Cambridge, Mass. (1950), pages 107-109.

17. P. C. Cross, R. M. Hainer and G. W. King, J. Chem. Phys., 12, 210-243 (1944).

18. M. W. P. Strandberg, Microwave Spectroscopy, Methuen Monograph, John Wiley and Sons, New York (1954):
(a) pages 5-18,
(b) page 4.

19. S. C. Wang, Phys. Rev., 34, 243-257 (1930).

20. G. W. King, R. M. Hainer and P. C. Cross, J. Chem. Phys., 11, 27-42 (1943).

21. N. F. Ramsey, Molecular Beams, Clarendon Press, Oxford (1956), page 74.

22. G. C. Dousmanis, Phys. Rev., 97, 967-970 (1955).

23. D. R. Hartree and W. Hartree, Proc. Roy. Soc. (London), A193, 299-304 (1948).

24. A. D. Walsh, J. Chem. Soc. (1953), I. 2260-2266, II. 2266-2288.

25. G. Herzberg, Infrared and Raman Spectra of Polyatomic Molecules, D. Van Nostrand, Princeton, N. J. (1945), pages 51-55.

26. H. Eyring, J. Walter and G. E. Kimball, Quantum Chemistry, John Wiley and Sons, New York (1944), pages 162-163.

27. D. J. E. Ingram, Spectroscopy at Radio and Microwave Frequencies, Butterworths, London (1955);
(a) page 71,
(b) pages 71-72.

28. A. K. Saha and T. P. Das, Theory and Applications of Nuclear Induction, Saha Institute of Nuclear Physics, Calcutta, India (1957), pages 163-282.

29. J. H. Van Vleck and V. F. Weisskopf, Revs. Mod. Phys., 17, 227-236 (1945).

30. P. W. Anderson, Phys. Rev., 76, 647-661 (1949).

31. C. P. Smyth, Dielectric Behavior and Structure, McGraw-Hill, New York (1955);
(a) page 383,
(b) pages 414-415.

32. B. Bleaney and D. J. E. Ingram, Proc. Roy. Soc. (London), A205, 336-356 (1951).

33. B. M. Kozyrev, Disc. Faraday Soc., 19, 135-140 (1955).

34. F. H. Verhoek and F. Daniels, J. Am. Chem. Soc., 53, 1250-1263 (1931).

35. Handbook of Chemistry and Physics, 37th Edition, Chemical Rubber Publishing Co., Cleveland, Ohio (1955);
(a) pages 842-845,
(b) page 3078.

36. C. K. Jen, S. N. Foner, E. L. Cochran and V. A. Bowers, Phys. Rev., 112, 1169-1182 (1959).

PROPOSITIONS

1. The molecular and electronic structure of the ground state of NO_2 has been under investigation for a long time. The microwave spectrum has yielded several lines corresponding to transitions between rotational energy levels (see Bird (1)). A theory dealing with the rotational energy levels and the magnetic perturbations associated with the unpaired electron spin and the N nuclear spin has been formulated by Lin (2, 3). Bird and Baird (4) have indicated that they have measured the various constants, which arise in Lin's theory, for $^{14}N^{16}O_2$. These constants are a measure of the interaction between the nuclear spin and the electron spin and between the molecular rotation induced magnetic moment and the electron magnetic moment. The E.P.R. (Electron Paramagnetic Resonance) spectrum of the gas phase $^{14}N^{16}O_2$ has been investigated by the author (5). The analysis of the complex, low pressure NO_2 E.P.R. spectrum is beclouded by the presence of three sets of lines (distinguished by different I_z values, where I_z is the projection of the ^{14}N nuclear spin quantum number, $I = 1$, onto the z-laboratory coordinate along which the static external magnetic field is polarized). Two sets of these lines behave in the same manner and are characterized by $I_z = \pm 1$. The third set of lines with $I_z = 0$ is the simplest to understand since it has zero nuclear spin-electron spin interaction. Since there exists a difference in behavior in the three sets of lines and the fact that the three sets of lines have a common origin, the resultant E.P.R. spectrum is very difficult to understand.

It is proposed that the E.P.R. spectrum of $^{15}N^{16}O_2$ be investigated at low pressure (as low as experimentally practical). The nuclear spin of ^{15}N is 1/2, which affords three advantages; namely, (1) the intensity of the individual lines increases by a factor of 3/2 as compared to the $^{14}N^{16}O_2$ spectrum, (2) the number of sets of lines is decreased from 3 to 2, and (3) the two sets of lines exhibit the same behavior with respect to the nuclear spin-electron spin and molecular rotation-electron spin coupling differing only in the nuclear spin sign. What has been said in reference 5 concerning the magnitude of the various interaction parameters is in need of modification for this case. The nuclear g factor for ^{15}N is: $g_N = -0.56626$ (6). The nuclear spin-electron spin coupling parameters cited in reference 5 have to be multiplied by the factor $g(^{15}N)/g(^{14}N) = -1.40624$ (6). According to reference 3, the energy of a transition between energy states in a strong magnetic field, H, corresponding to $\Delta S_z = 1$, $\Delta I_z = 0$, $\Delta M_N = 0$, $\Delta K = 0$, $\Delta N = 0$ is:

$$(1) \qquad E = -g|\beta|H - \left(f_\lambda \lambda \pm \frac{\delta'}{|K|}\tau - \sigma\right) I_z + \kappa M_N .$$

S_z is the quantized projection of S, the electron spin quantum number, onto the z laboratory coordinate (defined above); M_N is the projection of the rotational angular momentum quantum number, N, onto the z laboratory axis; κ is the projection of N onto the symmetry axis of NO_2; g is the spectroscopic splitting factor; $|\beta|$ is the absolute value of the Bohr magneton. In addition:

$$(2) \qquad f_\lambda = f_\tau \left(\frac{N(N+1)-3K^2}{N(N+1)} \right) = \frac{(N(N+1)-3K^2)(N(N+1)-3M_N^2)}{N(N+1)(2N-1)(2N+3)} \quad ,$$

and:

$$(3) \qquad \lambda = 2\, g\, g_N\, |\beta|\, \beta_N \left\langle \frac{3\beta^2 - 1}{2r^2} \right\rangle_{ave}$$

$$(4) \qquad \tau = \frac{3}{4}\, g\, g_N\, |\beta|\, \beta_N \left\langle \frac{\alpha^2 + \gamma^2}{r^2} \right\rangle_{ave}$$

$$(5) \qquad \sigma = \frac{8}{3}\, \pi\, g\, g_N\, |\beta|\, \beta_N \left| \psi(o) \right|^2$$

where $\left|\psi(o)\right|^2$ is the probability of "finding the electron" at the nucleus per unit volume

$$(6) \qquad \delta'_{|K|} = 0 \ (|K| = 1), \quad \delta'_{|K|} = 0 \ (|K| \neq 1);$$

and:

$$(7) \qquad K = \frac{1}{2}(\epsilon_{BB} + \epsilon_{CC}) - \left[\epsilon_{AA} - \frac{1}{2}(\epsilon_{BB} + \epsilon_{CC})\right] \frac{K^2}{N(N+1)} \pm \frac{1}{4}\, \delta'_{|K|} (\epsilon_{BB} - \epsilon_{CC});$$

where ϵ_{ii} are electron spin-rotational coupling constants with respect to the principal moments of inertia directions (A is in the molecular plane and perpendicular to the symmetry axis B, C is defined by the relation between the unit vectors, $\hat{g}_i$:

(8) $\hat{g}_C = \hat{g}_A \times \hat{g}_B$) .

Finally,

(9) $\alpha = \sin\theta' \cos\phi'$

$\underline{\beta} = \cos\theta'$

$\gamma = \sin\theta' \sin\phi'$;

where θ' is the angle from B to $\vec{r}$, the vector from the nitrogen nucleus to the unpaired electron, and ϕ' is the angle from C to the projection of $\vec{r}$ onto the AC plane.

In reference 5, the values of λ, τ, and σ have been calculated using the results of the theoretical calculation of the ground state wave function for NO_2 by McEwen (7) and the values of $\left\langle \frac{1}{r^3} \right\rangle_{ave}$ and $|\psi(o)|^2$ obtained for the N atom by Dousmanis (8). The results for ^{15}N are:

(10) $\sigma = 241$ Mcps, $\lambda = 15.3$ Mcps, $\tau = 11.5$ Mcps .

On the other hand, only the first term of K was considered in reference 5 due to the complexity of the spectrum and the low intensity of lines with $|K| = 1$. The spin-rotation coupling is of two types (see references 2, 3) each of which results in the same form of equation (the sums of the individual terms are the ϵ_{ii} of equation 7). The only parameters expected to change upon substitution of ^{15}N for ^{14}N which affect the spin-rotational coupling are the reciprocal moments of inertia. The change in the moments is a result of the mass difference of about

one atomic mass unit per molecule and the very slight alterations of bond lengths and angle. It is to be stressed, however, that the attendant change in spin-rotation coupling is expected to be small. The change is expected to be roughly proportional to the change in the moments of inertia. For $(\epsilon_{BB} + \epsilon_{CC})$ the change is expected to be less than 0.1% and for $[\epsilon_{AA} - \frac{1}{2}(\epsilon_{BB} + \epsilon_{CC})]$ the change is expected to be about 5%.

The purpose of this investigation is twofold:

(1) as has been intimated, the $^{15}N^{16}O_2$ E.P.R. spectrum affords a simpler analysis than that of $^{14}N^{16}O_2$. In addition, it allows one to check the magnitude of the constants which have been obtained in reference 5, taking into account that discussed above.

(2) the mechanism of the observed pressure broadening may be checked with the aid of the energy terms obtained. One would expect, in accordance with reference 5, an enhancement of intensity in two regions in the central part of the spectrum with increase in pressure. At higher pressures the many lines present at low pressures will become a doublet which upon further increase in pressure will overlap finally forming a pressure dependent singlet. Assuming the proposed mechanism in reference 5 to be correct and since the spin-rotation coupling constants are expected to exhibit little change (see above), one would expect the same broadening behavior for the gas phase E.P.R. spectrum of $^{15}N^{16}O_2$ as that observed in $^{14}N^{16}O_2$ (5).

Bibliography

1. G. R. Bird, J. Chem. Phys., 25, 1040-1043 (1956).

2. C. C. Lin, Dissertation, Harvard University, Cambridge, Mass. (1955).

3. C. C. Lin, Phys. Rev., 116, 903-910 (1959).

4. G. R. Bird and J. C. Baird, Bull. Am. Phys. Soc., Series 2, 4, 68 (1959).

5. S. B. Berger, Dissertation, California Institute of Technology, Pasadena, California (1961).

6. N. F. Ramsey, Nuclear Moments, John Wiley and Sons, New York (1953), p. 79.

7. K. L. McEwen, J. Chem. Phys., 32, 1801-1814 (1960).

2. A recent publication contains work done on the E.P.R. spectrum of gamma-irradiated L-cystine dihydrochloride (1), the structure of which is:

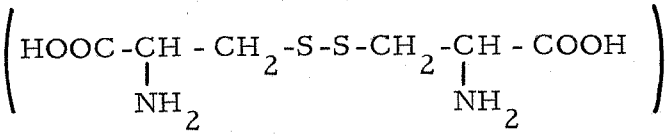

Kurita and Gordy, the authors, attribute the E.P.R. spectra obtained from the irradiated compound to the following radical species:

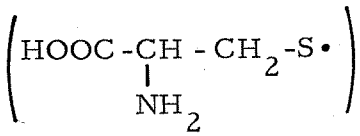

The following facts are established by the crystal structure work of Steinrauf, Peterson and Jensen (2):

(1) the molecule is in space group C2 , the b axis is unique.

(2) the crystal is monoclinic with $\beta = 103.6°$, $a_o = 18.61$ Å, $b_o = 5.25$ Å and $c_o = 7.23$ Å (unit cell dimensions).

(3) there are two molecules per unit cell which are equivalent in their orientations.

The following features of the E.P.R. spectrum of L-cystine dihydrochloride are presented by Kurita and Gordy (1):

(1) in some orientations of the single crystal one doublet is observed; specifically, when the magnetic field is along the y axis and when the magnetic field is in the xz plane

and the a'y plane. In this notation, x,y,z correspond to the crystallographic a,b,c axes, respectively. As shown by Kurita and Gordy, a set of orthogonal coordinates may be defined:

$$a' = x\ \cos(a',x) + z\ \cos(a',z) = 0.923x + 0.156z$$

$$b' = y$$

$$c' = x\ \cos(c',x) + z\ \cos(c',z) = 0.384x - 0.988z\ ;$$

where x and z represent distances in Angstroms.

(2) when the magnetic field is in the b'c' plane one obtains two doublets whose relative positions are dependent upon the angle the magnetic field makes with the b(or c) axis.

(3) the experimental data are well-fitted with respect to the g-tensor obtained with the p-type orbital assumed which is perpendicular to the C-S linkage. The conclusion necessitated to obtain the above fit is that the C-S bond must rotate in the crystal such that the two radicals formed from the one molecule of L-cystine dihydrochloride now have an S to S distance of 5.88 Å.

(4) the g value anisotropy of the radical is indicative of a large spin density on the sulfur atom since for carbon, nitrogen and oxygen it is known from work on other free radicals that the attendant g-value anisotropy is smaller and is explicable on the admixture of some 3d character

into the sulfur orbitals.

(5) the doublet observed arises from the interaction of the hydrogen nuclear magnetic moment with the electron magnetic moment and is essentially isotropic. The doublet, whose components are separated by 9 Mcps, is explained on the basis of hyperconjugation which places spin density on the CH_2 protons from the non-bonding orbital containing the unpaired spin on the sulfur atom. The reason given for there being only a doublet and not a triplet or quartet is that the unpaired electron hyperconjugates more strongly with one proton than the other.

It is proposed that another species would produce the same results and would not have the drawbacks of the above analysis. These liabilities are: (1) the large distance that the S atoms move in the crystal, (2) the large spin-spin coupling between the electrons on the sulfur atoms separated by only 5.88 Å which amounts to:

$$h^{-1} E_{dd} \approx \frac{g^2 \beta^2}{h} \frac{1}{r^3} = 3 \times 10^8 \text{ cps}$$ and which

would through lattice motion broaden the spectrum to an extent which would make the resolution of the hyperfine structure doubtful. In order to see this more clearly, consider a mean square amplitude of motion of the sulfur atom to be approximately 0.05 Å. Using the above energy,

E_{dd}, one can easily calculate an approximate frequency spread amounting to 15 Mcps. This crystal motion is expected therefore to produce a perturbation about equal to the doublet separation, 9 Mcps. (3) the necessity of requiring a different hyperconjugation between the sulfur non-bonding orbital and the two protons on the methylene group adjacent to the sulfur. There appears to be no forces which would constrain the p_x orbital on the sulfur to the required position. There are two non-bonding electrons in another orbital on the sulfur and no reason has been offered to require the specifying of orbital direction.

The radical proposed is:

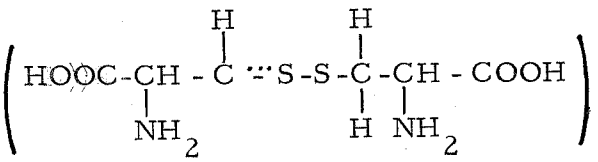

The orthonormalized orbitals required for the three electrons of the radical may be expressed as:

$$\psi_1 = (1 - \lambda^2)^{1/2} \psi_c(2p) + \lambda \psi_s(3p)$$

$$\psi_2 = \lambda \psi_c(2p) - (1 - \lambda^2)^{1/2} \psi_s(3p) .$$

Unfortunately, the values of the various terms of the energy expression are not known and an estimate of the value of λ is therefore not possible. To a rough approximation one may, due to the similar electronegativities of sulfur and carbon (3), consider $\lambda = \sqrt{2}^{-1}$. This assignment results in a three electron bond with two electrons (paired) in the

orbital of lower energy, ψ_1, and the unpaired electron in the other orbital, ψ_2. This situation does not appear to exist in the radical produced in light of the approximately isotropic behavior of the proton splitting (doublets). The available data imply a small λ, which means that the unpaired electron is more localized on the sulfur than on the carbon. An opposite situation accrues for the pair of electrons in the other orbital, ψ_1. This is a very interesting outcome, for with the value of λ, the value of the coulomb integral for sulfur may be estimated with respect to the coulomb integral for carbon. In a more sophisticated approach one would have to account for the additional complications of (1) orbital overlap with the adjacent sulfur orbitals, (2) admixture of higher orbitals, especially the 3d orbitals on sulfur. The expected orientation of the 3p sulfur orbital, $\psi_s(3p)$, is in concordance with the orbital required by Kurita and Gordy in the fitting of the g-tensor data. One notes that there are two sites for the radiation to promote the loss of a proton. The resultant radicals are analogous to those of Kurita and Gordy, differing only in the rotation that has changed the original species into their radicals. The hyperconjugation is now seen to arise only from the one available hydrogen on the carbon adjacent to the sulfur "containing" the unpaired electron.

An experiment intended to show the production of hydrogen atoms and subsequently hydrogen molecules is proposed. Namely, one should mass spectrophotometrically monitor the gaseous products produced by

the gamma-irradiation of L-cystine dihydrochloride in the powder form.

In order to ascertain the value of λ used before in conjunction with the orbitals ψ_1 and ψ_2, one could substitute a ^{13}C (with I = 1/2) in place of the ^{12}C adjacent to the sulfur atoms. An analysis of the effect of the ^{13}C nuclear spin-electron spin coupling on the E.P.R. spectrum and the magnitude of the effects produced would be interpretable in terms of the type of orbital involved and the magnitude of its contribution to the configuration of the unpaired electron. Similarly, the substitution of ^{33}S (with I = 3/2) in place of the ^{32}S would allow the same analysis for the ^{33}S nuclear spin-electron spin interaction. This experiment might not produce a very easily understood spectrum because of the nuclear quadrupole moment of ^{33}S. The experiment does appear to be worthwhile and the trouble of reconciling the effects of the quadrupole coupling does not seem overpowering. The type of analysis of the E.P.R. spectrum which would be required is analogous to that presented for other radicals, see reference 4.

Bibliography

1. Y. Kurita and W. Gordy, J. Chem. Phys., 34, 282-288 (1961).

2. L. K. Steinrauf, J. Peterson, and L. H. Jensen, J. Am. Chem. Soc., 80, 3835-38 (1958).

3. L. Pauling, Nature of the Chemical Bond, Cornell University Press, Ithaca, New York (1960), p. 93.

4. H. M. McConnell, C. Heller, T. Cole, and R. W. Fessenden, J. Am. Chem. Soc., 82, 766-775 (1960).

3. Consider the molecules FNY, where Y represents sulfur or oxygen. FNO has been investigated a little more thoroughly than has FNS. Nevertheless, a full article describing the work done on the microwave spectrum and the effect of the Stark effect thereon of FNO has not been published. The only available data reside in a letter to the editor (1) and an abstract (2). The data are interpreted to give bond distances: F-N = 1.52 Å, N-O = 1.13 Å and bond angle = 110° (1) and dipole moment μ = 1.8D with the N-F bond moment = 1.75D and the N-O bond moment = -0.17D. For FNS Glemser and associates (3) have found from electron diffraction data: F-N = 1.42 Å, N-S = 1.59 Å and angle FNS = 120±5° and more recently (4) N-S = 1.62 Å and angle FNS = 122°. Pauling (5a) shows the following resonant structures:

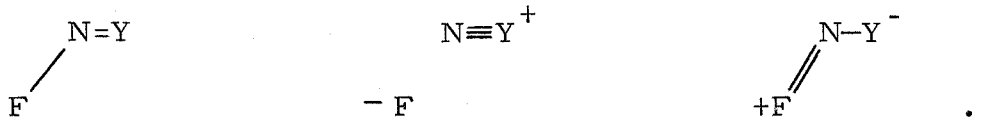

I II III

One may estimate the bond distances of each of the resonant structures using the interatomic distances found in Pauling (5b) in conjunction with the Schomaker-Stevenson electronegativity (χ_i) correction (5b). The equation given there is:

$$D(A\text{-}B) = r_A + r_B - c\left|\chi_A - \chi_B\right| \quad ;$$

where D(A-B) is the desired bond distance, r_i is the required

covalent radius and c is the Schomaker-Stevenson coefficient (c = 0.09 Å for N-O, N-F bonds and c = 0.08 Å for N-S bonds). The electronegativities are tabulated in Pauling (5c). For FNY one obtains:

Structure	D(F-N)	D(N-O)	D(N-S)
I	1.37 Å	1.20 Å	1.52 Å
II		1.06 Å	1.38 Å
III	1.13 Å	1.44 Å	1.74 Å

For FNO structures I and III are assigned the weights 0.25 and structure II is assigned the weight 0.5 on the basis of the bond distances and dipole moment data (5a). The no-bond form, structure II, would have a large bond distance since the ionic radius of F^- is 1.36 Å (5d).

The explanation afforded the unexpectedly high contribution of the no-bond configuration (structure II) is (1) that the N≡O bond is more stable than one would on first estimate figure and may be analogous to N≡N which likewise is very stable and (2) that the nitrosyl group is not as electronegative as either of the constituent atoms and therefore tends towards losing an electron (5a). The question now to answer is which structure is the most important for FNS. Since a sulfur atom is of lesser electronegativity than an oxygen atom, one on first reflection would consider enhancement of the contribution which structure II makes

to the total configuration. On the same grounds, the structure III would be expected to be of lesser consequence for FNS than for FNO. Therefore, one would predict that the N-F bond distance in FNO be shorter than it is in FNS and that N-S distance be closer to the triple bond length than the N-O distance is in FNO. From the data of Glemser and associates one sees that these trends are contradicted. The F-N bond distance may be considered to be fair. On this basis one notes that structure II makes less of a contribution to the molecular configuration than was at first expected. One can interpret this result as indicating that N≡S is not as stable as N≡O (probably considerably less stable). The electronegativity difference, $|X_N - X_Y|$ is 0.5 for both cases but the great size of the sulfur compared to the nitrogen is in contradistinction to the approximately equal size of the oxygen and the nitrogen. One may therefore expect that the great stability afforded to N≡O is a result of the similarity between N and O and that N≡S is not of equal stability. Using these arguments one diminishes the expected contribution of structure II while increasing the weight of structure I but probably not affecting the weight of structure III though the method of distribution of the fractional contribution which has been taken from structure II is not known. One might distribute that weight in proportion to the existent expectation (25% I, approximately 15% III). If the weight of structure II is taken as 0.40 then structure I has 0.375 and structure III has 0.225 contribution. These values are conjecture

and presented as an example with the hope to provide some reality. On this basis one would expect the N-S distance to be about 1.5 Å and the bond angle slightly less than 120°.

The values of Glemser and associates are not consistent with the above arguments. The N-S distance lies between the single and double bond values given above and give strong weight to structures I and III while the N-F distance lies between the single bond and no-bond values which give strong weight to structures I and III.

There are two principal conclusions which may be drawn; namely, (1) the values of Glemser and associates are incorrect, and (2) the theoretical bond distances used are in need of adjustment. In order to show which conclusion is correct, it is proposed that the microwave spectrum of FNS be investigated. The molecule is expected to be a near prolate symmetric top. The center of mass lies to the sulfur atom side of the line bisecting the FNS angle and about 0.8 the distance from the nitrogen to the line intersecting the sulfur and fluorine atoms. Calculation of the principal moments of inertia for the parameters of Glemser and associates with the FNS angle equal to 110 and 120° shows that Ray's asymmetry parameter, κ, for this molecule should be between -0.95 and -1. This proximity of κ to -1 means that the molecule is a very good approximation to a prolate symmetric top. κ is defined:

$$\kappa = \frac{2\frac{1}{I_B} - \frac{1}{I_A} - \frac{1}{I_C}}{\frac{1}{I_A} - \frac{1}{I_B}} \quad ;$$

where I_A, I_B and I_C are the three principal moments of inertia, given in order of increasing magnitude. The appropriate approximate equation for the energy is (6):

$$E = \frac{1}{2}(B+C)\,N\,(N+1) + [\,A - \frac{1}{2}(B+C)]\;K^2 \quad ;$$

where A, B and C are the reciprocal rotational constants (for example, $B = \frac{h}{8\pi^2 I_B}$) and K is the projection of the molecular rotational angular momentum (characterized by quantum number N) on the pseudo-symmetry axis (the bisector of the FNS angle). $\frac{1}{2}(B+C)$ is expected to be about 6KMcps and $[A - \frac{1}{2}(B+C)]$ is expected to be about 80KMcps. Substitution of ^{15}N and the obtaining of the altered rotational constants would allow the complete structure of FNS to be determined.

Application of Stark modulation in conjunction with the microwave experiment will allow one to investigate the dipole moment in the same manner as was done by Magnuson for FNO (1). This experiment is of interest since the large bond moment of N-F in FNO was completely unexpected in light of the 0.23 dipole moment of NF_3 which would allow a bond moment of 0.17 D for the N-F bond (7). The smallness of the dipole moment of NF_3 has been discussed and interpreted in terms of resonant structures with N=F double bonds (8) and in

terms of hybridization (9). A bond moment for N-F coupled with the bond length data can help decide the importance of the three structures in the molecular structure. Similarly the N-S bond moment may be obtained. The data then available would be sufficient to resolve the duality mentioned earlier.

Bibliography

1. D. W. Magnuson, J. Chem. Phys., 19, 1071 (1951).

2. D. W. Magnuson, Phys. Rev., 87, 226-227 (1952).

3. O. Glemser, H. Richert and F. Rogowski, Die Naturwissenschaften, 47, Part 4, 94-95 (1960).

4. R. C. Greenough, private communication from O. Glemser.

5. L. Pauling, Nature of the Chemical Bond, Cornell University Press, Ithaca, New York (1960).
   (a) pp. 345-347;
   (b) pp. 224, 228-230;
   (c) p. 93;
   (d) p. 514.

6. C. H. Townes and A. L. Schawlow, Microwave Spectroscopy, McGraw-Hill Book Co., New York (1955), pp. 83-86.

7. S. N. Ghosh, R. Trambarulo and W. Gordy, J. Chem. Phys., 21, 308-310 (1953).

8. P. Kisliuk, J. Chem. Phys., 25, 779 (1956).

9. M. Mashima, J. Chem. Phys., 24, 489 (1956); 25, 779 (1956).

4. It is proposed that the rate of energy transfer in a pure single crystal be measurable as a function of the N.M.R. spectral line width of a nucleus in a species which is directly involved in the energy transfer. The case to be considered involves a species which when excited to higher electronic energy states returns through a metastable triplet state to the singlet ground state. It will be necessary for the success of this experiment to have a sufficiently high concentration of species in the triplet state.

The rate of an electron exchange reaction may be obtained from a knowledge of the concentration of the species containing the odd electron and the normal and perturbed line width of the nuclear magnetic resonance spectrum of a nucleus in the species when certain conditions are fulfilled (1, 2). In a fashion analogous to the electron transfer, the rate of energy transfer between sites in a crystal may be investigated. The following lifetimes are defined: τ_m is the mean lifetime of the metastable state before phosphorescing to the ground state; τ_t is the mean lifetime of the metastable state before transferring the energy corresponding to E(triplet) - E(singlet) to another site (note that τ_t is dependent upon the concentration of singlet states); τ_d is the mean lifetime of a singlet state species before acceptance of the above cited energy (dependent upon the triplet state concentration). In order that the transference of energy be allowed to dominate the perturbation, it is required that:

(1) $$\tau_m >> \tau_t \ .$$

The conversion of energy into heat has not been considered and it will be assumed that the energy is transferred many times before dissipation into heat. In order that the nucleus under observation be primarily in the diamagnetic environment,

(2) $$\tau_d >> \tau_t \ .$$

Since the equilibrium condition is of interest (steady state), one obtains through kinetic considerations:

(3) $$\frac{1}{\tau_d} (N - n) = \frac{1}{\tau_t} n \ ;$$

where N is the total number of molecules in the crystal and n is the total number of excited molecules. In general, n will be much smaller than N, so that the inequality of equation 3 holds. In order that a change in line width be observable:

(4) $$\left(\frac{1}{T_2}\right)_d < \frac{1}{\tau_d} \ .$$

The final restriction is:

(5) $$(\delta\omega \tau_t)^2 >> 1 \ ;$$

where $\delta\omega$ is the perturbation energy (it is, in other words, the difference in energy between the nuclear spin in the diamagnetic and the

paramagnetic triplet environment). Note that only half of the substates of the triplet state are effective in this mechanism, since the projection of the electron spin angular momentum in the external magnetic field direction is quantized with the values of 1, 0, or -1 in the ratio of 1:2:1. From kinetics:

$$\tau_d = \frac{1}{nk} \quad ; \tag{6}$$

where k is the bimolecular rate constant describing the energy transfer.

The equation representing the line width as a function of τ_d under the conditions of equations 1, 2, 4, and 5 is:

$$\left(\frac{1}{T_2}\right)_{dt} = \left(\frac{1}{T_2}\right)_d + \frac{1}{2\tau_d} \quad ; \tag{7}$$

which is in direct analogy to that expressed for electron exchange in reference 1, The factor of 2 in the denominator of the term in τ_d arises from the fact that only half of the environments are effective in the line broadening mechanism. Note that electron spin relaxation has been neglected.

Bibliography

1. H. M. McConnell and S. B. Berger, J. Chem. Phys., 27, 230-234 (1957).

2. Stuart B. Berger, Dissertation, California Institute of Technology (1961).

5. At low temperatures (about at the NO liquifying temperature) NO exhibits dimerization to $(NO)_2$. The crystal structure of this dimer has been investigated (1). The results of this study show that there are two molecules per unit cell in space group P_{2_1}/a in a monoclinic form. The cell dimensions are unimportant for the present purpose. The residual entropy of $(NO)_2$ is 1.5 ± 0.2 e.u./mole dimer (2) indicating a disordered structure. Dulmage and associates (1) have advanced three possible positionings for the various atoms. The uncertainty is attributed to the disorder. The three spatial structures are (with the short distance constant):

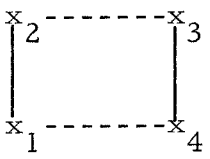

A

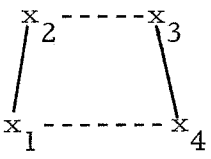

B

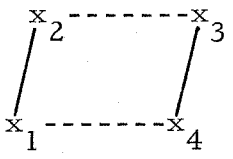

C

A	B
$x_1x_2 = x_3x_4 = 1.12 \pm 0.02$ Å	$x_2x_3 > 2.15$ Å
$x_2x_3 = x_1x_4 = 2.40 \pm 0.01$ Å	$x_1x_4 < 2.65$ Å
$< x_2x_3x_4 = 91.2 \pm 1.6°$	

Dulmage and associates as seen through their proposed structures state that they can, at best, take the 2.40 Å distance as an average distance. In addition, on the basis of their data, they prefer A. They further propose three molecular arrangements:

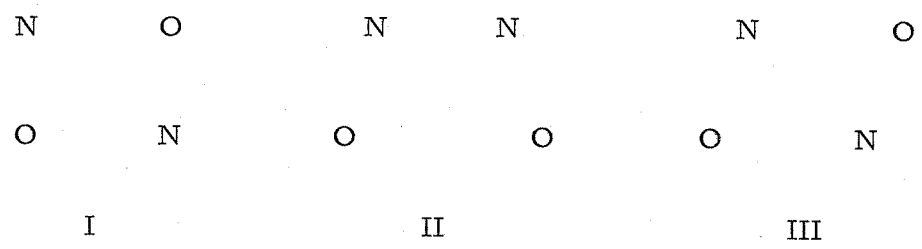

I II III

In support of I, these authors cite the similarity with the NO monomer with respect to bond distance and bond order (about 2.5) and propose the resonance structures:

The coincidence of the infrared and Raman spectra was interpreted as favoring a non-centrosymmetric structure (3). Dulmage and associates note that the coupling between NO groups is weak and that the coincidence observed may be accidental. Finally reflection upon the structure of $(NO_2)_2$ recalls its long N-N bond thereby making II and III attractive.

Two methods are advanced in the hope of clarifying the structure. First, one might try mixing $^{15}N^{18}O$ with $^{14}N^{16}O$ and quickly crystallizing. After leaving set for a reasonable length one would mass spectrophotometrically determine the species present. The production of the species $^{15}N^{16}O$ and $^{14}N^{18}O$ in a reasonable quantity would be fair evidence for I and III. The problem of whether or not the

exchange will be sufficiently fast to observe the new species precludes any conclusion as to the absence of I and III. Secondly, one could observe the nuclear quadrupole resonance spectra of $(NO)_2$. All three species will produce an axially symmetric electric field at the ^{14}N nucleus. The energy equation is then (4)

$$E_m = \frac{e^2qQ}{4I(2I-1)} \left[3m^2 - I(I+1)\right] ;$$

where the eigenvalues of I_z are diagonal and $I = 1$ is the nuclear magnetic moment of nitrogen, m is its z projection and e^2qQ is the quadrupole coupling. The magnitude of the latter is dependent upon the field gradient at the nitrogen, Q. One would expect that the gradient of III > I > II, since the number of close atoms decreases in that order. A detailed analysis of this problem seems to be of value.

Bibliography

1. W. J. Dulmage, E. A. Meyers and W. N. Lipscomb, Acta Cryst., 6, 760-764 (1953).

2. H. L. Johnston and W. F. Giauque, J. Am. Chem. Soc., 51, 3194-3215 (1929).

3. A. L. Smith, W. E. Keller and H. L. Johnston, J. Chem. Phys., 19, 189-192 (1951).

4. T. P. Das and E. L. Hahn, Nuclear Quadrupole Resonance Spectroscopy, Solid State Physics Supplement No. 1, Academic Press, New York (1958, Chapter I.